UNIVERSITÀ DEGLI STUDI
DI MILANO

Scuola di Dottorato in Scienze Biochimiche, Nutrizionali e Metaboliche,
Dottorato di Ricerca in Biochimica (BIO/10), XXI ciclo

Low Molecular Weight Heparins: in depth structural characterization to understand their different biological properties

Davide VECCHIETTI

Matricola **R06792**

Tutor: Prof. Sandro SONNINO,
Dott.ssa Antonella BISIO
Coordinatore: Prof.ssa Silvia PAGANI

Anno accademico 2007/2008

To my Mother

By convention there is sweet, by convention there is bitterness, by convention hot and cold, by convention color; but in reality there are only atoms and the void.

Democritus

1.0 Introduction

“ *- Dr. Howell, I have discovered antithrombin! - He smiled and said, - Antithrombin is a protein, and you are working with phosphatides. Are you sure that salt is not contaminating your substance? - I told him I was not sure of that, but it was a powerful anticoagulant* ”.

It was 1916 and Jay McLean, a second year medical student, accidentally discovered the Heparin! The name was derived from cuorin (a cephalin isolated from heart) and heparphosphatide (a cephalin isolated from liver).

The discovery of heparin was not followed by immediate practical use and only twenty years later its clinical utility in the treatment of post traumatic venous thrombosis of the lower extremities was recognized, by the Canadians Charles Best and Gordon Murray. Jay McLean expired in 1957, dismayed and depressed with the indifference devoted by the scientific community to its discovery and only several years later the fact was recognized in a simple ceremony to testify its participation in the discovery of a drug that promoted the progress and development of vascular and cardiac surgery, the extracorporeal circulation, the haemodialysis, the organ transplantation, the treatment and prevention of arterial and venous thromboembolism and has been critical in more other fields in the modern medicine.

1.1 Heparin

Heparin is a sulfated polysaccharide belonging to the family of glycosaminoglycans (GAG) (1). The structure of heparin has been extensively investigated for more than 50 years, with the particular aim of unravelling the features associated with its potent anticoagulant activity (2). The emerging interest in no anticoagulant properties of heparin (3) and their therapeutic applications (4) has extended these studies in an attempt to gain an understanding of the molecular basis and possible interplay of different sequences. The present knowledge of structure and structure–activity relationships of heparin has emerged steadily over the years. The regular sequences in the prevalent product of heparin biosynthesis that constitute the majority of the sequences of beef lung heparins used in several structural studies has long been thought to be exclusively responsible for the anticoagulant activity. The discovery that this activity is mainly dependent on an antithrombin (AT)-binding domain which is present in only about one third of pharmaceutical grade heparin chains, and that this domain is a specific pentasaccharide sequence, has led to the reappraisal of the role of minor sequences in determining specificities of biological interactions of heparin. Such a reappraisal has, in turn, been stimulated by an increasing interest in heparan sulfate (HS), a structural analogue of heparin that plays important roles in a number of physiological and pathological processes. Heparin thus accompanied HS into the world of ‘‘new biology’’, with the perception that distinct domains of both GAGs preferentially bind proteins that modulate a number of physiological and pathological processes (6).

A deeper elucidation of the structure and information on biological interactions of both heparin and HS was made possible by the availability of structurally well-defined heparin oligosaccharides obtained by chemical synthesis (7) and by developments of methods for sequencing heparin/HS fragments (8). Developments in understanding the structure–activity relationships of heparin are covered in several reviews (5,9–13).

1.1.1 Monosaccharide Residues

Like most of the GAGs, heparin is a linear polysaccharide constituted by alternating disaccharide sequences of a uronic acid and an aminosugar. The uronic acid residues of heparin are L-iduronic acid (IdoA) and D-glucuronic acid (GlcA), and its only aminosugar is D-glucosamine (GlcN). Indeed, IdoA, GlcA and GlcN, together with the minor components D-galactose (Gal) and D-xylose (Xyl) belonging to the terminal of GAG chains linked to the peptide core of the original peptidoglycan, are the only monosaccharide residues identified in purified heparins (2).

Whereas both IdoA and GlcN residues are linked α-1,4 to the next residue in the chain, GlcA is linked β-1,4. GlcN is prevalently N-sulfated in heparin, and N-acetylated in minor sequences. Both the uronic acid (especially IdoA) and the aminosugar bear O-sulfate groups in position 2 and 6 respectively. The formulas of the most represented monosaccharide residues in heparin are shown in figure 1.

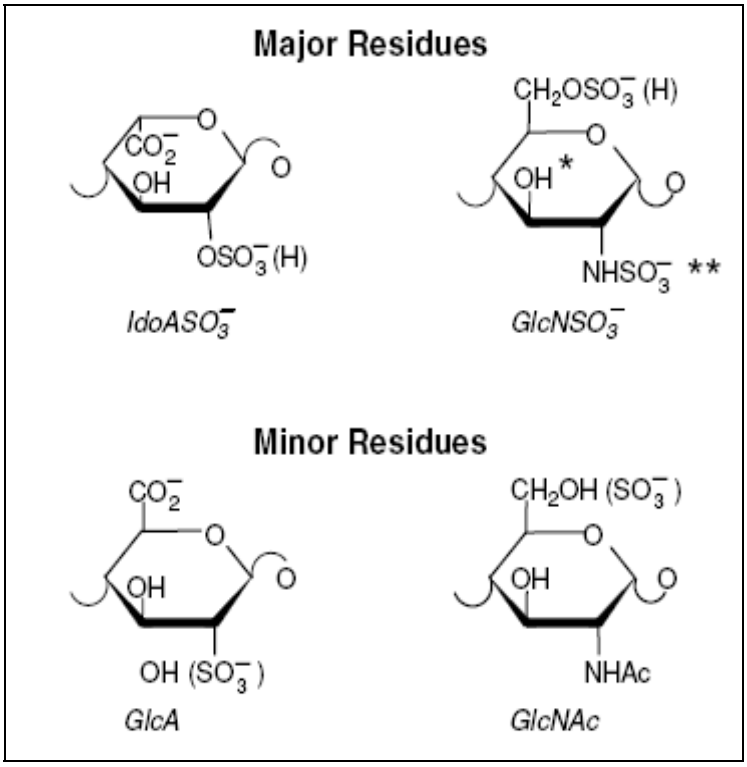

Fig 1 Monosaccharide components of heparin. Forms in parenthesis occur less frequently. Minor GlcN residues bear a SO3 substituent (*), or a free NH2 group instead of a NHSO3 group (**) (see text).

Heparin chains are made up of various combinations of these building blocks. As schematized in figure 2, different sulfation patterns are unevenly distributed along the heparin/HS chains, with less charged sequences mostly concentrated towards the reducing side of the chains (R) and the most charged ones towards the non-reducing side (NR), with mixed domains (NA/NS) in between the two regions.

The relative proportion of the different domains and the actual composition within the same domains of heparins vary depending on the animal and organ source and, to some extent, also on the purification procedures (14). Some of the heparin chains terminate, at the R end, with the ‘‘linkage region’’ (LR) reminiscent sequence of the attachment, through a serine (Ser) residue, to the peptide core of the original proteoglycan (2). As a result of the limited cleavage by β-d-glucuronidases of GlcA–GlcN linkages in the last step of biosynthetic modification of carbohydrate chains of the heparin proteoglycan, the terminal residue on the NR end of heparin chains is usually a GlcN (5). Depending on the extent of this latter modification and on its possible erosion during manufacturing/purification processes, heparins from different origins widely differ in their content in LR (see later).

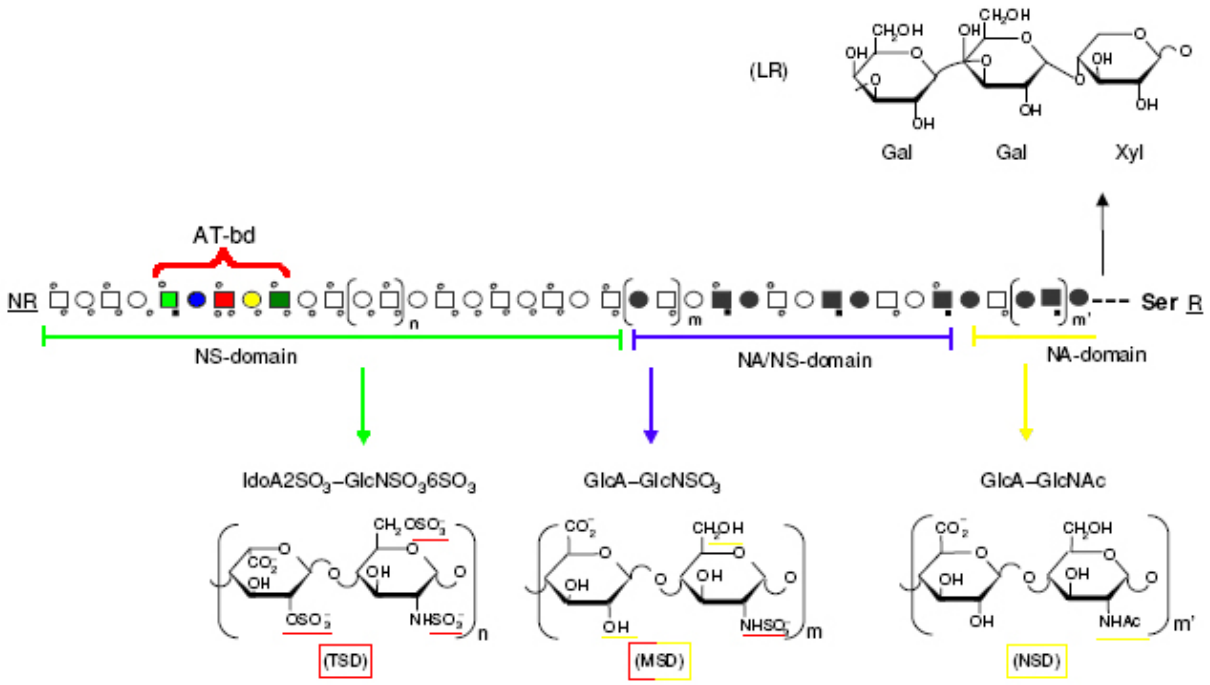

Fig 2 Schematic representation of a heparin chain constituted of N-acetylated (NA), N-ulfated (NS), and mixed NA/NS domains also containing an antithrombin-binding domain (AT-bd). The chain is conventionally represented as extending from its reducing (R) to its ‘‘nonreducing’’ end. In fact, its biosynthesis starts from the LR. Formulas of major disaccharidic sequences within NS, NA/NS and NA domains and of the LR originally linked to the Gly-Ser polypeptide core, are shown.

1.1.2 Major disaccharide Units

The composition of heparin is usually expressed in terms of their content in different disaccharide units. As illustrated in figure 2, the major disaccharide repeating sequences of heparin are those of the trisulfated disaccharide (TSD) IdoA2SO3 - GlcNSO36SO3, which are concentrated in NS domains, where glucosamine residues are prevalently N-sulfated. TSD units represent up to 60–75% of heparins obtained from pig mucosa and up to 85% of heparins from beef lung (15,16). These relatively long segments of ‘‘fully sulfated’’ (i.e., N-, 2-O-, and 6-Osulfated) disaccharide units along the heparin chains are often referred to as constituting ‘‘regular regions’’ and are the major contributors to the polyelectrolytic properties of heparin. Also 2-O-sulfated GlcA residues have been identified in fully sulfated regions of heparin (17).

Although rare components [less than 0.5% (w/w)], these residues may play important functions (10,17).

As segments of a macromolecule, NS regions of heparin exclusively constituted by TSD sequences should not be defined as copolymers of repeating disaccharide units. In fact, the α-l configuration of IdoA residues involves a trans orientation of pairs of TSD units and heparin should thus be referred to as a copolymer of hexasulfated tetrasaccharide (HST) units, featuring arrays of three sulfate groups (NSO_3,2-O-SO_3, and 6-O-SO_3) that alternate on both sides of the chains, as shown in figure 3.

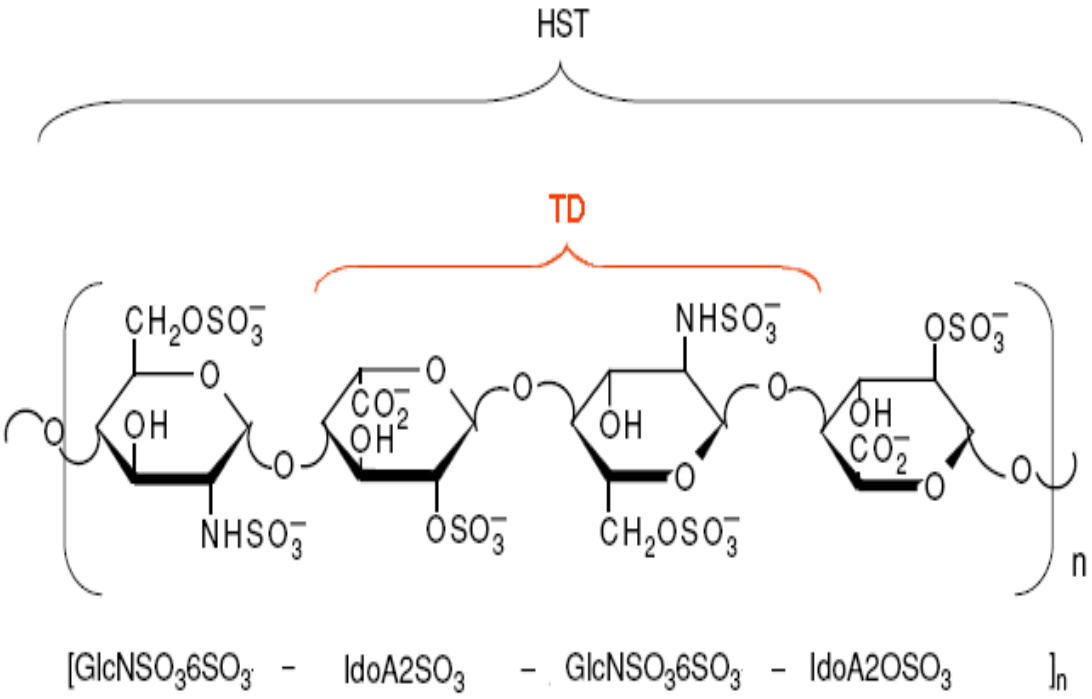

Fig 3 Heparin as a poly-tetrasaccharide: major sequences in the NS region

The length of repeating TSD units along the heparin chains has been assessed only in statistical terms and for a limited number of heparin types, mainly through size profiling of oligosaccharides generated by cleavage of heparins oxidized with periodate at the level of nonsulfated uronic acids (18,19). Without isolation and sequencing of individual oligosaccharides, this analytical approach quantify only

sequences made up of 2-O-sulfated disaccharide units and does not take into account occasional 6-O-desulfated glucosamine residues. The length of repeating ‘‘TSD’’ sequences in pig mucosal heparin corresponds to 4–12 disaccharide units (18), with an average size of eight disaccharide units (19). As illustrated in Fig. 4, the 2-O-sulfated sequences are separated from each other by GlcA-containing (less frequently by IdoA-containing) sequences (see later) (18).

Fig 4 Proposed distribution of disaccharide units along an average heparin chain (18). TSD, trisulfated disaccharide. For simplicity, possible AT-binding and linkage regions are omitted. Arrows indicate possible insertion of GlcA-containing units.

1.1.3 Undersulfated Sequences

As schematically illustrated in figure 2, minor undersulfated repeating units (such as the monosulfated disaccharide (MSD) GlcA-$GlcNSO_3$) are part of mixed N-sulfated/N-acetylated, GlcA-containing NA/NS domains. The NA domain close to the linkage region LR is prevalently constituted of nonsulfated disaccharide (NSD) GlcA–GlcNAc repeating units. However, NA/NS regions may incorporate 2-O-sulfated IdoA and 6-O-sulfated $GlcNSO_3$/NAc residues, and some GlcN residues in the NA domains are 6-O-sulfated. Heparins from different animal species and/or organs significantly differ from each other in their degrees of heterogeneity as revealed by disaccharide analysis (14) or NMR analysis of their sulfation patterns (20). The relative contents of non-6-Osulfated glucosamine and non-2-O-sulfated iduronic acid

of pig mucosal heparins are consistently different from those of beef mucosal heparins (14,16,20). Also the extent of undersulfation associated with occurrence of nonsulfated GlcA residues widely varies among different types of heparin, ranging from a few percent of total uronic acids for beef lung heparins to up to 20% of pig mucosal heparins (16,20). As illustrated in figure 2, nonsulfated GlcA (together with N-acetylated GlcN) residues are prevalently (though not exclusively) concentrated in NA and NA/NS regions. However, 2-O-desulfation of iduronic acid residues and 6-O-desulfation of glucosamine residues is spaced out along the heparin chains (21). Figure 5 schematically illustrates the concept that sulfation gaps associated with O-undersulfation in the NS/NA and NS regions of heparin separate fully sulfated sequences of different lengths. Due to the different requirements in terms of size of fully sulfated sequences as effective ligands for most of the heparin-binding proteins (5,10,12), different frequencies of sulfation gaps conceivably modulate the protein-binding properties of heparins and heparin fractions.

A large number of heparin oligosaccharide fragments arising from the irregular regions of heparin are listed in Ref. 5. The number of identified heparin/HS oligosaccharides is steadily increasing (22–24). Recurrent patterns, such as the trisulfated hexasaccharide IdoA(GlcA)2SO_3-GlcNSO_3–IdoA–GlcNAc–GlcA–GlcNSO_3, have been identified in the low sulfated irregular region of pig mucosal heparin, the underlined trisaccharide sequence being shared by a number of the isolated oligosaccharides (25).

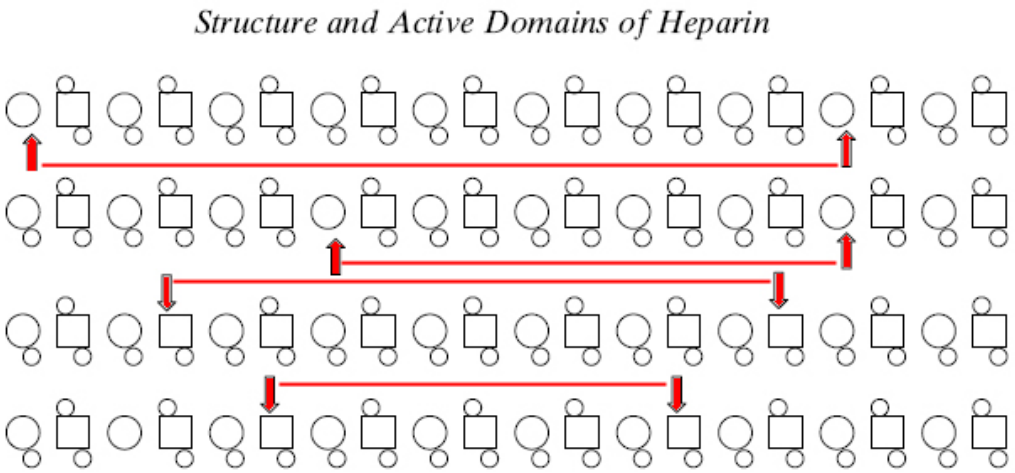

Fig 5 Idealized representation of heparin NS chains with 6-O- and 2-O-sulfation gaps (indicated by arrows) spaced out along the chains. For simplicity, AT-binding sequences are not shown. Sulfation gaps determine the length of ‘‘fully sulfated’’ segments made up of TDS sequences and modulate protein-binding and associated biological properties of heparin.

1.1.4 Specific sequences

As illustrated in figure 2, some of the heparin chains contain a specific sequence constituting the antithrombin binding domain (AT-bd). This sequence is the pentasaccharide AGA*IA shown in figure 6, where the red star denotes a rare 3-O-sulfated $GlcNSO_3$ residue. The figure also indicates the three sulfate groups that are essential for high-affinity binding for AT (red rhombus), and underlines the fact that the GlcA residue is also essential (half moon). The IdoA residue preceding the pentasaccharide shown in the formula (yellow), though invariably present in natural AT binding domains, does not contribute to the affinity for AT. Some natural variants compatible with high affinity for AT (i.e., N-sulfation instead of N-acetylation of the first aminosugar residue and 6-O-sulfation of the 3-O-sulfated residue) are also shown (5).

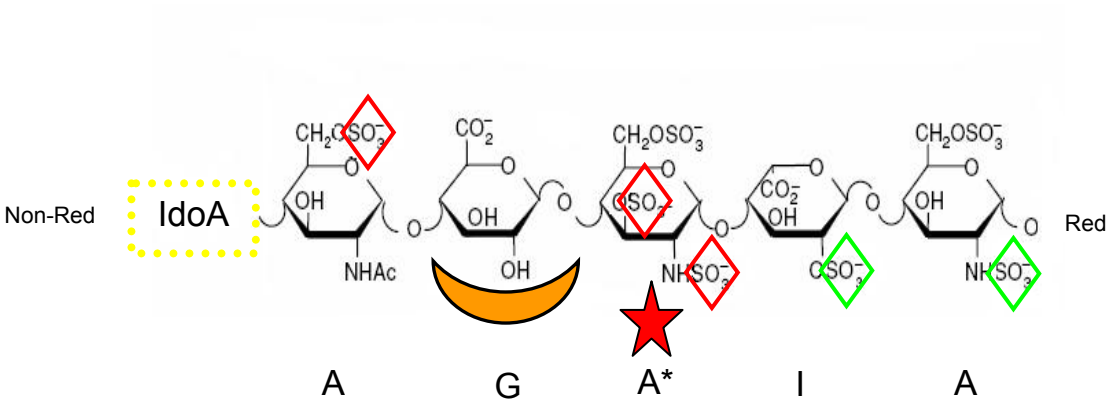

Fig 6 Pentasaccharidic antithrombin-binding sequence AGA*IA (where A is either GlcNAc6SO3 or GlcNSO36SO3; A*, GlcNSO33,6SO3; G, GlcA; I, IdoA2SO3). The red star marks the typical 3-O-sulfated glucosamine residue. The circled sulfate groups are either essential (red rhombus) or marginally essential (green rhombus) for high affinity. The ''half moon'' below GlcA indicates that this residue is also essential. The IdoA residue preceding the pentasaccharide (yellow) is not essential for AT binding, but invariably occurs in natural AT-binding domains of heparin and HS.

The information summarized in figure 6 has been obtained since the unexpected finding (made independently by three research groups) that only about one third of the chains constituting heparin currently used in therapy bind to AT and that most of the anticoagulant activity of heparin is attributable to species with high affinity (HA) for AT (26–28). The discovery that the rare 3-O-sulfated glucosamine residue is an essential component of the AT-bd (29) was followed by full elucidation of the structure of this active domain (30) and by chemical synthesis of heparin oligosaccharides, finally leading to a synthetic pentasaccharide exactly reproducing the structure of the natural one (7).

The location of the AT-bd along the heparin chain is still uncertain. Whereas an early study suggested that this domain was located prevalently towards the NR end of the molecule (32), another study suggested a more random distribution (33).

On the other hand, the observation that the NMR signals typical for the ''linkage region'' concentrated exclusively in the heparin fraction with no affinity for AT (34) is in favour of the first hypothesis. Several oligosaccharides obtained by controlled

depolymerization of heparin fractions with high affinity for AT contributed to defining structural features around the AT-bd (35–38). As illustrated in figure 2, the linkage region is another well-characterized sequence common to heparin and HS, as well to other GAGs (2,39). It consists of a trisaccharide β1,3-linked to the last GlcA residue of the glycosaminoglycan chain and is constituted by three neutral residues: one D-galactose (Gal) residue β-1,3 linked to a second Gal, which is β-1,4-linked to a D-xylose (Xyl) residue β-1,Olinked to Ser (39). The content of LR in heparins varies widely depending on the origin of heparin [i.e., it is lower than 1% in beef lung heparins and up to 5% in pig mucosal heparins (39,40)]. Depending on treatments for purification and bleaching during the manufacturing process, heparin may lose the terminal Ser of the LR and most of the LR as well. Though potentially implicated in antiangiogenic properties of heparin/HS (41), the sequence of the LR is commonly regarded as a biologically inactive component of heparin.

The AGA*IA pentasaccharide is not the only specific sequence present within the heparin chains responsible for the binding toward a protein, since most of the principal biological effects of the heparin are sequence mediated. In table 1 the principals minimal binding sequences of the heparin chains are summarized.

Tab 1 Principals binding sequences existing within the heparin chains and interaction who are mediated.

Interaction	Minimal binding sequence
Heparin – AT	$\mathbf{A_{NS,6S}}$ **-** **G** **-** $\mathbf{A_{NS,3,6S}}$ **-** $\mathbf{I_{2S}}$ **-** $\mathbf{A_{NS,6S}}$
Heparin -- Heparin cofactor II	$\mathbf{I_{2S}}$ **-** $\mathbf{A_{NS,6S}}$ **-** $\mathbf{I_{2S}}$ **-** $\mathbf{A_{NS,6S}}$ **-** $\mathbf{I_{2S}}$ **-** $\mathbf{A_{NS,6S}}$
Heparin -- Fibroblast growth factor 2	$\mathbf{A_{NS}}$ **-** $\mathbf{I_{2S}}$ **-** $\mathbf{A_{NS}}$ **-** $\mathbf{I_{2S}}$
Heparin -- Fibroblast growth factor 1	$\mathbf{A_{NS,6S}}$ **-** $\mathbf{I_{2S}}$ **-** $\mathbf{A_{NS,6S}}$ **-** $\mathbf{I_{2S}}$
Heparin -- Heparanase	$\mathbf{I_{2S}}$ **-** $\mathbf{A_{NS,6S}}$ **-** **G** **-** $\mathbf{A_{NS,6S}}$

1.1.5 Molecular conformation of heparin residues and sequences

The molecular conformation of GAGs, especially of those containing IdoA such as heparin, HS and dermatan sulfate, has long been a matter of controversy (42). Modelling of 3D structures of polysaccharides in solution involves the assumption of the conformation of individual residues and building up the polymer chains with these residues in a way that minimizes the overall conformational energy. Molecular models must then be experimentally validated, usually by NMR spectroscopy.

The assumption and experimental validation of the conformation of heparin components such as GlcN and GlcA is unproblematic. Whereas energy calculations and NMR parameters indicate a classic chair ($^4C_1$) conformation for both residues, apparently anomalous experimental data has long made the conformation of IdoA (and IdoA2SO_3) elusive (43).

The availability of a number of synthetic heparin oligosaccharides (7) has permitted extensive studies on the conformation of IdoA (and IdoA2SO_3) in different sequences, leading to the finding that IdoA pyranose rings may assume one of three equienergetic conformations (the chairs $^4C_1$ and $^1C_4$, and the skew-boat $^2S_0$). In fact, the shape of the IdoA residues flips from one to at least another of these conformations in rapid dynamic equilibrium (44). The relative population of two (or three) conformers depends on sulfation on the same residue (i.e., IdoASO_3 vs IdoA) and on adjacent GlcN residues (44, 45). Whereas IdoA2SO_3 residues in the NS domains of heparin are about 60% in the $^1C_4$ and 40% in the $^2S_0$ conformation, 3-O-sulfation of GlcNSO_3 as in the AT-binding domain reverses to 40:60 the population of these conformers (44,46). Such a proportion further varies in different heparin/HS oligosaccharides (45–49) as a function of sequence. Also, the $^1C_4$ form contributes to the conformational equilibrium of IdoA and IdoA2SO_3 residues in terminal positions (45). Conformer populations are also affected by extrinsic factors, such as the type of counter ions (45,47).

The capability of iduronate residues to assume more than one conformation confers on IdoA-containing chains a peculiar local flexibility (‘‘plasticity’’), with important bearing on binding and associated biological properties (50). This concept is illustrated in figure 7.

Molecular modeling studies on heparin sequences in the regular region generated helices, as shown in A and B for chain built-up with IdoA2SO_3 residues in the $^1C_4$ and $^2S_0$ conformations, respectively (51). Both A and B helices feature arrays of three sulfate groups (ANS, I2S, and A6S) on alternate sides of the chain, as expected from configurational considerations on the primary structure (Fig. 2). However, the orientation in space of different substituent groups (including the anionic ones SO_3^- and COO^-) is widely different in the two helices and involves different spacings between the sulfate groups within each cluster. By contrast, the conformation of N-acetyl heparosan, taken as representative conformation in the NA domains of heparin/HS (fig. 7C), is essentially invariant due to the stable $^4C_1$ conformation taken up by β-linked GlcA residues (43,52). Apart from affecting the relative conformer populations, sulfation gaps along the heparin chains do not involve substantial changes in the conformation of each type of helix (53).

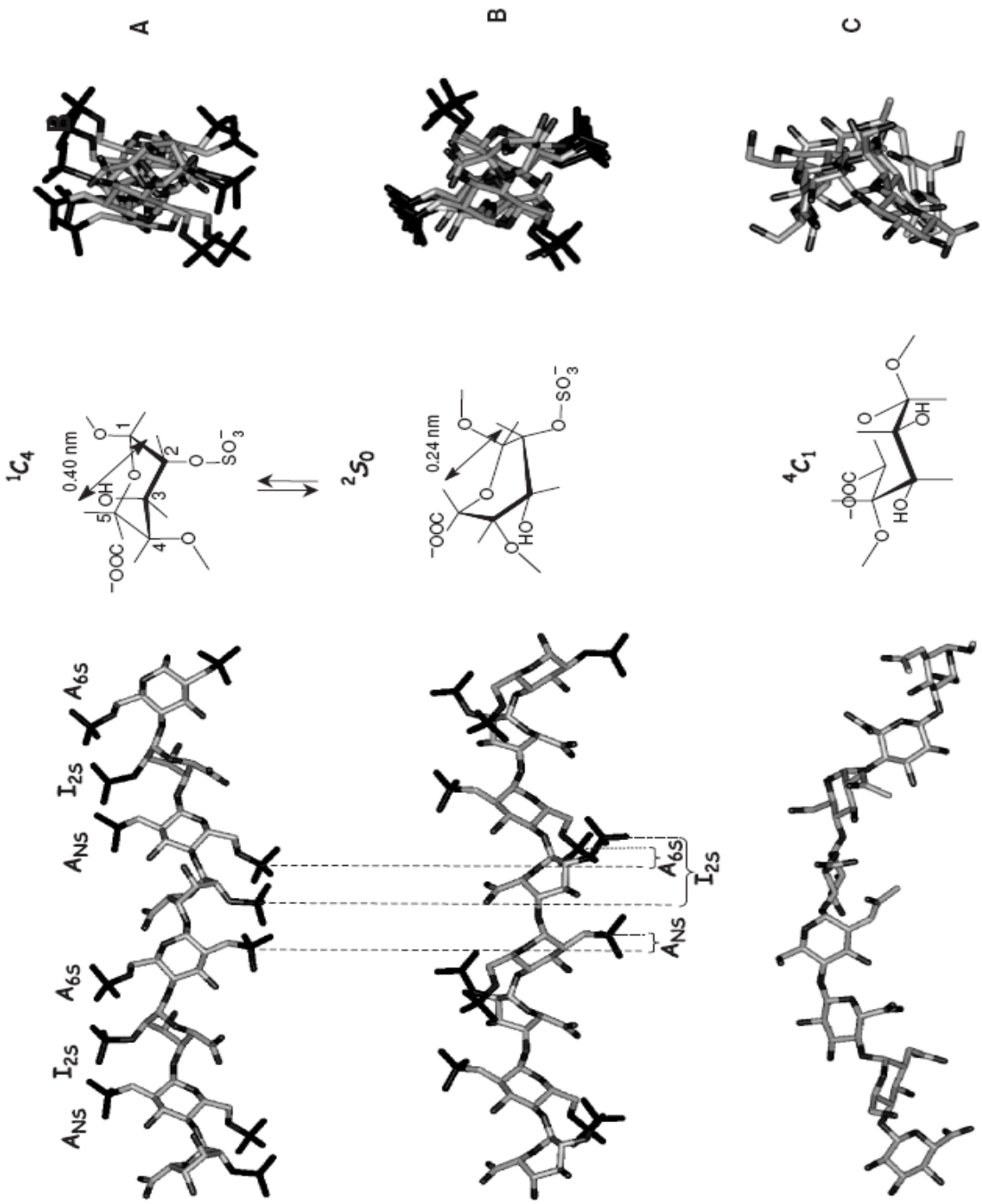

Fig 7 Molecular conformation of heparin NS chains (A, B) and NA chains (these latter represented by the biosynthetic precursor N-acetyl heparosan, C), illustrating the dramatic influence of changes (from $^1C_4$ to $^2S_0$) in the conformation of IdoA2SO3 residues of heparin on spacing of sulfate groups along and across the chains (52). The rigid ($^4C_1$) conformation of GlcA residues in N-acetyl heparosan does not involve significant changes from the chain conformation shown in C, even when some of the OH groups are sulfated (M. Guerrini and M. Hricovini, unpublished). Structures A and B are redrawn from Ref. 51. The figure also shows that the three conformations of uronic acid residues are characterized by different dihedral angles between vicinal C–H bonds and distances between nonbonded atoms (i.e., between H5 and H2), typically measurable by NMR spectroscopy (44).

1.1.6 Biosynthesis of heparin and HS

Heparin, heparan sulfafate (HS), dermatan sulfate (DS) and condroitin sulphate (CS) contain the common GAG-protein linkage tetrasaccharide, GlcAβ1-3Galβ1-3Galβ1-4Xylβ1-O-Ser. After the translation of the core protein, xylosilation of a Ser residue of the core protein is initiated by xylosyltranferase (XylT) in the endoplasimic reticulum (ER) and the *cis*-Golgi (54,55). XylT catalyzes the transfer of a Xyl residue through a β-linkage from UDP-Xyl to a Ser residue in the core protein substrates (fig 8), the amino acid sequences of which are conserved as Ser-Gly-X-Gly (where Gly and X stand for glycine and any amino acid, respectively) as revealed by comparison with the GAG attachment sites in the core proteins (56).

In Human and rats two different β-XylTs have been cloned (57), but the catalytic role of the second one has not been shown and its biological function remain unclear. Subsequently, two Gals are attached to the Xyl residue by galactosyltransferase-I and galactosyltransferase-II (GalT-I and GalT-II) (fig 8). GalT-I is one of the seven β1-4GalT family members, which appears to have exclusive specificity for the donor substrate UDP-Gal. On the other hand GalT-II wich transfers Gal from UDP-Gal to a β-linked Gal residue is one of the six β1-3GalT family members (58).

Finally the linkage region is completed by the transfers of a GlcA through a β1-3 linkage from UDP-GlcA to Galβ1-3Galβ1-4Xylβ1-O-Ser (fig 8), which is catalyzed by glucuronyltransferase-I (GlcAT-1) (59, 60).

Chain polymerization of the repeating disaccharide region in heparin and HS is evoked by the transfer of the αGlcNAc residue from UDP-GlcNAc to the linkage region tetrasaccharide, which is mediated by GlcNAcT-I (fig 8). On the other hand the addition of β1-4-linked GalNAc to the linkage region by β1-4N-acetylgalactosaminyltranferase-I (GalNAcT-I) initiates the formation of the repeating disaccharide in CS and DS.

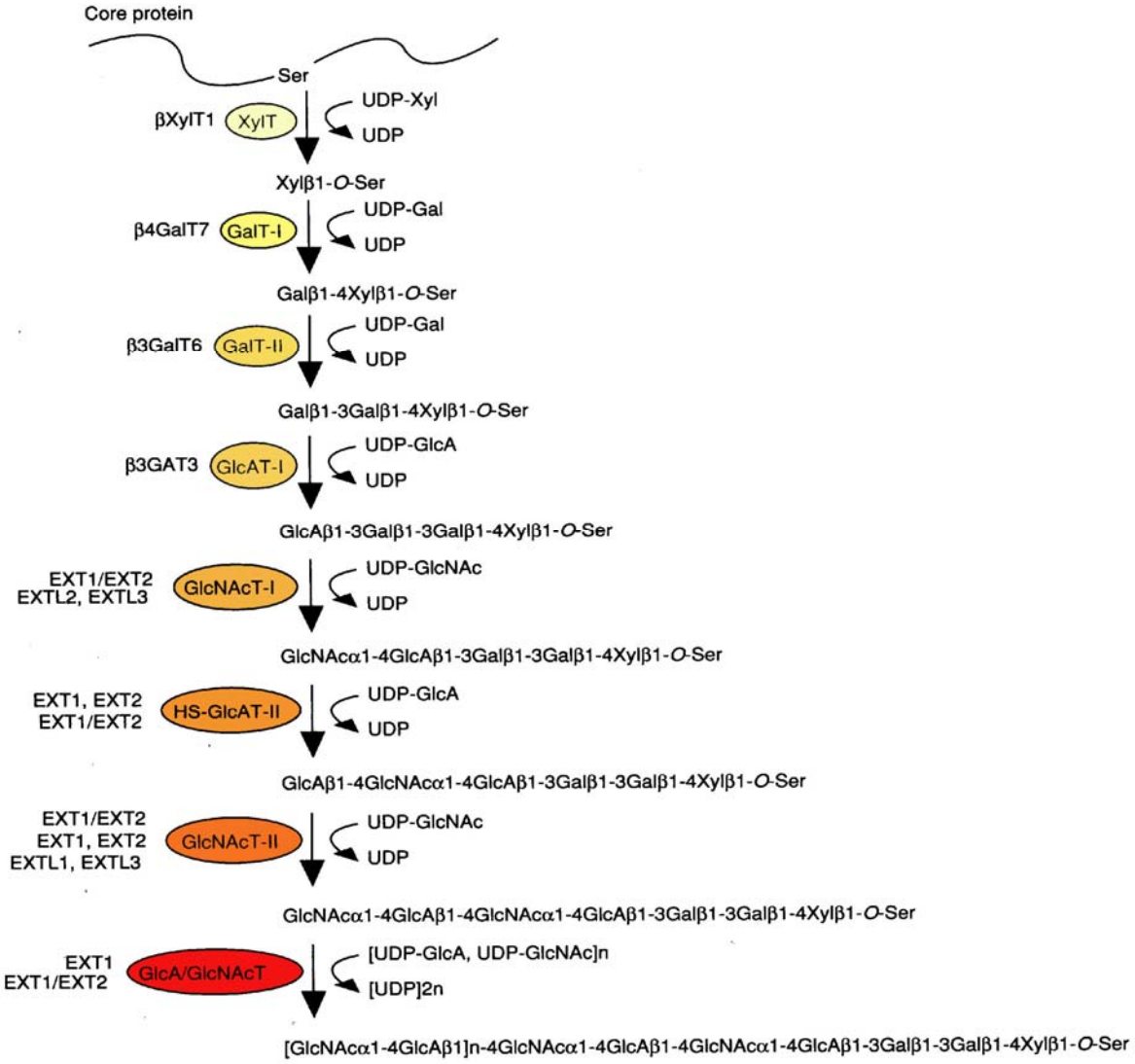

Fig 8 Scheme of the assembly of the heparin/HS backbones by various glycosyltranfereses. Each enzyme shown in an oval requires UDP-sugar as donor substrate, and then transfers a sugar residue to the nonreducing terminal sugar of an acceptor substrate. EXT1/EXT2 indicates a heterodimeric complex. XylT, xylosyltransferase; GalT-I, galactosyltransferase-I; GalT-II, galactosyltransferase-II; GlcAT-I, glucroonyltransferase-I; GlcNAcT-I, N-acetylglucosaminyltransferase-I; GlcNAcT-II, N-acetylglucosaminyltransferase-II; HS-GlcAT-II, HS-glucuronyltransferase-II; GlcA/GlcNacT, GlcA and GlcNAc transferase.

N-Deacetylation and N-sulfation of GlcNAc residues in heparin and HS are initial modifications of precursor chains and essential for all the subsequent modifications (fig 9). Both reactions are catalyzed by bifuncional enzymes, GlcNAc N-deacetylase/N-sulfotranseferase (NDSTs).

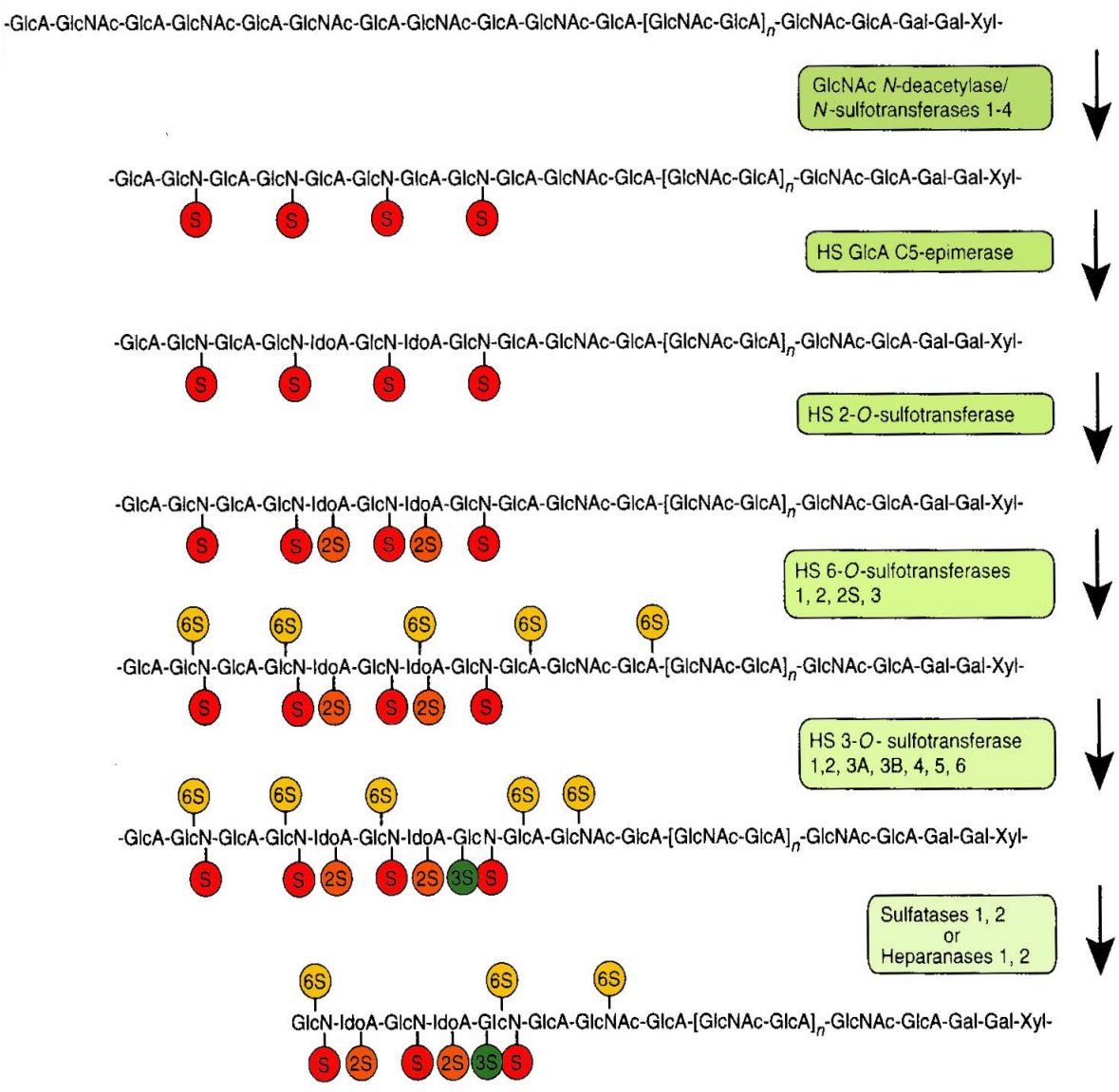

Fig 9 Pathways of biosynthetic modifications of heparin and HS chains. Following synthesis of the backbone of heparin or HS polymerases belonging to the EXT gene family, modifications of the precursos heparin/HS chains are conducted by various sulfotranserases and a single epimerase.

1.1.7 Nuclear Magnetic Resonance for Structural Analysis of Heparin and Heparan Sulfate

The presence of unnatural residues in LMWHs preparations, generated by certain depolymerization or chemical modification procedures, causes signal overlapping in monodimensional NMR spectra, preventing in many cases their use for quantitative analyses. By resolving signals hidden in the monodimensional spectra, $^{1}H–^{13}C$ correlation NMR spectroscopy (HSQC) permits identification of the constituent monosaccharides of LMWHs. However, HSQC experiments cannot be straightforwardly applied for quantitative analysis since the measured ‘‘volume’’ response of signals is also dependent on the one-bond proton–carbon coupling constant ($^{1}J_{C–H}$) values and relaxation effects. Luckily, for heparin and other GAGs with similar hydrogen/carbon atoms such as H2/ C2 in differently substituted GlcN residues, differences in both $^{1}J_{C–H}$ coupling and relaxation times are small, with consequently small effects on the volume of the corresponding signals..On the other hand, variations of $^{1}J_{C–H}$ between α anomers of L-IdoA and ß anomers of D-GlcA, which can induce significant changes on the corresponding signal volume intensities, should also be taken into account (193). Integration of HSQC signals has been recently used for quantitative analysis of urinary GAGs from patients with different mucopolysaccharidoses and the same method has been used to compare the relative amounts of GlcA in low-molecular-weight heparins obtained by depolymerization by γ-ray irradiation(194-195) .

However, none of these quantitative applications of 2DNMR have taken into account the influence of differences in the $^{1}J_{C–H}$ values of the integrated cross-peak signals. Recently, a quantitative method, of general applicability for obtaining $^{1}H–^{13}C$ correlation NMR spectra by suppression of $^{1}J_{C–H}$ dependence, has been reported. However, the pulse sequence used in that work reduces the sensitivity of HSQC spectra by about 25%, making it useless for detection of minor peaks using the

common NMR instruments with medium magnetic field intensities (400–500 MHz) (196).

On the base of these observations, it was demonstrated that standard HSQC experiments can be used for quantitative analysis of GAG samples by proper selection of magnetically comparable signals, where the impact of differences in $^{1}J_{C-H}$ coupling is minimized. The method was validated using two different pig mucosal heparin preparations and applied to profile the substitution patterns chemically modified K5-PS derivatives (186).

This NMR method was also applied to analyse LMWHs samples. Together with a detailed analysis of the structural peculiarities of LMWHs (tab 2), typical of each manufacturing process, variation in the heparin monosaccharidic composition among the analyzed samples was found (189).

Tab 2 Most important chemical shifts of terminal residues (reducing and non reducing) and signals of the LR (Linkage Region), obtained through HSQC spectra recorded at 35°C with Bruker Avance 600 spectrometer equipped with high sensitivity TCI probe (189).

	H1	C1	H2	C2	H3	C3	H4	C4	H5	C5	H6	C6
$A_{NS\text{-}red\alpha}$	5.47	93.9										
$A_{NS\text{-}red\beta}$	4.71	98.6	3.02	60.7								
$A_{NAc\text{-}red\alpha}$	5.23	93.5										
$M_{NS\text{-}red\alpha}$	5.41	95.6	3.63	60.3								
1,6-an.M	5.59	103.9	3.49	55.0					4.84	76.2	4.24 3.79*	67.5
1,6-an.A	5.63	104.3	3.22	58.6					4.84	76.2	4.22 3.82*	68.1
$I_{2S\text{-}red\alpha}$	5.44	95.6										
$I_{2S\text{-}red\beta}$	4.99	94.8										
Unknown	5.15	94.5										
ΔU_{2S}	5.53	100.1					6.01	108.7				
ΔU	5.18	103.9					5.83	110.4				
$AM.ol_{6S}$	3.67/ 3.59	65.4	4.01	86.0	4.14	78.2	4.15	88.0	4.29	82.4		
AM.ol	Nd	Nd	3.93	85.5	nd	nd	4.20	88.7	4.08	84.3		
(LR)Gal+G	4.65	106.5							4.69	74.5		
(LR)Gal	4.55	104.2										
(LR)Xyl	4.55	106.3							4.15 3.42*	66.0		

Tab 3 Most important chemical shifts of residues of LMWHs samples, obtained through HSQC spectra recorded at 35°C with Bruker Avance 600 spectrometer equipped with high sensitivity TCI probe.

	H1	C1	H2	C2	H3	C3	H4	C4	H5	C5	H6	C6
A*	5.52	98.9	3.46	59.4								
A_{6S}											4.50 e 4.20*	69.0
A_{6OH}											~ 3,80*	62.0
A_{NS} - G	5.58	100.4										
A_{NS} - I	5.35	98.3										
A_{NS}- I_{2S} + A_{Nac}-G	5.41	99.4										
A_{NS}			3.35	61.0								
A_{Nac}			3.97	57.0								
G_{2S}	4.75	102.8	4.17	97.582.4								
G - A_{NS}	4.61	104.6										
G-A_{Nac}	4.51	105.0										
G-A*	4.62	103.8										
I_{2S}	5.22	102.0							4.69	74.5		
I-A_{6S}	5.01	104.8										
I-A_{6OH}	4.94	104.6										
I_{2S}-1,6an	5.38	101.5										
G_{nr}					3.54	78.1	3.55	74.8				
Epoxide	5.42	98.9	3.82 3.74	53.4 54.3								

1.2 Low Molecular Weight Heparins

LMWHs are defined as salts of sulphated GAGs having an average Mw of less than 8000 Da and for which at least 60% of all molecules have a Mw of less than 8000 Da (61). As the minimum Mw for anti-IIa activity is about 5,000, the anti-IIa specific activity of LMWH is drastically reduced. The ratio of anti-Xa to anti-IIa activity is greater than 1 and, like the Mw distribution, is a defining characteristic of each separate LMWH product (see Table 2). LMWH may in principle be prepared by fractionation of UFH or by its depolymerization. None of the current LMWH products are prepared by fractionation, though early work on LMWH used fractions rather than depolymerised fragments (62). About 20-30% of LMWHs components are already present in the UFH. Almost all of these agents are produced by chemical or enzymatic depolymerization of porcine mucosal heparin, which specifically introduce structural changes in each of the LMWH products. Thus, depending on the patented depolymerization procedure, differents products are formed and each one has to be regarded as a distinct drug entity.

Early studies of the relationship between anticoagulant activity and Mw revealed a puzzling anomaly, in that the activity in the traditional activated partial thromboplastin time (APTT) assay decreased with decreasing Mw, but when measured by the newer anti-Xa assay the activity was maintained or even increased in the lower Mw fractions (63). Subsequent studies using purified antithrombin confirmed these trends, and it became clear that acceleration of inhibition of thrombin and FXa by heparin had different Mw requirements (64, 65). This difference was emphasized in studies by Holmer (66) and Barrowcliffe (67,68); high-affinity (for antithrombin) oligosaccharides with chain lengths mostly below 16 units, had very high anti-Xa activity, over 1,000 IU/mg, but their activity in thrombin inhibition and APTT assays was less than 10 IU/mg. While the anticoagulant effect are initially present at dosages that are antithrombotic, these agents have been found to produce sustained antithrombotic effects without any detectable *ex vivo* anticoagulant actions. These evidences,

particularly the possibility to induce a response non-trombin mediated with molecules with low Mw (safer, see next session, 1.3) were the starting point to the development of LMWHs as anticoagulant drugs. Whether various LMWHs can replace heparin for all its indications remains unclear at this time.

1.2.1 Therapeutic applications of LMWHs

The LMWHs are now globally regarded as drugs of choice for postsurgical prophylaxis of deep venous thrombosis (DVT) and the management of acute coronary syndromes. Recently, these agents have also been approved for the treatment of thrombotic disorders. Several products are currently available for clinical use worldwide. Because of manufacturing differences, each LMWH exhibits distinct pharmacologic and biomedical profiles (69). The specific activity of these agents in the anticoagulant assays ranges from 35 to 45 anti-IIa U/mg, whereas the specific activity in terms of anti-Xa units is designed as 80-120 antiXa U/mg. The LMWHs are capable of producing product-specific dose and time-dependent antithrombotic effects in animal models of thrombosis.

In experimental animal models and various clinical trials, these agents have been found to release tissue factor pathway inhibitor (TFPI) after both intravenous (IV) and subcutaneous (SC) administration (70). Repeated administration of LMWHs produces progressively stronger antithrombotic effects. However, the hemorrhagic responses vary and are largely dependent on products. The release of TFPI following IV and SC administration in humans has demonstrated the product individuality and relevance of this inhibitor to the actions of LMWHs (71). Antithrombotic and hemorrhagic studies are reported that compare the pharmacologic profile of some of the available LMWHs. Product individuality in terms of relative potency in different assays and the failure of standardization protocols to provide any guidelines for product substitutions and prediction of the clinical effects has remained a major consideration (72).

Initially, the clinical batches of LMWHs were prepared by ethanolic fractionation of heparin. Although the depolymerization process results in LMWHs products (Mw 4-8 kDa), these products exhibit differences in both their molecular, structural, and functional properties. Safety and efficacy comparison of these agents in well-designed clinical trials to demonstrate clinical differences in each of the individual products have only become available recently. Initial attempts to standardize LMWHs on the basis of their biologic actions, such as anti-Xa potency, have failed. A potency designation on the basis of the anti-Xa actions only represents one of the several properties of these agents. Furthermore, this assay only measures the AT affinity based actions of some of the components of these agents. Many of the pharmacologic actions of LMWHs are based on the non-AT affinity components of the drugs. These include the release of TFPI, t-PA, inhibition of adhesion molecule release, decrease in the circulating von Willebrand factor and modulation of blood flow. Most of these effects are not measurable by using conventional methods to assay heparin, such as the anti-Xa, anti-lla, and global anticoagulant tests. Despite the clinical effectiveness of the LMWHs in various indications, the mechanism of action of these agents is not completely understood.

It has been suggested that endogenous release of a Kunitz-type inhibitor, TFPI, may be a contributing factor to the mediation of the antithrombotic actions of these agents. It is interesting to note that most of the studies on LMWH have alluded to the relevance of the anti-Xa effect with the antithrombotic action of these agents.

However, after subcutaneous administration of these agents, circulating anti-Xa activity is not detectable in samples collected 12 h after the administration of prophylactic dosages. Despite this, the patients remain in an antithrombotic state.

Thus, additional mechanisms, such as the release of TFPI, may contribute to the overall action of these agents. LMWHs are also known to produce endothelial modulation and may release fibrinolytic activators, such as t-PA and antiplatelet substances, such as prostacyclin and nitric oxide. Endothelial dysfunction, platelet activation, white cell activation, and plasmatic process contribute to this process.

Since LMWHs are polycomponent drugs with multiple sites of action, these agents are capable of controlling of thrombogenesis at several target sites.

Unfortunately, most of the clinical trials have been designed to determine the clinical outcome with these drugs and very little is known of the pharmacologic mechanisms involved in the mediation of their action.

Pharmacologic differences and non-equivalence of these agents have been reported previously (69,70). Recent clinical trial results also show that each of these drugs produces its own product-specific therapeutic index. Thus, unlike unfractionated heparin, these drugs are not interchangeable on the potency-adjusted dosage.

Anticoagulant potency of unfractionated heparin is usually measured in terms of USP U/mg. This method, however, is not applicable to the LMWHs because of their relatively weaker and varied effect on the coagulation process. However, since LMWHs exhibit anticoagulant action at higher concentrations (>5.0 μg/mL), their anticoagulant actions can be compared in this assay. The anti-Xa activity of various LMWHs is now considered to be of limited importance in the potency evaluation and marketing of these agents. Similarly, the anti-Xa/IIa ratio is only of pharmaceutical value and may not have any clinical meaning. The relative anti-Xa anti-IIa ratio also changes after the administration of these agents and is dependent on several factors.

The first clinical trial on LMWH for the prophylaxis of post surgical DVT was published in 1986 (73). The initial clinical development of LMWHs remained restricted to the European continent for the first few years. Almost 10 years later, these drugs were introduced in the US. In the initial stages of the development of these drugs, only nadroparin, dalteparin, and enoxaparin were used. Subsequently, several other LMWHs, such as ardeparin, tinzaparin, reviparin, and parnaparin were introduced. Today, some eight LMWHs constitute a group of important medications with total sales reaching nearly 2.5 billion dollars with expanded indications reaching far beyond the initial indications for the prophylaxis of post- surgical DVT. Only two of the LMWHs identified have been approved for multiple indications.

In addition to the currently approved indications, these drugs are also used in several off-label indications, as depicted in figure 10. Moreover LMWHs are currently being evaluated for anticoagulant use in percutaneous interventions and surgical procedures.

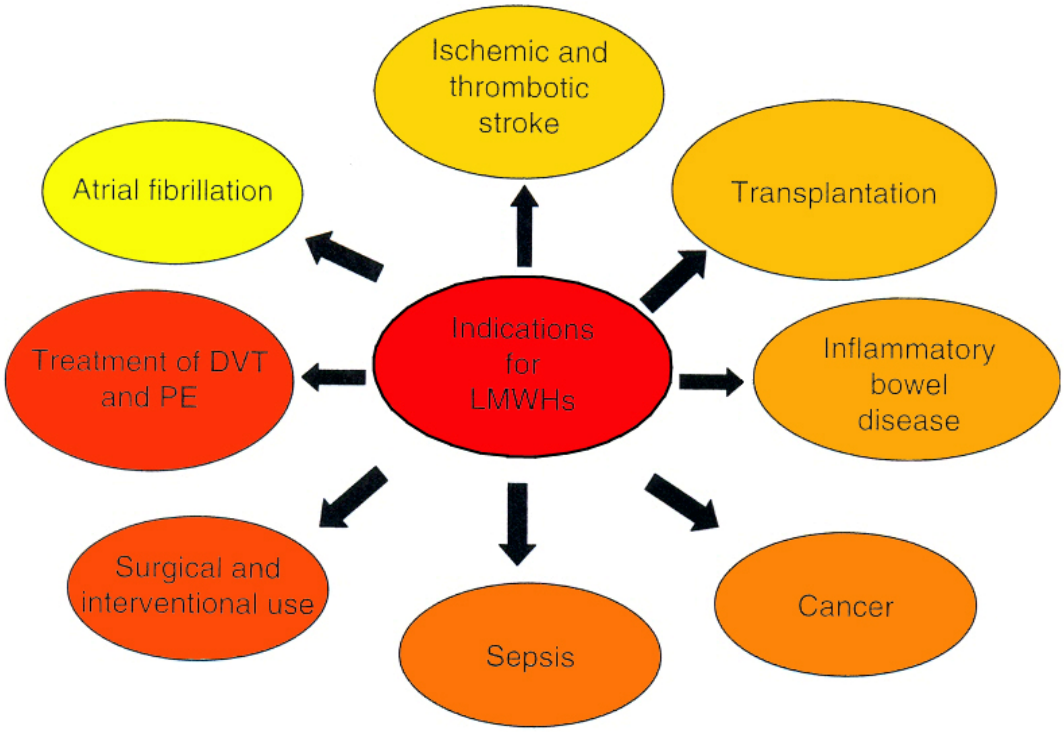

Fig 10 There is a wide range of indication for the potential use of LMWHs.

Clinical trials have clearly demonstrated the safety and efficacy of some of the LMWHs in the outpatient prophylaxis and treatment of thromboembolic diseases (74-76). In addition, these drugs have also been used for the management of acute coronary syndrome. Additional clinical evidence has also provided supportive evidence for the efficacy of these agents in such patient groups as thrombotic and

vascular stroke, peripheral arterial diseases, cancer, thrombotic process associated with pregnancy, old age, and inflammatory disorders (76-81).

While the clinical studies have only been performed on a select number of LMWHs, it is likely that different products at individually optimized dosages may prove to be effective. In this regard, product individuality and the available clinical trial data should be considered a priority to a recommendation being made for a given LMWH. This poses a challenge to the clinicians and requires a clear decision on the selection of a given product for single or multiple indications. Since the pharmacologic profile of each of these drugs is different and some of the comparative data have shown varying clinical performance, it is likely that the optimized dosage for these agents may be significantly different, requiring individual dosing recommendations. Thus, it is of crucial importance to consider each of these products as different drugs, and make each of these different agents available for specific indications.

Dose adjustments, optimization of drug combinations, and assurance of the safety of combined drugs are areas where clinical trials will be very helpful. Despite the expanded use of LMWHs in thrombotic and cardiovascular indications, several issues remain unresolved.

Although these agents are used in high dosages for anticoagulation purpose, at this time it is no available any antidote (82). In addition, there are no guidelines available for the management of bleeding with these agents with the exception of the use of protamine sulfate. The adjustment of dosage in weight compromised patients, such as in paediatrics and geriatric patients remains unclear. Furthermore, the guidelines for the monitoring of the effect of these agents especially in drug combinations are not available.

In the coming years, the role of LMWHs will be expanded in both thrombotic and nonthrombotic indications. A greater emphasis is currently placed on the non-anticoagulant properties of these agents. Some of the clinical effects of many of these products are not explainable in terms of anticoagulant effects. Newer formulations, drug combinations, extended use, and long-term effects of these drugs

will be important in the optimization of these drugs. Pharmacoeconomics will play a key role in the expanded usage of these drugs and the optimization in years to come. Identification of products for specific indications and knowledge of individual LMWHs will be extremely helpful in the proper usage of these agents.

1.2.2 Different depolymerization methods

LMWH is currently obtained from UFH by different chemical and enzymatic depolymerization processes, most of which introduce special structural modifications at the site of cleavage, generating novel end-chain residues (Fig. 12). Both heparinase digestion of unmodified heparin and β-eliminative cleavage by alkaline treatment of heparin benzyl esters introduce unsaturated uronic acid at the non reducing end (83-85), whereas deaminative cleavage (with nitrous acid or isoamyl nitrite) produces an anhydromannose residue at the reducing terminus (86). In the β-eliminative cleavage through an enzymatic method with heparinise I and II (fig 11) the cleavage takes place only at the 2-O-sulfoiduronic acid residue. In the β-eliminative cleavage by alkaline treatment the cleavage occurs specifically at iduronic acid without preference for the presence or absence of a 2-O-sulfo group. Heparin can also be oxidatively cleaved via hydrogen peroxide, which, by generating hydroxyl radicals, cleaves glycosidic bonds without modifying the end residues on both sides of the point of attack (87). As a consequence of strong acidic or basic treatments, other structural alterations, such as N- or O-desulfation, may sometimes occur along the heparin sequences (88,89).

In addition, also the AT binding site could be partially modified by some of the depolymerization reactions, with a consequent decrease of AT-mediated activity (90). In fact, while a mild nitrous acid treatment preserve the structural integrity pf AT-BR, strong reaction conditions can generate a fragment ending with a trisulfated anhydromannose residue (91). Also the enzymatic treatment with a heparinase I and II has been recently demonstrated to be able to cleave the AT binding site leaving the $A_{N,3,6S}$ as reducing terminal residue (92,93) (fig 11).

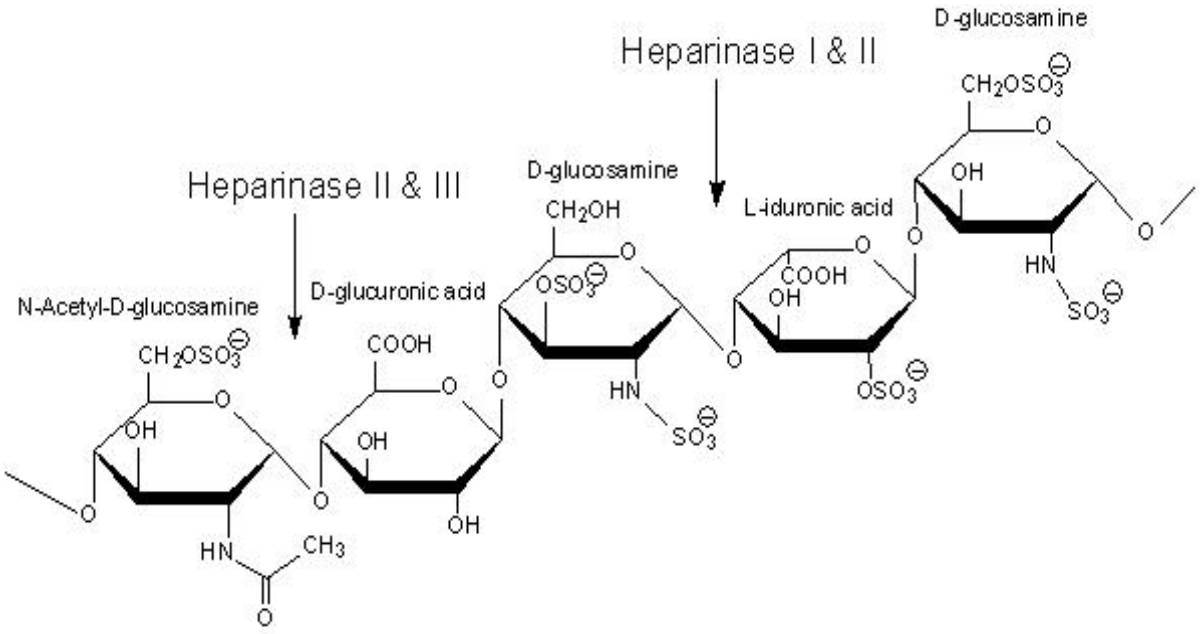

Fig 11 Site of cleavage of Heparinese I, II, III.

At present, no data are available on the possible specialty of action of both β-elimination and hydrogen peroxide. Moreover, none of the above degradative processes result in an accurate control of the degree of depolymerization of heparin chains.

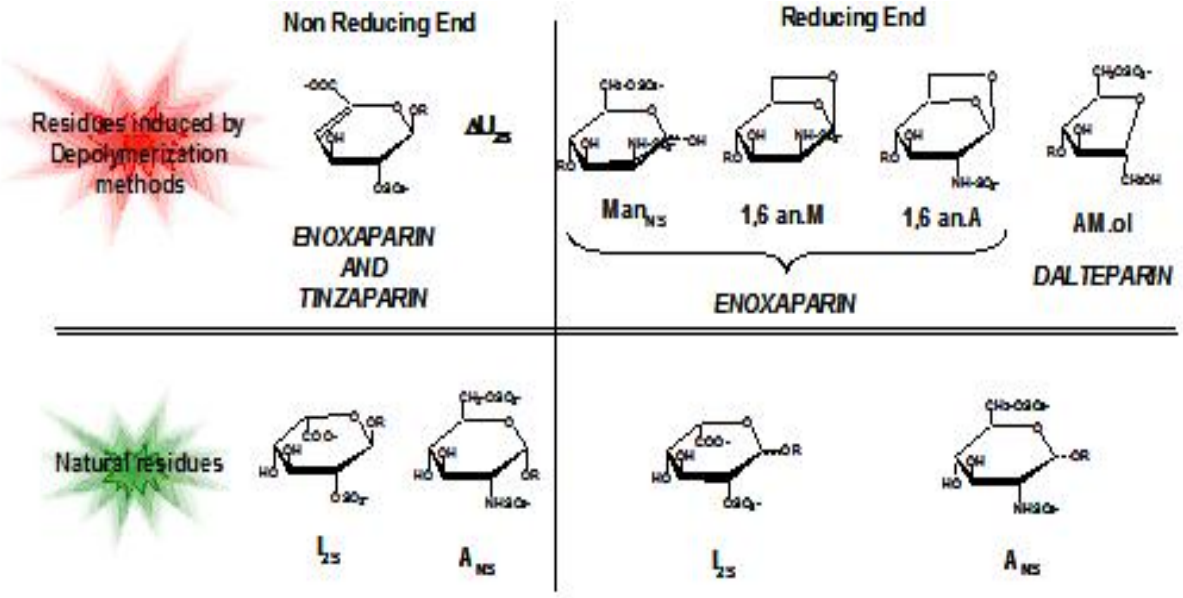

Fig 12 Typical residues of LMWHs compared to natural residues of the end terminus of heparin chains.

More recently, a physical method based on controlled gamma irradiation of heparin has been developed to produce a LMWH (94). A correlation between the amount of irradiation to which heparin is exposed and the reduction of the average size of fragments, as well as a good correlation between USP potency and extent of irradiation, were observed. In table 4 all the LMWHs actually available worldwide and the depolymerization methods used to obtain each product are reported (95).

Tab 4 Names and Properties of LMWHs Available Worldwide

Name	Manufacturer	Trade Names	Depolymerization Method	Average Molecular Weight (Daltons)	Anti Xa:IIa Ratio
Ardeparin sodium	Wyeth-Ayerst	Normiflo RD 11885 WY-90493-RD	Peroxidation treatment	5500-6500	1.8:1
Certoparin sodium	Novartis	Alphaparin Mono-Embolex NM Sandoparin Troparin	Amyl nitrate treatment	6000	2:1
Dalteparin sodium	Pharmacia	Fragmin Boxol FR 860 Kabi 2165 Low Liquemine Tedelparin	Nitrous acid treatment	5600-6400	2:1
Enoxaparin sodium	Aventis	Lovenox Clexane Decipar Enoxaparine Pharmuka 10169 PK-10169 Plaucina RP-54563 Thrombenox	Benzylation and alkaline treatment	5000	2.7:1
Nadroparin calcium	Sanofi-Winthrop	CY-216 Fraxiparin Fraxiparina Fraxiparine Seleparina	Nitrous acid treatment	4300	3.2:1
Parnaparin sodium	Aventis	Alpha LMWH Fluxum Minidalton	Cupric acid and hydrogen peroxide treatment	4500-5000	3:1
Reviparin sodium	Knoll	Clivarin LU 473111	Nitrous acid treatment	4150	3.5:1
Tinzaparin sodium	DuPont Pharma	Innohep Logiparin Novo LHN 1	Enzymatic degradation	8000	1.9:1

1.2.3 Synthetic Heparin Polysaccharides

The generation of the synthetic heparin pentasaccharide reproducing the At-bd (fig 13) has addressed an important issue in the pharmacology of heparin: it greatly helped to understand the contribution of the inhibition of factor Xa in the mediation of the antithrombotic effect of LMWHs and heparin oligosaccharides. The first studies using heparin derived oligosaccharides failed to demonstrate a functional relevance of the inhibition of factor Xa to an antithrombotic effect in experimental animal models. It was suggested that inactivation of thrombin was required for inhibition of thrombosis and that agents with predominantly anti-factor Xa activity were weakly effective antithrombotic agents. Those studies were inconclusive, however, since the agents used were heterogeneous in structure and relatively low potency. It remained questionable whether a highly active anti-factor Xa agent could be antithrombotic *in vivo*.

Pentasaccharide is a synthetic heparin-related agent representing the minimum saccharidic sequence of critical structure required for the high affinity binding of heparin to the AT molecule and eliciting solely a high inhibitory action against factor Xa (opposed to the multiple antithrombotic mechanism of heparin). Since pentasaccharide is synthetic, it is known to be homogeneous in molecular size and structure, thus representing an optimal tool for studies related to antithrombotic agents expressing sole anti-factor Xa activity. Pentasaccharide proved that sole factor Xa inhibition elicits an antithrombotic affect by decreasing the generation of thrombin, resulting in a controlled and selective modulation of coagulation.

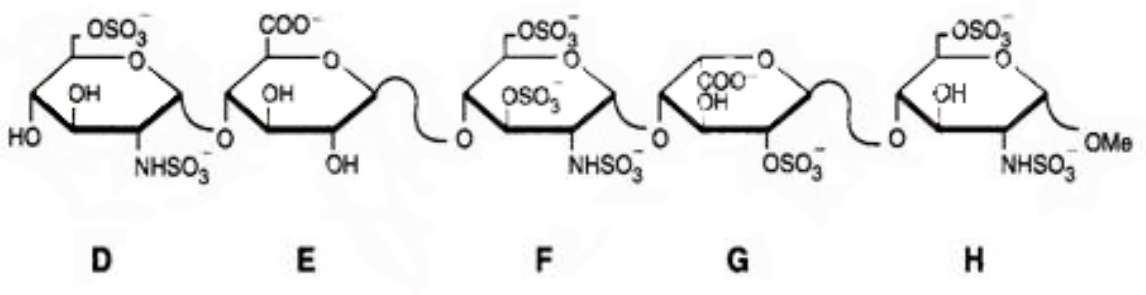

Fig 13 Fondaparinux (Arixtra®; GlaxoSmithKline) has been approved for prophylaxis and treatment of DVT and PE in certain clinical interactions. It continues to undergo clinical development.

The ^{13}C-NMR spectroscopy of the synthesized product revealed the anticipated spectral characteristics consistent with a pentasaccharide structure containing the desired sulphate, carboxyl and amino groups (96). Antithrombin affinity analysis demonstrated a high affinity (3 x 10^{-8} M) (97). Anti-protease activities of 2800 anti-factor Xa U/mg in human plasma by a clotting method and 4000 anti-factor Xa U/mg in human plasma by an amidolytic method were demonstrated (98). Pharmacologic studies confirmed that this pentasaccharide was biologically active *in vivo* (99).

Due to the hypothesized critical nature of the 3-O-sulfate group (A*) of this pentasaccharide for eliciting high affinity to AT, anti-factor Xa activity and thus antithrombotic effect, a structurally modified pentasaccharide devoid of the A* group was synthesized (fig 14) (100,101).

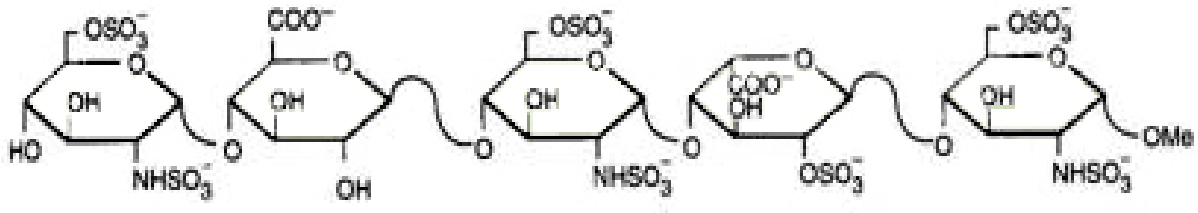

Fig 14 Structure of 3-O-desulfated pentasaccharide. Removal of A* group (replaced by a hydroxyl group) abolishes binding of the pentasaccharide to AT.

Biochemical studies did not show the extra signal in the ^{13}C-NMR spectrum that was previously speculated to result from A* residue. This material did not possess high affinity for AT (5 x 10^{-4} M) (102), nor did posses detectable anti-factor Xa activity

(102). Moreover both tetrasaccharides contained within the pentasaccharide (units AGA*I- and -GA*IA) exhibited decreased affinity to AT and decreased anti-factor Xa activity (99,102), thus demonstrating that not only A* residue was critical for the desired properties of this pentasaccharide.

Tab 5 Comparison of the properties of Fondaparinux, LMWH and Heparin

	Fondaparinux	**LMWH**	**Heparin**
Molecular weight	1.728 Da	~5000 Da	~15000 Da
Source	Chemically synthesized	Porcine mucosa, bovine lung	Porcine mucosa, bovine lung
Dispersity	Homogeneous	4000 – 9000 Da	3000 – 30000 Da
Protease specificity	Xa inhibition	Xa and some IIa inhibition	Inhibit most coagulation protease
AT-mediated activity	Xa inhibition	Xa>IIa inhibition	Inhibit most coagulation protease
HC-II mediated activity	Only at high concentration	Weak inhibition of thrombin	Moderate inhibition of thrombin
TFP release	None	Strong	Strong
HIT response	Not known	Cross-react when heparin is positive	Positive
Bioavailability	~100 %	≥80%	≤30%
Half-life	Long when bound to AT	Longer than heparin	Relatively short

Recently Idraparinux an O-sulfated O-methylated pentasaccharide derivative of fondaparinux was synthesized (fig 15) (103). Due to the increased sulfation, this agent exhibits a 30-fold higher binding affinity to AT than fondaparinux, and a higher anti-factor Xa potency. Idraparinux exhibits a significantly longer elimination half-life of about 120 h, which allows for once-weekly dosing (104). It has 100% subcutaneous bioavailability (104).

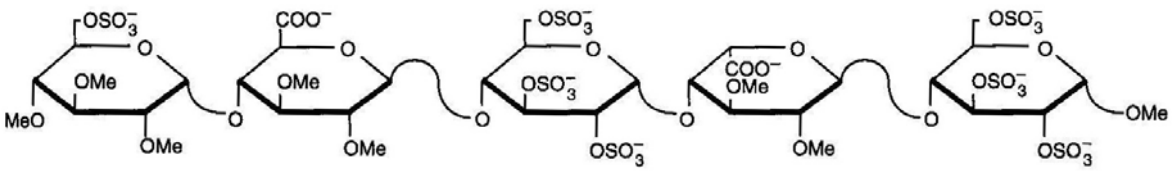

Fig 15 Chemical structure of idraparinux. This 2-O-Sulfated, O-metylated pentasaccharide exhibits higher affinity to AT compared to the native pentasaccharide, a higher anti-factor Xa potency and a longer elimination half-life. Idraparinux (Sanofi-Aventis).

1.3 Heparin vs low molecular weight heparins

In contrast to unfractionated heparin (UFH), low molecular weight heparins (LMWHs) have a lower binding affinity toward plasma proteins, endothelial cells (ECs), and macrophages. Since difference in binding profile explains the pharmacokinetic differences observed between LMWHs and UFH. The binding of UFH to plasma proteins reduces its anticoagulant activity, which combined with the variations in plasma concentrations of heparin-bindings proteins, explains its unpredictable anticoagulant response.

LMWHs exhibit improved subcutaneous bioavailability; lower protein binding; longer half-life; variable number of ATIII binding sites; variable glycosaminoglycan contents; variable anti-serine protease activities (anti-Xa, anti IIa, anti-Xa/anti-IIa ratio, and other anti-coagulation factors); variable potency in releasing tissue factor pathway inhibitor (TFPI); and variable levels of vascular EC binding kinetics (105-108). For these reasons (Tab. 6), over the last decade LMWHs have increasingly replaced UFH in the prevention and treatment of venous thromboembolic disorders (VTE). Randomized clinical trials have demonstrated that individual LMWHs used at optimized dosages are at least as effective as and probably safer than UFH. The convenient once or twice daily subcutaneous (SC) dosing regimen without the need for monitoring has encouraged the wide use of LMWHs.

It is well established that different LMWHs vary in their physical and chemical properties due to the differences in their methods of manufacturing. These differences translate into differences in their pharmacodynamic and pharmacokinetic characteristics (106). The world health organization (WHO) and USA FDA regard LMWHs as individual drugs that cannot be used interchangeably (106).

Bioavailability of LMWHs after intravenous (IV) or SC administration is greater than for UFH and was determined to be between ≈87% and ≈98%. UFH, by contrast, has a bioavailability of 15-25% after SC administration. LMWHs have biological halflife ($t_{½}$) (based on anti-Xa clearance) nearly double that of UFH. The $t_{½}$ of the most

commercial clinically used LMWHs (enoxaparin, dalteparin, tinzaparin and others) has been documented to be between ≈100 and 360 min, depending on whether the administration of LMWH was IV or SC. The anti-Xa activity persists longer than antithrombin activity, which reflects the faster clearance of longer heparin chains (109). LMWH, in doses based on patient weight, needs no monitoring, possibly because of the higher bioavailability, longer plasma $t_{½}$ and more predictable anticoagulant response of LMWHs compared with UFH, when administered SC.

Though LMWHs are more expensive than UFH, a pilot study in pediatric patients found SC LMWH administration to reduce the number of necessary laboratory assays, nursing hours and phlebotomy time (110).

LMWHs are expected to continue to erode UFH use, through development programs for new indications and increased clinician comfort with use of the drugs.

Tab 6 Heparin vs LowMolecularWeightHeparins

UFH (unfractionated heparin)	**LMWHs (Low Molecular Weight Heparins)**
Continuous, IV infusion	twice daily or daily subcutaneous injections
Primarily administrated in hospital	Administrated everywhere
Administrated by health care professionals	Administrated by professionals or patients
Unpredictable anticoagulant response	Predictable anticoagulant response
Monitoring and dose adjustments	No monitoring, fixed or weight based dosing
Frequent dosing errors	More precise dosing
Risk of thrombocytopenia and osteoporosis	Decreased risk of adverse events
Cheap, but not cost-effective	Demonstrated pharmacoeconomic benefits
Requires 5-7 days in the hospital	Requires 0-2 days in the hospital

1.4 Antithrombin

1.4.1 Serpin structure

Serpins were identified as a protein family by Hunt and Dayhoff in 1980 based on the sequence similarities of AT, α_1-antitrypsin and ovalbumin (117). To date, over 1500 serpins have been implicated in the genomes of organisms representing all branches of life, and have been implicated in diverse physiological processes (111,118). Although most serpins are inhibitors of serine proteases, as the acronym suggest (serine protease inhibitors), many are incapable of protease inhibition and others posses additional functions (cell signalling, hormone carriers) (116). The highly conserved serpin-fold consist of three β-sheets (A,B and C) and nine α-helices (A-I), organised into an upper β-barrel domain and a lower α-helical domain, which are bridged by five stranded β-sheet. In the classic serpin orientation, β-sheet A is facing, and the Reactive Centre Loop (RCL), the region that interacts with the protease, is on top (fig 16).

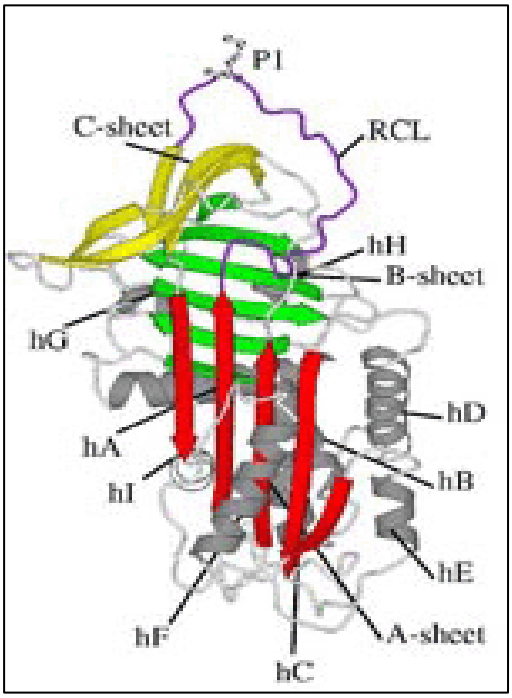

Fig 16 The serpin architecture.

Unlike all other families of serine protease inhibitors, the RCL of serpins is long and flexible and serves as bait by presenting a favourable protease cleavage site. The serpins fold is also unusual in its thermodynamic properties, as the native state is not the most stable. Under certain conditions, serpins undergo a change in topology to a hyper stable state, with the insertion of RCL as the fourth strand as the now six-stranded β-sheet A. This transition is triggered by proteolytic nicking of the RCL to generate the cleaved form, or in the absence of cleavage to generate the so-called “latent” form (10).

1.4.2 The suicide substrate mechanism

Serpins utilise a suicide substrate mechanism for the inhibition of serine proteases (112), which is best described by the kinetic model of protease substrate hydrolysis (fig 17). Unlike the typical reversible lock-and-key type inhibitors (e.g.,Kunitz family inhibitors such as BPTI), the serpin is consumed during inhibition (hence suicide-substrate). However, serpins have evolved to be very poor substrates of serine proteases, with the very last step in the proteolytic cycle, deacylation (K_{hyd}), slowed several orders of magnitude. How deacylation is slowed has been revealed by the recent structure of the final serpin-protease complex (128). As shown in figure 17, rapid recognition of the serpin RCL by the protease (formation of the michaelis complex) is followed by the formation of the acyl-enzyme intermediate and separation of the C-terminal peptide of the serpin RCL from the active site of the protease (126). At the acyl-enzyme intermediate step, where the seprin and protease are covalently linked via an ester bond between the reactive centre p1 residue and the active site Ser of the protease, the seprin rapidly inserts the RCL into β-sheet A. The protease is thus flung 70 Å from the top of the seprin to the bottom and the new hyperstable serpin crushes the protease by exerting a pulling force on the active site loop.

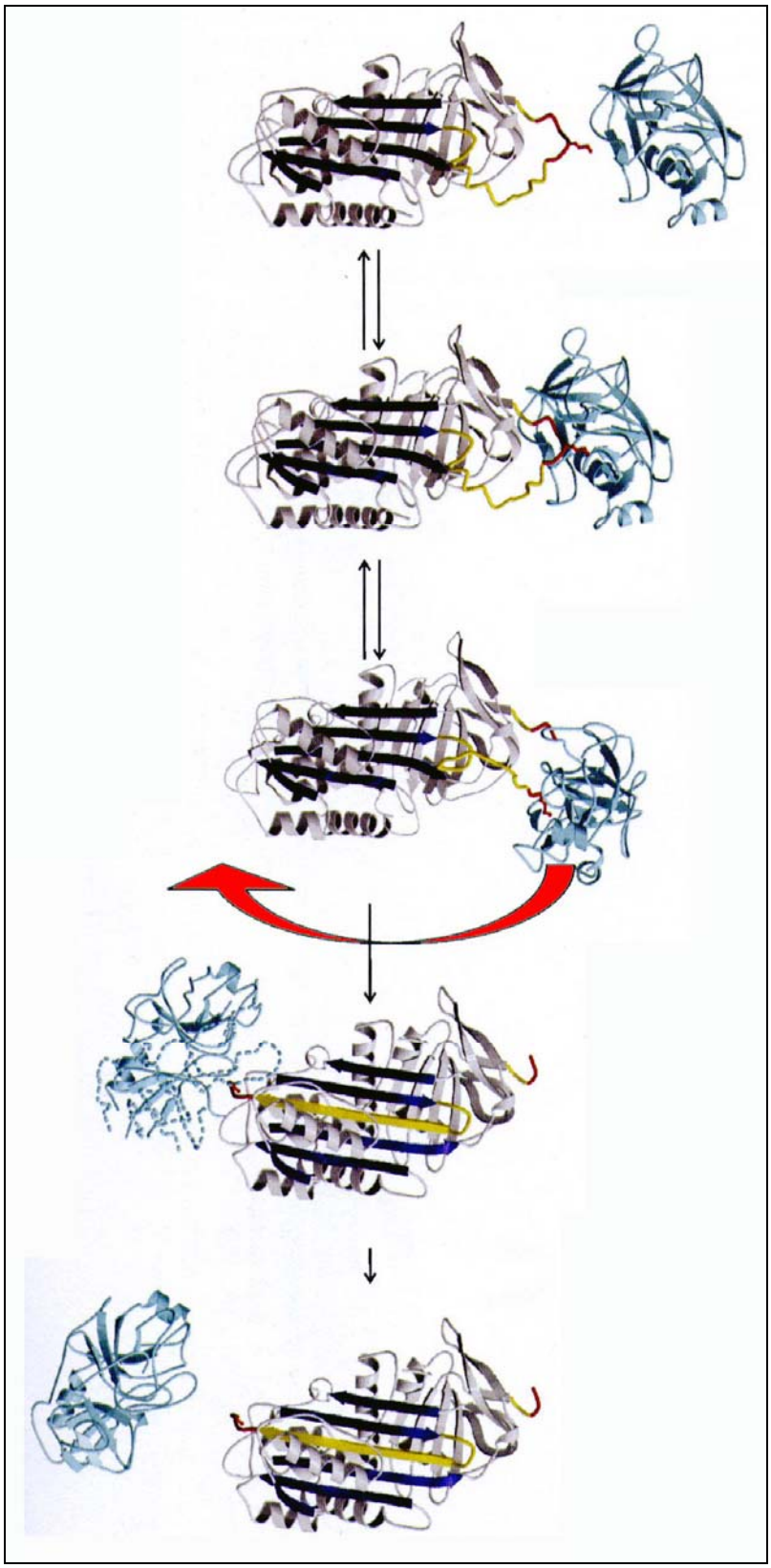

Fig 17 The suicide substrate mechanism of serpins.

The effect of the pulling force is a stretching out of the catalytic loop of the protease, which contains the active site serine and the residues which form the oxyanion hole, thus rendering the protease catalytically inert. Clashes between the hyper stable serpins and the protease also lead the unfold of roughly 40% of the protease structure, as evidenced by the lack of density in the crystal structure (128), the acquisition of profound proteolytic susceptibility (129,130) and the change of NMR resonance (131).

1.4.3 Physiological functions

Antithrombin (AT) is the most important serpin in hemostasis (147). It is a plasma which circulates at 2,3 μM and is capable of inhibiting all of the serine proteases that promote blood coagulation, but based on rates of inhibition, its primary targets are factors IXa, Xa and thrombin (fig 18). The importance of AT is demonstrated by the high association of deficiency with venous thrombosis (148), by the embryonic lethal consumptive coagulopathy in the knockout mouse (149), and by the continued success of therapeutic heparin. The anticoagulant effect of natural heparin and the new synthetic heparins, is mediated primarily through the activation of AT as an inhibitor of the coagulation proteases (150,151). Of course, heparin, which is produced and secreted exclusively by mast cells, is not a physiological activator of AT; instead it is the closely related cousin heparan sulfate which lines the vascular wall, and which, ensures the fluidity of the microvasculature through interaction with a fraction of the circulating AT (152). Heparin differs from heparan sulfate only in degree of sulfation and in the fraction of the highly flexible iduronic acid; both factors are key in determining affinity for AT. Heparan sulfate is highly heterogeneous and contains patches of high sulfation and iduronic acid levels, providing the sites of interaction with AT (153). While some 30% of heparin chains bind AT with high affinity, only a small fraction of hepapan sulfate chains possess the high affinity site (152). The early identification of AT as the effector of heparin anticoagulant activity has spurred intense research effort aimed at understanding how it binds to and is

activated by heparin. The AT-heparin interaction now serves as a paradigm for the heparin binding serpins as a whole.

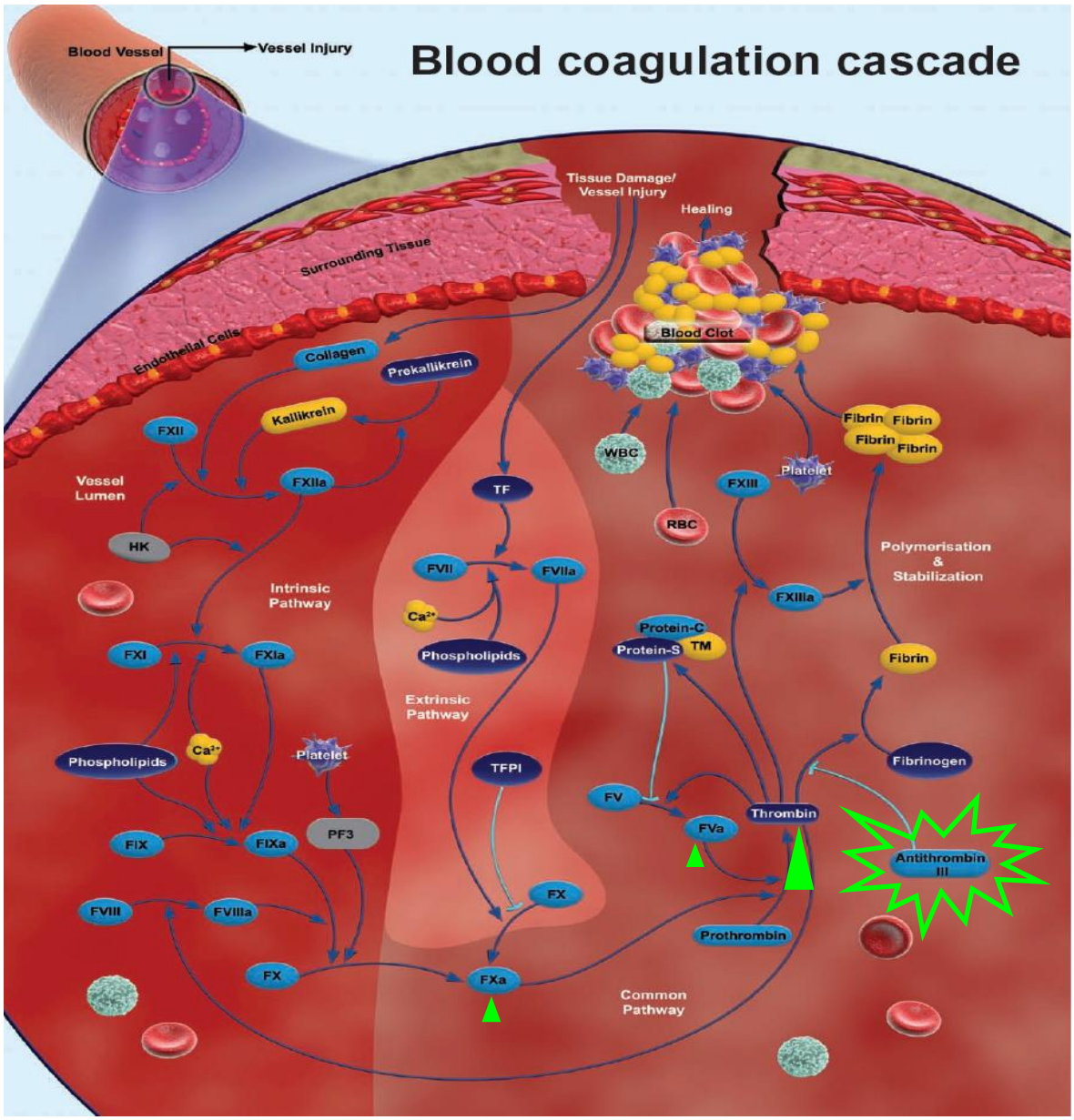

Figure 18 Blood coagulation cascade. Antithrombin (green star) is the most important serpins and its activity is focused on the final step of the coagulation cascade: inhibition of thrombin (green triangle) ad also factors Xa and Va (small green triangles).

1.4.4 Mechanism of Heparin binding

The interaction with the pentasaccharide is exquisitely specific and small alterations in either the sulfation pattern of the AGA*IA or in the sequence of the heparin binding region of AT can significantly reduce binding affinity (156). The region of AT which bind to heparin was initially identified from a heparin binding deficient variant of AT found in a patient who had experienced a thrombotic event (157). Subsequent alignment of the sequence of AT on the template of the first serpin structure by huber and Carrell (146) revealed the heparin binding site and it has since been confirmed by mutagenesis (158) and crystallographic (159-161) studies. A diagram detailing the individual interactions between the pentasaccharide and AT is given in figure 19. The heparin binding residues of AT have been mutated to determine their individual contributions to the free energy of pentasaccharide binding; by far the most important residue is Lys114 (162,163), found on the loop just N-terminal to helix D, which is induced into a helical conformation through interaction with the pentasaccharide and two other residues, Lys125 and Arg129, also contribute significantly to the energy of binding (164,165). It is interesting to note that the sum of energetic contributions of the three residues, Lys114, Lys125 and Arg 129, is greater than the total free energy of binding, implying cooperativity. AT also has an N-terminal loop containing Lys11 and Arg13, which contacts the pentasaccharide and may serve a capping role (166), but also Arg 46,47 and Asn 45 are involved in the interaction with the pentasaccharide (fig 19, dotted lines). Of eight-to-ten negatively charged groups on the pentasaccharide available for interaction with AT, six interact with AT; this is consistent with the number of ionic interactions inferred from the dependence of binding affinity on ionic strength (five-to-six) (167).

It had been established through biochemical studies that heparin binding induces a large-scale conformational change in AT (168-170) and this has subsequently been confirmed by crystallographic structures of native and pentasaccharide bound AT.

AT binds the pentasaccharide by an induced-fit mechanism involving an initial weak interaction (K_1= ~ 25 μM), followed by a conformational change (k_2) to the high-affinity state, with an overall dissociation constant of ~50nM (170). The structures of AT reveal conformational changes in the vicinity of the pentasaccharide and in other regions, indicating a global conformational change in response to heparin binding. In the heparin binding region, helix D is extend toward its C-terminus, a new helix P extends from its N-terminus and helix A appear to extend towards its N-terminus. The global conformational change involves the expulsion of the RCL from β-sheet A and the consequent closing of β-sheet A to the five-stranded form seen for other native serpin structures. The tertiary structure of AT is also altered by heparin binding , with a 10° rotation of helix D and the repositioning of the upper β-barrel domain relative to the lower helical domain (173).

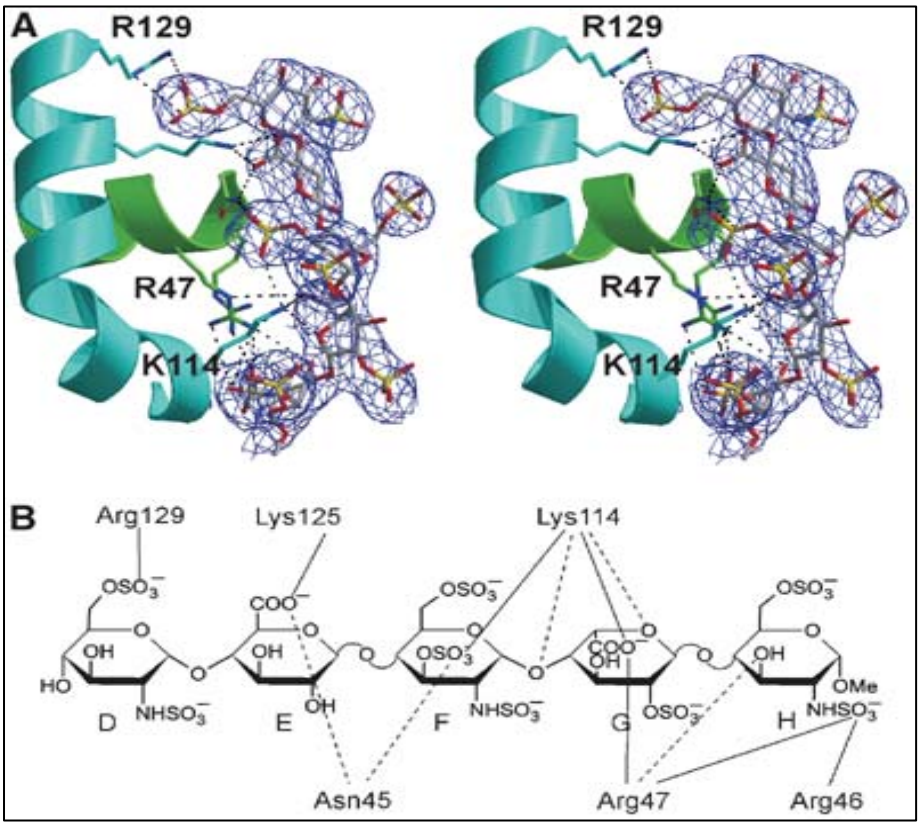

Fig 19 Mechanism of heparin binding, pentasaccharidic sequence involved in the Antithrombin binding.

Just how local changes in the heparin binding region result in the expulsion of the RCL and the closure of sheet A is unclear. Molecular modelling (174) and biochemical studies (175,176) suggest a link between the C-terminal elongation of helix D and loop expulsion and this has been supported by the recent crystal structure of AT in an intermediate pentasaccharide-bound conformation (161). Cleavage of RCL of AT reverse the induced fit, causing a 1000-fold loss in affinity for the pentasaccharide (177,178). It is expected that such a mechanism would allow AT-protease complexes to be released from heparin sulfate for receptor-based clearance.

1.4.5 Acceleration of protease inhibition

Heparin acceleration of protease inhibition by AT involves two distinct mechanisms, depending on the targets involved (179). Pentasaccharide binding to AT is sufficient to accelerate the inhibition of Factors IXa and Xa by 300-500-fold and as the pentasaccharide binds only AT and induces a conformational change, this mechanism of activation is considered allosteric. In contrast, activation of thrombin inhibition requires both AT and thrombin to bind the same heparin chain (at least 18 monosaccharide units in length) (180), with the heparin serving a bridging function. A scheme of the allosteric and bridging mechanism is given in figure 20.

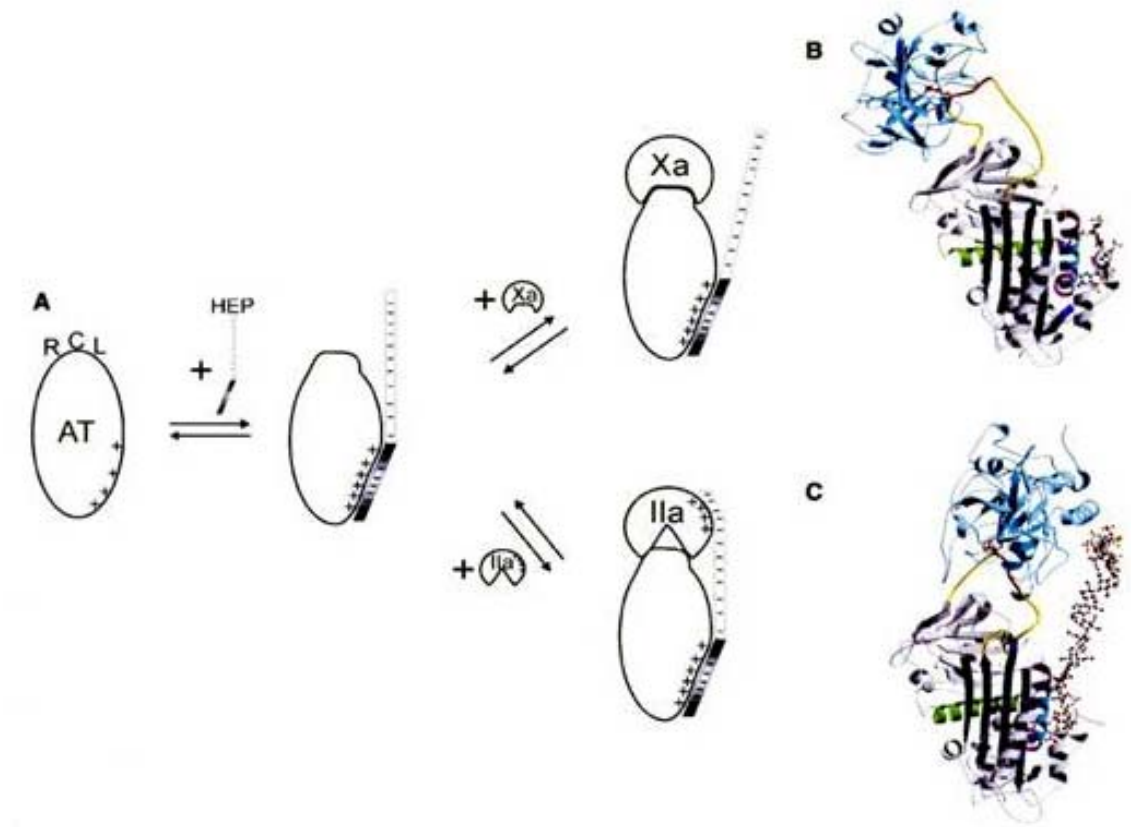

Fig 20 Inhibition mechanism heparin induced At-mediated (A), toward factor Xa (B) and factor IIa (C).

Although it is convenient to consider the two mechanisms as distinct, recent studies have demonstrated that in the presence of physiological levels of Ca^{2+} factor Xa (and IXa) inhibition is further accelerated through the addition of a bridging component to the allosteric mechanism (132,133). The molecular basis of improved protease recognition by AT in the presence of heparin is currently under investigation and it has become clear that exosite contacts, outside to the RCL of AT, are critical (182,183). Two crystal structures of AT in complex with inert thrombin and a synthetic heparin mimetic (SR123781) have recently been published (160,184).

In the higher resolution structure by Li et al., electron density was observed for the entire heparin chain and revealed the expected thrombin-heparin interactions; it is thus considered more likely to represent the bridged complex (fig 20 C).The position of the thrombin relative to AT in the structure explains why the rate of thrombin inhibition is insensitive to the expulsion of the hinge region, as partial insertion of the hinge is observed. In contrast, heparin acceleration of factor IXa and Xa inhibition is

completely dependent on the expulsion of the hinge region from β-sheet A (181), probably due to the requirement of exosite contacts towards the back of AT (185) (fig 20 B).

2.0 Aim of the Work

In the last decade the diffusion of LMWHs is rising up and for the future these drugs are destined to replace totally the unfractionated heparin in all clinical fields in which they are actually utilised. The advantages of the LMWHs are described above (1.2) but for now the knowledge of these heterogeneous compounds do not allow to directly correlate their structure and composition with clinical effects. In fact ideally, LMWHs should differ from their parent heparins only for their average molecular weights, which are approximately one third than those of the original polysaccharides, but actually, according to the methods used for manufacturing LMWHs, they can differ from parent heparin even in terms of monosaccharide composition and oligosaccharide sequence.

With the aim of deepening the knowledge of structural features correlating with biological activities of LMWHs, the present work focused on the detailed investigation of the oligosaccharide composition of the three most popular commercial LMWH preparations, enoxaparin, tinzaparin and dalteparin.

Those LMWHs, currently approved for the use in the United States, are produced by three different means of depolymerisation, each resulting in unique structural alterations at either the reducing and/or non-reducing end of the cleaved heparin chains (189). Dalteparin, is produced through deaminative cleavage with nitrous acid, resulting in formation of an anhydromannitol ring at the reducing end. Tinzaparin, is the result of enzymatic β-eliminative cleavage of unmodified heparin by heparinase-I, that generates a Δ4,5 uronic acid residue at the non-reducing end. Enoxaparin, prepared through chemical β-eliminative cleavage by alkaline treatment of heparin benzyl esters, is once again featured by non-reducing unsaturated uronate residues. For such LMWH also the presence of 1,6-anhydro structures at the reducing end is described.

3.0 Results

3.1 Gel permeation chromatography

The three LMWH preparations were separated into their oligomeric components through gel permeation chromatography on Biogel P10, obtaining noticeably different chromatographic profiles (figure 21,22,23). A series of peaks, each one corresponding to oligomeric families, ranging in size from dp4 to dp16 (enoxaparin) (fig 21) or dp18 (tinzaparin) (fig 22) and from dp8 to dp22 (dalteparin) (fig 23), were resolved. The larger unresolved oligosaccharides were present in different proportions for each LMWH. The average chain length of most of the components was determined through mass spectrometry analysis, by collecting the fractions corresponding to individual peaks (data not shown). Moreover, in the enoxaparin elution profile, in between the various peaks of shorter even oligomers (tetra-hexamers etc.) small peaks were observed and were identified as odd oligomers (trimer in front of the tetramer; pentamer in between the tetramer and hexamer).

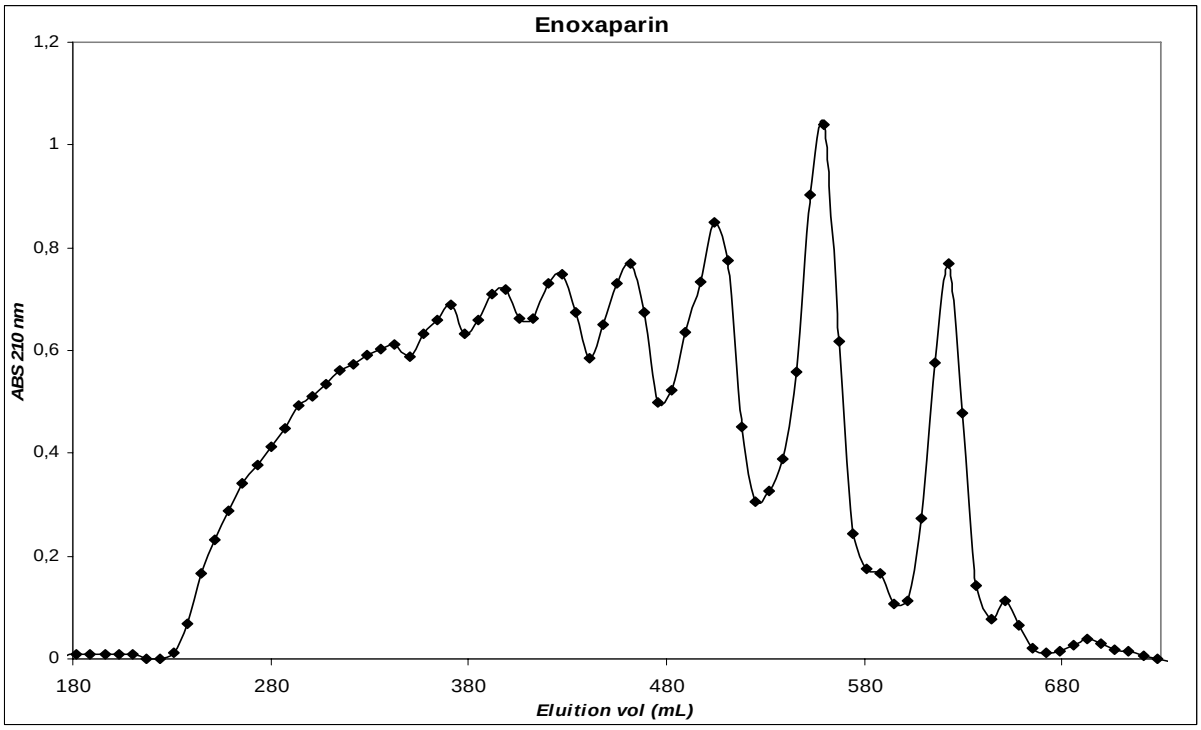

Fig 21 Gel permeation elution profile of Enoxaparin.

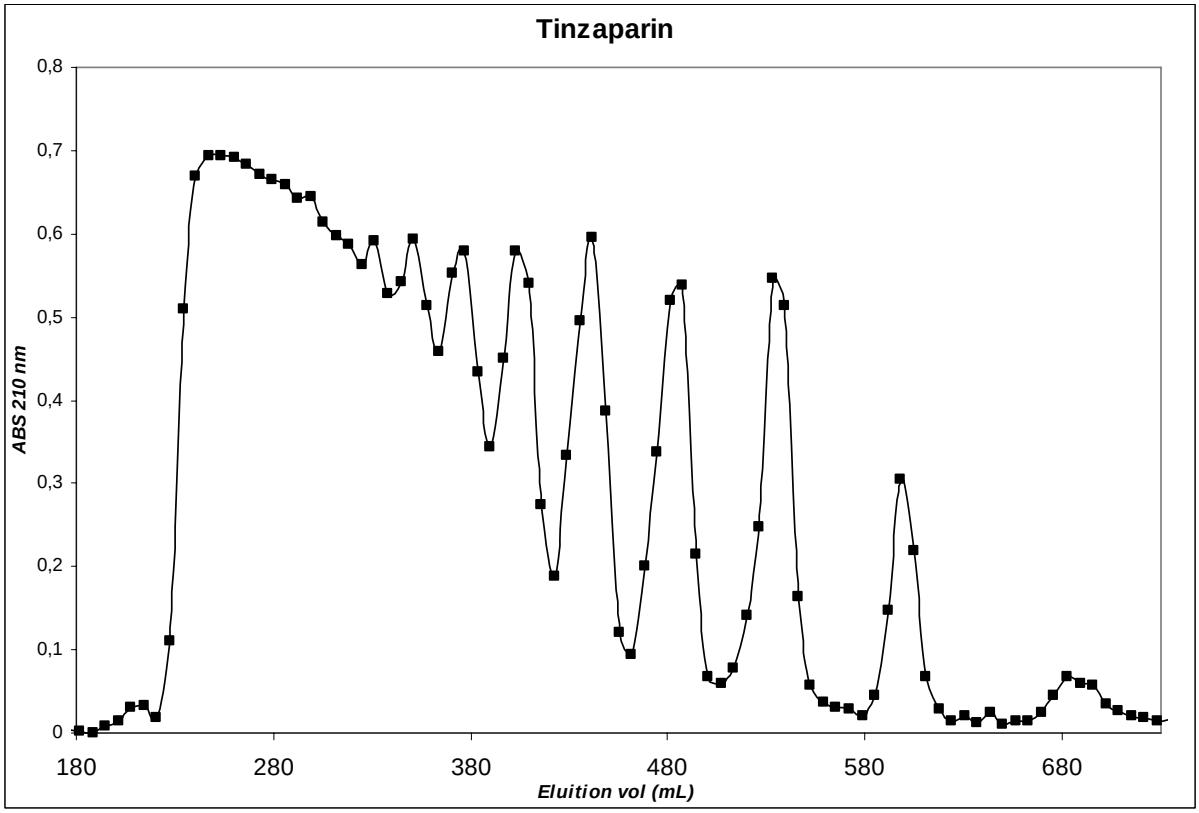

Fig 22 Gel permeation elution profile of Tinzaparin.

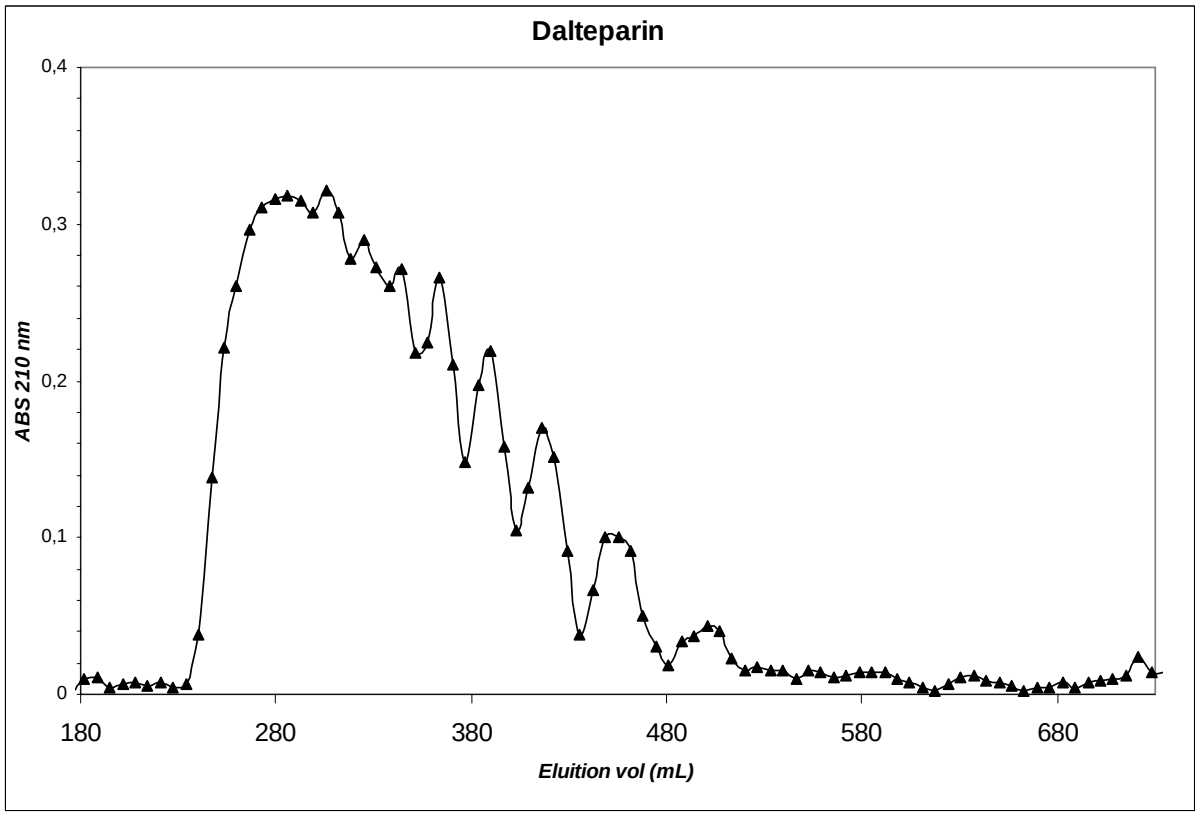

Fig 23 Gel permeation elution profile of Dalteparin.

A first important compositional difference is pointed out: the three LMWHs are composed by different percentages of a single oligosaccharidic population, particularly Enoxaparin is richer in small oligosaccharidic chains instead Dalteparin is richer in long oligosaccharidic chains. Tinzaparin is the LMWH with the highest polydispersity and all different populations of oligosaccharidic chains are represented. Each oligosaccharidic population was collected and the relative percentage with respect to the total compound has been estimated (in table 7 are summarized the percentages of abundance of the three LMWHs)

Tab 7 Evaluation of the relative abundance of the oligosaccharidic components of the three LMWHs studied (weight %) (n.d. not detected). All the percentages were calculated on the basis of the weight recovery after the biogel p10 column.

Oligosaccharide	Enoxaparin	Tinzaparin	Dalteparin
dp 1 to dp 3	3,6	1,6	n.d.
dp 5 and 4	8,9	3,5	n.d.
dp 6	10,7	4,9	n.d.
dp 8	17,8	5,1	n.d
dp 10	12,7	6,1	10,0
dp 12	10,1	5,1	11,0
dp 14	0,5	7,5	9,2
dp 16	9,3	7,1	17,2
dp 18	20,4	7,6	12,6
larger oligos	6,0	51,5	40,0

3.2 Affinity chromatography

Affinity chromatography on AT-Sepharose of LMWHs, enoxaparin, dalteparin and tinzaparin, resulted in separation of two portions: the first one, eluted at lower ionic strength, represented the non adsorbed material and was designed as no affinity (NA) fraction; the second one, eluted at higher salt concentration, was designed as high affinity (HA) fraction. The relative contents of HA fraction of the three LMWHs, calculated as a mean of three experiments, appear very similar (tab 8).

Table 8 Evaluation of High affinity content (relative percentage) of three LMWHs.

LMWH	% HA
Enoxaparin	13.6 ± 0.71
Tinzaparin	14.2 ± 0.62
Dalteparin	13.6 ± 1.21

Such a percentage of HA fraction mainly depends on two factors: the presence along heparin chain of sequences specifically interacting with AT and the length of oligosaccharide chains. In fact, the longer is the heparin oligosaccharide interacting with AT-Sepharose column and the higher is its response to carbazole reaction. As the average chain length of the three LMWHs is rather different, as shown in figure 21,22 and 23, also the oligosaccharide composition of the corresponding HA fractions is expected to be qualitatively dissimilar.

With the aim of further fractionating HA components, AT-Sepharose column was overloaded with an amount of each LMWH exceeding three times the retention capacity of the resin. Following the procedure described in Material and Method section, three HA subfractions endowed with graded strength of interaction with AT were separated from each LMWH (HA1, HA2 and HA3, in scaling order of affinity), together with the corresponding no-affinity fraction (NAr).

3.3 Molecular weight evaluation

Molecular weight parameters of enoxaparin, tinzaparin and dalteparin, and of their corresponding NA and HA fractions, were evaluated by high performance-size exclusion chromatography/ triple detector array (HP-SEC/TDA) (manuscript in preparation). HP-SEC on-line with triple detector array permits the evaluation of polymeric samples by exploiting the combined and simultaneous action of three detectors: laser light scattering (RALLS/LALLS) refractometer and viscometer. The

method, already successfully employed to determine the molecular weight of UFH and dermatan sulfate (190), does not require any chromatographic column calibration. The resulting molecular weight parameters, Mw, Mn and polydispersity (D), are shown in table 9.

Tab 9 Evaluation of molecular weight parameters by HP-SEC/TDA.

Sample	Fraction	Mn	Mw	D
Enoxaparin	Parent	3850	4975±171	1,30
	HA	8080	9000	1,12
	NA	3450	4700	1,32
Tinzaparin	Parent	5715	8100±295	1,41
	HA	9060	11000	1,23
	NA	5600	7000	1,61
Dalteparin	Parent	5700	7000±155	1,21
	HA	7950	10200	1,23
	NA	4800	6500	1,30

In agreement with the featuring diversity of Biogel P10 elution profiles (fig. 21, 22 and 23), the parent LMWHs exhibited very different molecular weight and polydispersity values.

Fig 24 HP-SEC/TDA chromatograms of the three LMWHs: refractive index response.

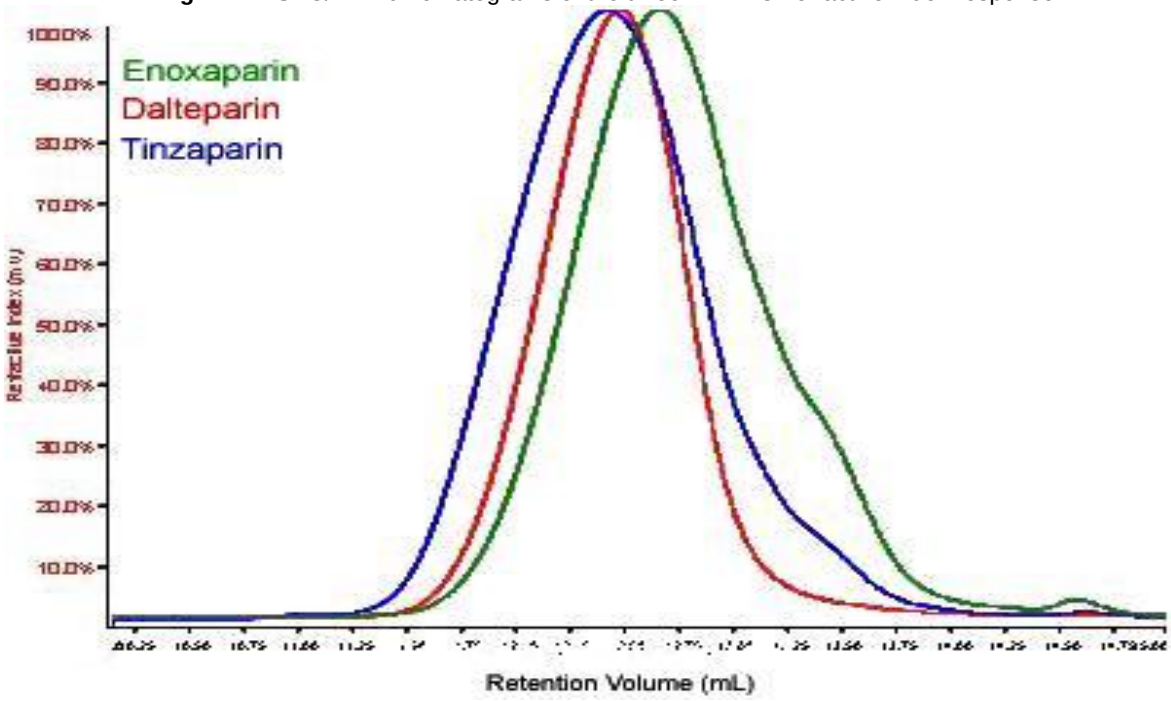

All the HA fractions exhibited significantly higher molecular weight with respect to their corresponding parent LMWH and a reduced polydispersity only in case of enoxaparin and tinzaparin. In figure 25 the elution profiles of tinzaparin and its HA fraction are compared and a significant difference in retention volume is pointed out.

Fig. 25 HP-SEC/TDA **e**lution profile of tinzaparin (red) and its high affinity fraction HA (black).

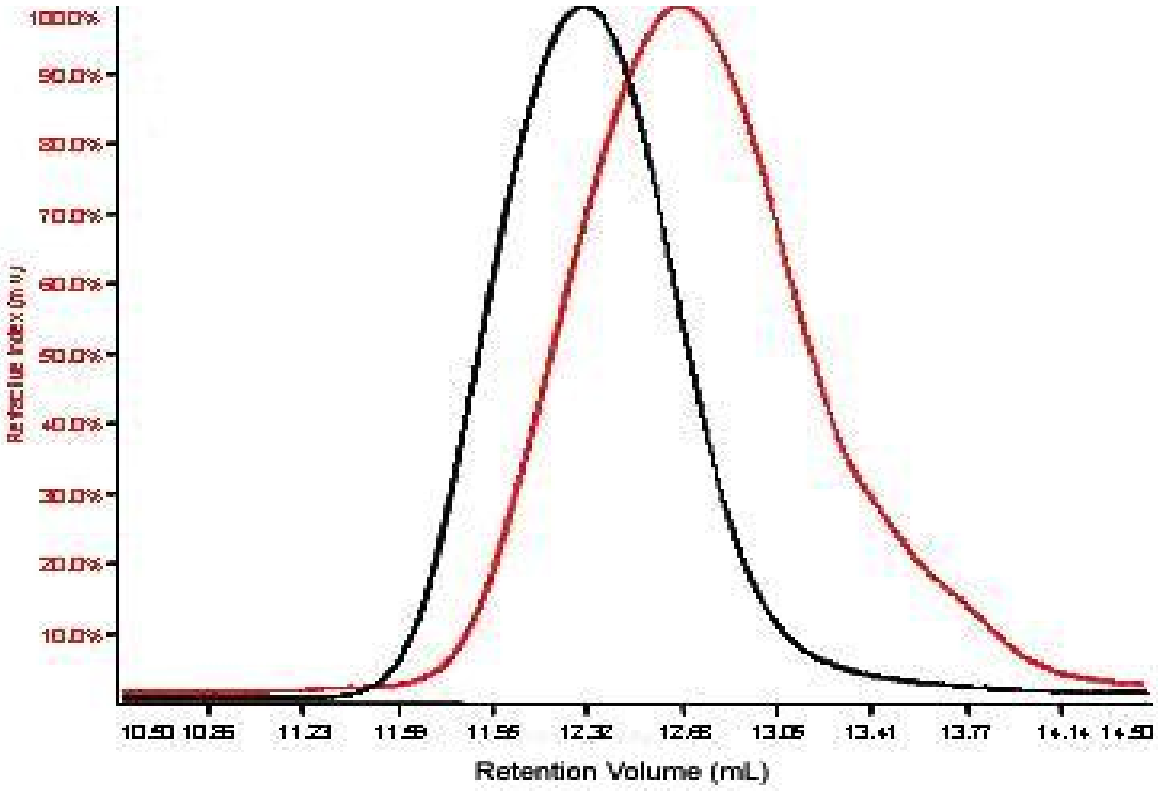

To evaluate the molecular weight of high affinity subfractions HA1, HA2 and HA3, an alternative method was applied, mainly to overcome the relatively large requirement of material from HP-SEC/TDA analysis (about 2,5-5 mg for each analysis). Then a HP-SEC coupled both to a UV detector and to an electronspray ionization source, equipped with a hybrid quadrupole/time-of-flight (ESI-Q-TOF) mass spectrometer. In this case the chromatrographic column employed was a Superdex 75 (see Material and Methods section) and the amount of material required for each analysis was 0.2-0.4 mg. Chromatographic column was calibrated by using the mass values for the smaller components (i.e. Tetra, Hexa, Octa) and five heparin fraction previously characterized through HP-SEC/TDA (Mp=5400, 6000, 6500, 8400, 9800). The total ion chromatograms (TIC) of all LMWH heparin fractions and the UV chromatograms,

available only for enoxaparin and tinzaparin fractions, were elaborated through a GPC program.

To assess the concordance of molecular weight values obtained with the two techniques, the three parent LMWHs have been analysed with both HP-SEC/TDA and HP-SEC/UV-ESI-Q-TOF. Results obtained are shown in table 10.

Tab 10 Molecular weight parameters evaluation through HPLC-ESI and TDA.

Sample	Analysis	Mn	Mw	D
Enoxaparin	HP-SEC/TDA	3850	4975±171	1,30
	HP-SEC/UV-ESI	3500	4600	1,33
Tinzaparin	HP-SEC/TDA	5715	8100±295	1,41
	HP-SEC/UV-ESI	4900	7100	1,43
Dalteparin	HP-SEC/TDA	5700	7000±155	1,22
	HP-SEC/UV-ESI	5800	7800	1,28

For enoxaparin and dalteparin, both Mn and polydispersity (D) values are in good agreement, and the difference between Mw values is held down 10%. In the case of tinzaparin whereas D is unvaried, Mn and Mw values obtained with the two techniques exhibited the larger difference. In particular, Mn and Mw values found with HP-SEC/ESI-Q-TOF are lower with respect to those found with HP-SEC/TDA. Such a difference could be explained by considering that different chromatographic columns have been employed in the two systems and Superdex 75 GPC column employed in HP-SEC/UV-ESI-Q-TOF could resolve less efficiently higher molecular weight oligomers with respect to the TSK columns employed in HP-SEC/TDA. Since tinzaparin is the richest in larger oligosaccharides among the three LMWHs studied, (see table 5), as a consequence, HP-SEC/UV-ESI-Q-TOF could result in an underestimation of its molecular weight.

Since the comparison of molecular weight parameters of LMWHs and of their subfractions aimed at pointing out a trend of variation inside homogeneous families,

the differences detected between HP-SEC/TDA and HP-SEC/UV-ESI-Q-TOF was considered not influential.

Molecular weight parameters of HA1, HA2, HA3 and NAr subfractions of each LMWH were finally obtained (tab 11).

Tab 11 Evaluation of molecular weight parameters through HP-SEC/UV-ESI-Q-TOF.

Sample	Fraction	Mn	Mw	D
Enoxaparin	Parent	3500	4600	1,33
	HA1	6500	7350	1,13
	HA2	5200	6200	1,23
	HA3	6300	7000	1,12
	NAr	4000	5000	1,25
Tinzaparin	Parent	4900	7100	1,43
	HA1	8100	9200	1,13
	HA2	8500	9500	1,11
	HA3	9000	10000	1,12
	Nar	5200	6500	1,25
Dalteparin	Parent	5800	7800	1,28
	HA1	6150	8300	1,35
	HA2	5800	8400	1,47
	HA3	5800	8500	1,45
	NAr	4300	7000	1,50

In agreement with the results obtained by HP-SEC/TDA, all HA fractions have higher Mw compared to parent LMWHs, moreover the correlation between affinity and molecular weight is different in the three cases (fig 27).

The elution profile of a single LMWH and its fractions (Tinzaparin) is shown in figure 26 (Total Ion Chromatogram).

Fig 26 Elution profile of the tinzaparin parent (black), non affinity fraction (brown) and high affinity fractions (HA1 red, HA2 green, HA3 blue).

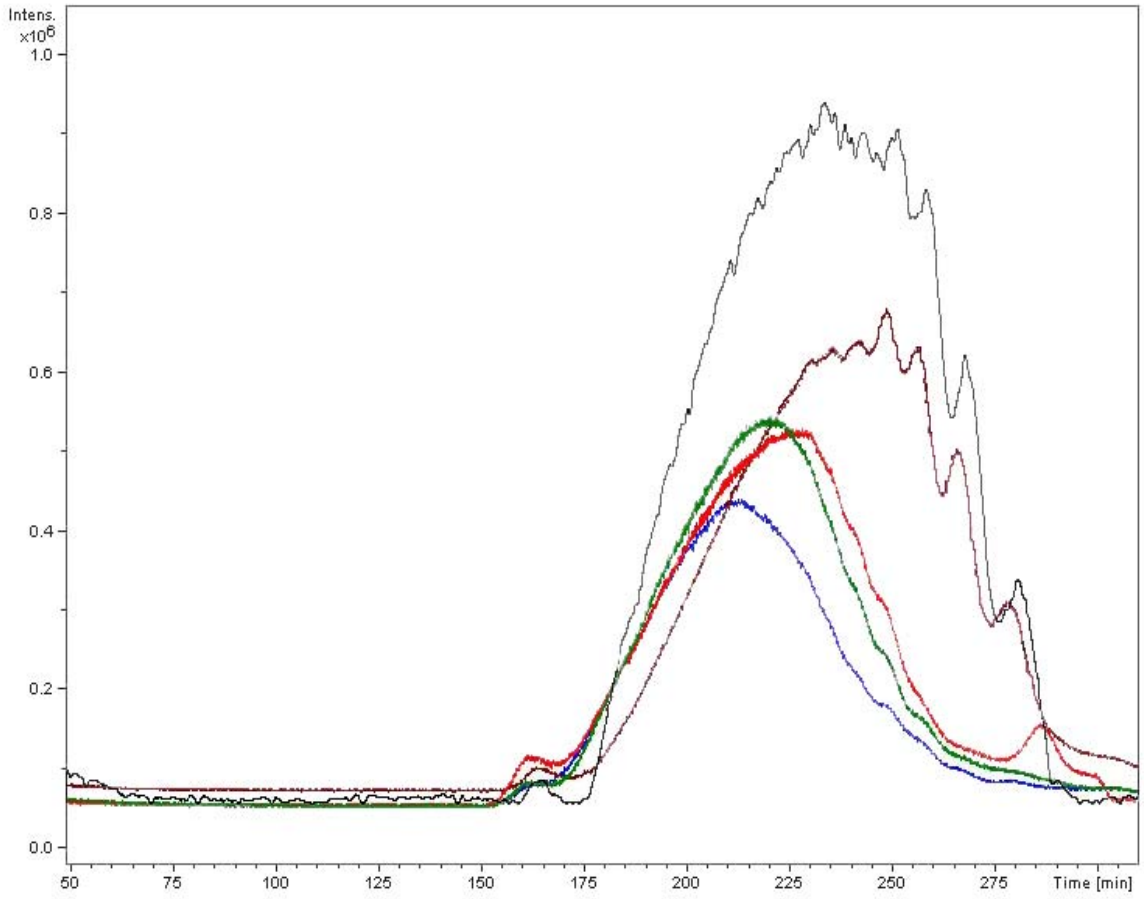

Fig 27 Correlation between AT-affinity and molecular weight: comparison among the series of fractions with graded affinity (HA1, HA2, HA3, and NAr) obtained from enoxaparin, tinzaparin and dalteparin.

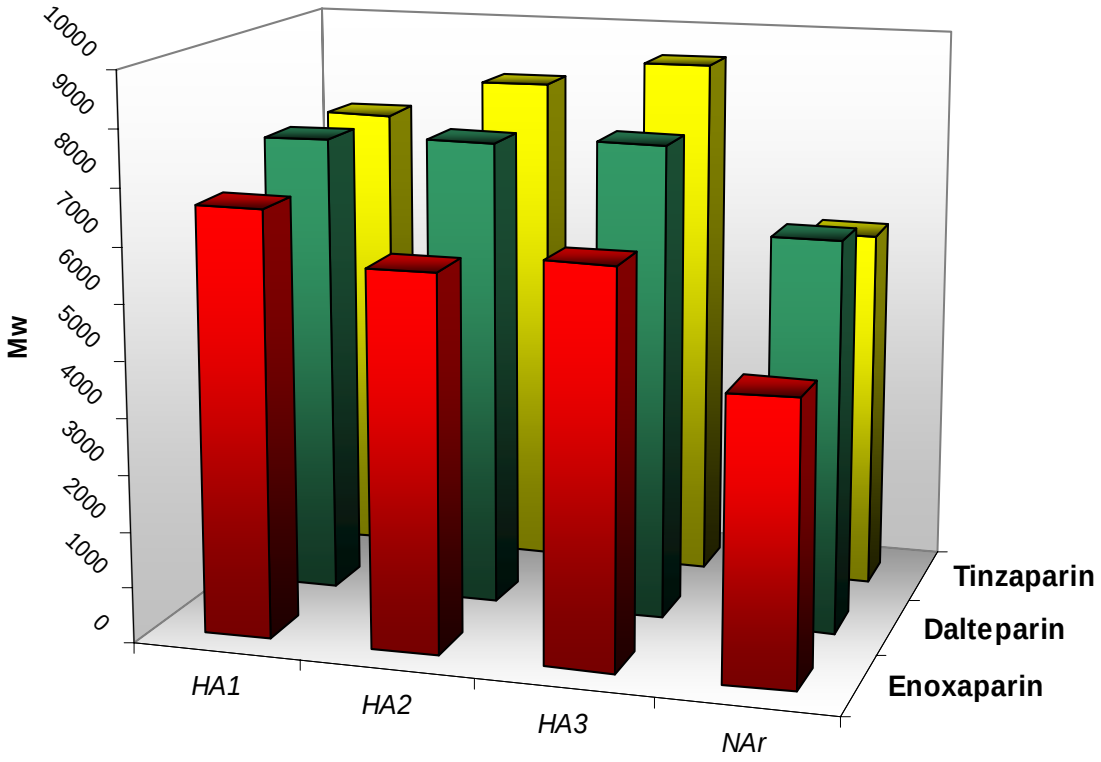

As shown in figure 27 the molecular weight (Mw) of HA fractions of Tinzaparin increased with the decreasing of affinity toward AT (yellow boxes), whereas Dalteparin is the most homogenous compound, apart from a very slight increase of Mw (green boxes) and for Enoxaparin (red boxes) the Mw decreases together with the affinity degree. In all cases the NAr component exhibit the lowest Mw mainly due to the presence of the shorter oligosaccharides.

Larger oligosaccharides species are expected to exhibit the highest affinity toward AT because the probability to contain the specific pentasaccharidic sequence (AGA*IA) is higher than for shorter chains. In fact all HA fractions are longer than the corresponding NA fractions. Nevertheless, by considering the HA subfractions of each LMWH, no correlation was found between degree of affinity and molecular weight: even for tinzaparin, fraction with the highest affinity exhibited the lowest molecular weight value.

3.4 NMR characterization

All fractions and subfractions separated by affinity chromatography were studied through NMR by applying the quantitative compositional analysis method based on two-dimensional (2D) ^{1}H-^{13}C correlation experiments (heteronuclear single quantum coherence, HSQC) already successfully applied to characterize the corresponding parent LMWHs (189). The average contents of monosaccharide components of the three LMWHs and of all their fractions are compared in tables 12 and 13. Enoxaparin and its fractions exhibited a notable structural complexity because of the number of reducing residues detectable in their spectra with respect to those displayed by tinzaparin and dalteparin LMWHs and fractions: eight ,*vs* two, *vs* one, respectively. Anyway, the most important difference displayed by each HA and NA fraction with respect to the corresponding parent LMWHs are due to the average contents of $A_{NS,3S}$ and G-$A_{NS,3S}$ considered as markers of the pentasaccharidic sequence AGA*IA. The percentage of $A_{NS,3S}$ (A*), the central residue of the pentasaccharidic sequence (AGA*IA), is always higher than the percentage of glucuronic acid linked to A*, G-(A*). Actually, A* was also found in heparin fractions with no affinity for AT (189), indicating that this residue can be located also in sequences not directly involved in the interaction with AT.

Tab 12 Determination of variously substituted monosaccharide components (percentage) of Enoxaparin, Tinzaparin and Dalteparin (amines).

Sample	A_{ns} I_{2s}	A_{ns} I	A_{ns} G	$A_{ns,3s}$	A_{nac}	A_{nac} α-red	A_{ns} α-red	A_{ns} β-red	1,6 anA	1,6 anM	M_{ns} α-red	An. M.ol	A_{6s}
Enoxaparin													
parent	48.8	7.0	11.8	4.3	10.3	0.5	8.6	1.0	2.2	2.5	3.0	0.0	83.8
HA	35.3	13.8	10.4	14.0	16.0	0.4	4.8	0.0	2.0	1.5	1.8	0.0	89.5
NA	48.4	6.7	14.1	2.8	8.7	0.5	9.3	1.2	2.6	2.8	3.0	0.0	84.0
HA1	33.5	14.6	11	16.8	12.5	0.3	6.6	0.0	1.4	1.7	1.5	0.0	90.1
HA2	42.1	12.4	8.6	11.7	12.5	0.4	6.7	0.0	1.7	2.1	1.9	0.0	90.2
HA3	38.1	13.6	8.9	11.5	15.8	0.7	6.5	0.0	1.3	1.8	1.7	0.0	88.7
NAr	50.8	6.8	12.5	1.8	7.8	0.3	10.2	0.1	2.6	2.9	3.3	0.0	82.1
Tinzaparin													
parent	53.2	7.6	8.6	3.4	14.0	0.6	11.1	1.3	0.0	0.0	0.4	0.0	86.3
HA	43.4	13.5	8.0	7.9	19.6	0.6	6.3	0.4	0.0	0.0	0.0	0.0	85.6
NA	55.8	6.5	10.9	1.5	11.6	0.6	12.0	1.6	0.0	0.0	0.0	0.0	85.0
HA1	40.2	14.3	9.1	10.1	18.7	0.5	5.2	1.5	0.0	0.0	0.3	0.0	87.0
HA2	42.4	13.9	8.0	9.2	19.4	0.2	6.3	0.6	0.0	0.0	0.0	0.0	83.1
HA3	45.6	13.3	8.6	5.3	20.6	0.0	5.7	0.9	0.0	0.0	0.0	0.0	80.8
NAr	58.8	6.5	9.0	1.4	9.5	0.4	13.4	1.5	0.0	0.0	0.0	0.0	85.2
Dalteparin													
parent	55.3	8.9	6.0	5.4	9.6	0.0	0.0	0.0	0.0	0.0	0.0	14.8	91.5
HA	41.9	15.5	6.0	14.0	13.2	0.0	0.0	0.0	0.0	0.0	0.0	9.3	89.8
NA	60.6	7.6	7.0	4.3	7.2	0.0	0.0	0.0	0.0	0.0	0.0	13.4	91.7
HA1	41.8	13.5	8.8	12.9	12.0	0.0	0.0	0.0	0.0	0.0	0.0	10.9	94.1
HA2	41.1	15.5	5.0	13.9	12.8	0.0	0.0	0.0	0.0	0.0	0.0	11.7	94.6
HA3	44.3	14.2	4.7	12.8	12.8	0.0	0.0	0.0	0.0	0.0	0.0	11.2	91.7
NAr	59.6	6.8	7.0	3.7	7.4	0.0	0.0	0.0	0.0	0.0	0.0	15.4	91.8

Tab 13 Determination of variously substituted monosaccharide components (percentage) of Enoxaparin, Tinzaparin and Dalteparin (uronic acids).

Sample	I_{2s}	I A_{6S}	I A_{6OH}	G $A_{ns,3s}$	G A_{ns}	G A_{nac}	G_{2s}	ΔU_{2s}	ΔU	I_{2s} red	U_{2s} red	Epox
Enoxaparin												
parent	52.8	5.7	1.3	3.3	8.2	4.5	2.6	17.6	1.0	1.1	0.9	0.3
HA	49.1	13.8	0.0	11.2	6.9	3.8	1.5	10.6	2.4	0.0	0.0	0.0
NA	54.1	4.7	1.1	2.1	8.7	4.3	2.6	18.4	1.1	1.5	0.9	0.0
HA1	49.4	12.4	0.7	10.7	6.0	2.3	1.1	14.4	2.9	0.2	0.0	0.0
HA2	49.0	9.8	1.7	7.6	7.1	3.2	3.4	14.4	2.0	0.9	0.8	0.0
HA3	49.8	13.4	0.0	9.7	7.0	3.3	1.7	12.2	2.1	0.7	0.0	0.0
NAr	53.5	3.9	0.6	1.1	9.5	6.5	2.4	18.9	0.5	1.5	0.8	0.0
Tinzaparin												
parent	64.0	6.8	1.5	2.0	9.0	3.2	0.0	12.7	0.0	0.0	0.3	0.0
HA	56.8	13.1	1.6	6.2	6.4	3.8	0.0	11.8	0.0	0.0	0.0	0.0
NA	62.3	5.1	1.9	1.4	9.6	4.8	0.0	15.2	0.0	0.0	0.0	0.0
HA1	54.6	13.9	1.9	7.2	6.6	4.5	0.0	9.9	0.0	0.3	0.0	0.0
HA2	57.8	13.4	1.5	5.6	6.1	4.1	0.0	11.0	0.0	0.0	0.0	0.0
HA3	60.7	12.0	1.4	3.1	6.9	3.5	0.0	11.8	0.0	0.0	0.0	0.0
NAr	63.5	4.9	1.8	1.3	9.0	5.1	0.0	14.3	0.0	0.0	0.0	0.0
Dalteparin												
parent	76.3	8.5	0.7	4.4	6.5	3.5	0.0	0.0	0.0	0.0	0.0	0.0
HA	60.9	14.1	2.3	12.4	6.6	3.8	0.0	0.0	0.0	0.0	0.0	0.0
NA	74.4	7.3	1.2	4.6	7.8	4.8	0.0	0.0	0.0	0.0	0.0	0.0
HA1	65.0	13.5	1.4	12.3	4.8	3.0	0.0	0.0	0.0	0.0	0.0	0.0
HA2	66.4	14.5	2.2	9.7	4.2	3.0	0.0	0.0	0.0	0.0	0.0	0.0
HA3	66.5	14.7	0.8	10.6	4.6	2.8	0.0	0.0	0.0	0.0	0.0	0.0
NAr	77.5	6.5	2.0	3.3	6.6	4.1	0.0	0.0	0.0	0.0	0.0	0.0

The possible importance of the average sulfation degree of heparin chains with respect to AT-affinity, was also considered. As described in Materials and Methods (see 3.6.1) the evaluation of the percentage of abundance of sulfated residues provided an estimation of the average sulfation degree *per* disaccharide for the LMWHs and their fractions was provided.

Fig 28 Correlation between AT-affinity and sulfation degree: comparison among the series of fractions with graded affinity (HA1, HA2, HA3, and NAr) obtained from enoxaparin, tinzaparin and dalteparin.

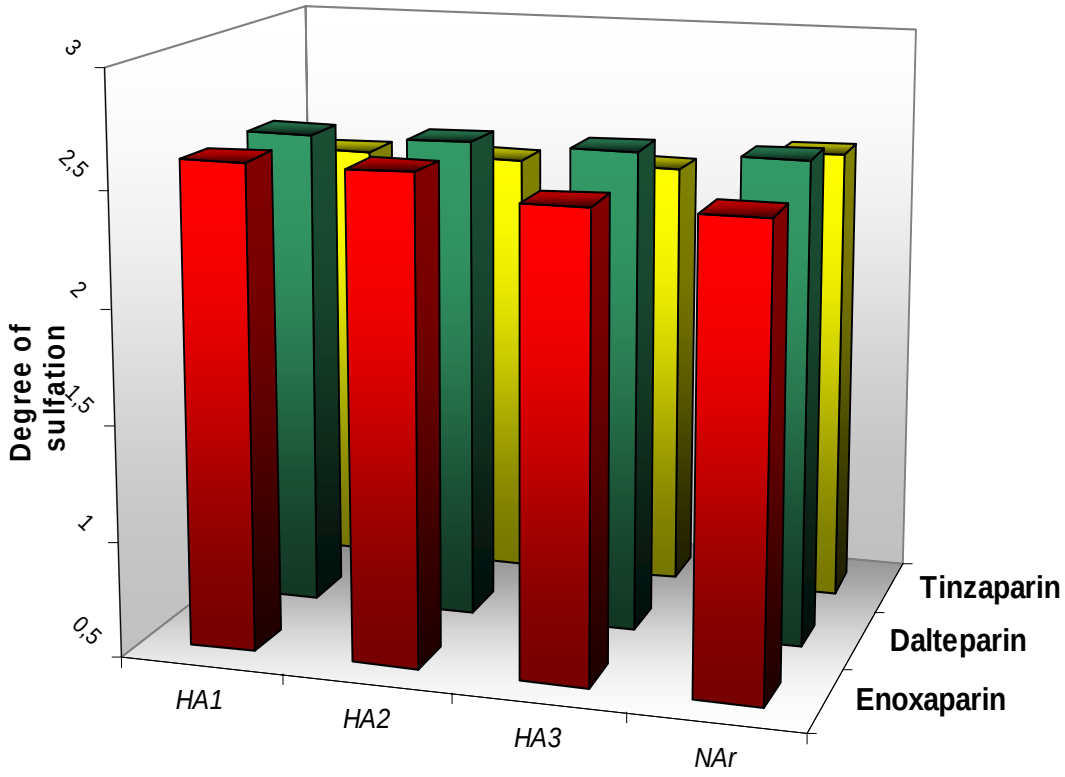

In contrast with some recent literature data, pointing to a significant role of charge the density of GAG chains in their affinity for AT (197), the present results did not reveal any correlation between the average degree of sulfation of the low molecular weight heparin chains and the affinity toward AT.

As a consequence, if neither molecular weight (fig. 27) nor degree of sulfation can explain the different degree of affinity of the analysed fractions, other factors are expected to contribute to the affinity for AT, in addition to the presence of the specific pentasaccharide sequence (AGA*IA). Possible factors include the positioning of

AGA*IA within the oligomeric chain, the pattern of sulfate groups and the chain flexibility of reducing and nonreducing extension of the pentasaccharide, or even the presence of more than one AGA*IA per chain. These hypotheses were previously pointed out by our group (40,190).

As described in Material and Methods (see 3.6.2) information about the molecular weight of LMWHs can be obtained also through NMR spectra, by evaluating the percentage of reducing end residues (192). Being NMR a conservative technique towards sample, such a way was considered as further alternative to estimate the molecular weight of LMWH subfractions, HA1, HA2, HA3 and NAr, which were available only in low amount, not sufficient for HP-SEC/TDA analysis. It is important to underline that the molecular weight estimated by such a way represents an average Mn value which does not take in account the real polydispersity of the sample. Anyway, it is useful to evaluate the possible variation of molecular weight within a homogeneous family of fractions.

Due to the different relaxation times of the terminal residues with respect to residues in chain, NMR generally overrates the amount of ending groups and consequently underestimates the Mn values.

In table 14, the comparison of the reliable Mn values obtained by HP-SEC/TDA analysis ($Mn_{(TDA)}$) of each parent LMWH and of the corresponding HA and NA fractions with the Mn value calculated via NMR ($Mn_{(NMR)}$) points out such a difference. To overcome this problem a correction factor was calculated as follows:

$$f = Mn_{(TDA)} / Mn_{(NMR)}$$

for all HA and NA fractions and applied to obtain a "correct $Mn_{(NMR)}$" estimation of the corresponding HA1, HA2, HA3, and NAr fractions, respectively (tab. 14).

Tab 14 Determination of the correction factor for Mn values obtained through NMR.

Sample	Fraction	Mn HP-SEC TDA	Mn NMR	Correction Factor *f*
Enoxaparin	Parent	3850	3100	1,24
	HA	8000	5700	1,40
	NA	3500	2900	1,21
Tinzaparin	Parent	5350	4650	1,15
	HA	9000	8600	1,05
	NA	5650	4450	1,27
Dalteparin	Parent	5850	4300	1,36
	HA	7950	6700	1,19
	NA	4800	4700	1,02

Crossing information about the average Mn and the relative percentage content of G-(A*), regarded as marker of the active pentasaccharide sequence, it was possible to estimate for each LMWH and HA subfraction the average content of AGA*IA *per* chain, together with the average number of disaccharide *per* chain (tab. 15).

Tab 15 Estimation of the average content of AGA*IA sequence *per* chain.
[a] Mn values calculated by introducing the corresponding correction factor *f* as described in the text (see table 12). For parent LMWHs correct Mn = $Mn_{(TDA)}$
[b] values between brackets are referred to HP-SEC/ESI-Q-TOF-MS measurements.

Sample	fraction	Determinations *via* NMR					ESI-MS	disacch. *per* chain	AGA*IA *per* chain
		Red. ends %	avg Mn dis.	Mn	Corr. Mn[a]	% G-(A*)	Mn		
Enoxaparin	Parent	20,4	631	3100	3850[a]	3,3	3500	6,1 (5,6)[b]	~0,2 (~0,1)[b]
	HA1	11,7	639	5400	7600[a]	10,7	6500	11,8 (10,4)[b]	~1,3 (~1,2)[b]
	HA2	14,3	637	4500	6300[a]	7,6	5200	9,9 (8,9)[b]	~1,0 (~0,8)[b]
	HA3	12,7	630	4900	6900[a]	9,7	6300	10,9 (10,0)[b]	~1,0 (~1,0)[b]
	NAr	23,1	630	2700	3300[a]	1,1	4000	5,2 (6,2)[b]	~0,1 (~0,1)[b]
Tinzaparin	Parent	13,7	633	4650	5350[a]	2,0	4900	8,4 (7,8)[b]	~0,2 (~0,2)[b]
	HA1	7,9	626	7900	8200[a]	7,2	8100	13,4 (13,1)[b]	~1,0 (~1,0)[b]
	HA2	7,3	625	8600	9000[a]	5,6	8500	14,4 (13,6)[b]	~0,8 (~0,7)[b]
	HA3	7	622	9000	9400[a]	3,1	9000	15,1 (14,5)[b]	~0,5 (~0,4)[b]
	NAr	15,3	633	4200	5300[a]	0,7	5200	8,4 (8,2)[b]	~0,1 (~0,1)[b]
Dalteparin	Parent	14,7	631	4300	5850[a]	4,4	5700	9,0 (9,2)[b]	~0,4 (~0,4)[b]
	HA1	11,0	628	5700	6700[a]	12,3	6150	10,8 (10,6)[b]	~1,4 (~1,3)[b]
	HA2	11,7	631	5400	6400[a]	9,7	5800	10,2 (10,1)[b]	~1,0 (~1,0)[b]
	HA3	11,2	626	5600	6600[a]	10,6	5800	10,7 (10,6)[b]	~1,1 (~1,1)[b]
	NAr	15,3	633	4100	4200[a]	3,3	4300	6,7 (6,6)[b]	~0,2 (~0,2)[b]

As expected the average chain length is directly related to the molecular weight. Instead the average AGA*IA for a single chain is a further confirm of the “sequence effect” hypothesis: fractions with higher affinity toward the AT (HA1) have more than one AGA*IA sequence for a single chain for Enoxaparin and Dalteparin. On other hand Tinzaparin fractions with intermediate affinity (HA2) and lowest affinity (HA3) toward the AT have less than one AGA*IA for a single chain, that result confirm once again the “sequence effect” hypothesis, by pointing out the existence of sequences with affinity toward AT but without the complete AGA*IA sequence.

3.5 Activity

Since the final aim of the present research is the correlation of the structural characterization of LMWHs with their functional properties, all the isolated fractions were planned to be submitted to a series of biological tests, including anti-Xa assay, anti-IIa assay, pharmacokinetics assays.

Preliminary experiments were performed by testing the anti–Xa activity of some selected fractions with graded affinity toward AT (i.e. HA1, HA3, and NAr), in comparison with parent LMWHs. Preliminary results obtained, shown in table 16, pointed out a direct relationship between affinity and anti-Xa activity: all fractions endowed of AT-affinity exhibited a high AT-mediated factor Xa inhibition, whereas fraction devoid of AT-affinity (NAr) did not exhibit any significant inhibitory effect.

Tab 16 Determination of anti Xa-activity of selected fractions in comparison with the corresponding parent LMWH.

Sample	Fraction	Anti Xa activity (U/mg)
Enoxaparin	Parent	95
	HA1	361
	HA3	199
	NAr	0
Tinzaparin	Parent	82
	HA1	291
	HA3	133
	NAr	7
Dalteparin	Parent	133
	HA1	245
	HA3	234
	NAr	10

As concern the comparison among the three LMWHs, while for HA1 and HA3 fractions of both enoxaparin and tinzaparin the anti-Xa activity is widely different (361 *vs* 199 and 291 *vs* 133, respectively), for the same fractions of dalteparin the difference is negligible, proving once again the high degree of homogeneity of that LMWH preparation.

To meet the requirement of high amount of material to carry out all the planned biological tests, further affinity chromatography fractionations of the three LMWHs by employing the preparative AT-Sepharose column are being performed.

4.0 Discussion

During the last decade the need to investigate more in depth the differences among various low molecular weight heparins is acquiring importance due to their continuous development and the increasing trend to substitute unfractionated heparin (69, 71). As described in the introduction, the actual and potential therapeutic uses of the low molecular weight heparins are wide (72-82). In this work we focused our attention on their anticoagulant properties (105-108). The fact that LMWHs are considered not interchangeable in the antithrombotic therapy (69) is an evidence of the importance of structural differences as starting point to explain differences in the biological properties and clinical effects of the LMWHs.

With the aim to explain from a structural and compositional point of view their different biological properties, this work was focused on the in depth study of the three most commonly employed commercial LMWHs: enoxaparin, tinzaparin, and dalteparin. Their compositional differences were determined by analyzing their oligosaccharidic populations by gel permeation chromatography. The elution profiles provided a fingerprint for each LMWHs, revealing very characteristic oligosaccharidic compositions, differing as regards the number of oligomeric species, their size and their relative proportion.

Enoxaparin was shown to be characterized by a consistent presence of short oligosaccharidic chains, i.e. tetra-octasaccharides. Tinzaparin exhibited the highest degree of polydispersity, being composed of oligosaccharidic chains of various lengths. Dalteparin revealed the lowest polydispersity, appearing richer in longer oligosaccharidic chains. These differences were confirmed by determination of molecular weight and polydispersity by HP-SEC/TDA. Enoxaparin was the LMWH with the lowest molecular weight, tinzaparin was the one with higher polydispersity, and dalteparin the most homogenous of the three LMWHs.

Since the anticoagulant/antithrombotic effect of the LMWHs is primary due to the interaction with AT, the analysis of LMWH fractions endowed with high affinity toward the protein was particularly important. Affinity chromatography on AT-Sepharose was performed to separate and quantify the high affinity fraction. Despite the different length of oligomeric components of the three LMWHs, the relative percentage of their HA and NA fractions, evaluated as uronic acid content of interacting and non interacting species respectively, was very similar.

The composition of HA fractions was studied more in detail. In particular, their molecular weight in comparison with the corresponding NA fractions and with the parent LMWHs was determined. All the HA fractions exhibited a considerably higher molecular weight and a reduced polydispersity with respect to NA fractions, suggesting that the longer are the oligosaccharides and the higher is the probability that they contain the specific pentasaccharidic sequence mainly responsible for AT interaction. Such an evidence holds also for dalteparin despite the parent LMWH displayed the most reduced polydispersity, thus appearing as the most homogeneous HA fraction from a compositional point of view.

To deepen the characterization of HA components, HA heparin chains of each LMWH were further fractionated into three subfractions with graded affinity toward AT (HA1, HA2, and HA3), also obtaining their corresponding no-affinity fraction, NAr. All these fractions were in turn characterized for Mw and, in addition, analysed for their mono-disaccharide composition, in comparison with the corresponding parent LMWHs and HA fractions, through quantitative analysis of their bi-dimensional proton-carbon NMR spectra (186).

The molecular weight of all HA subfractions were estimated by two different methods: HP-SEC/ESI-MS, by calculating molecular weight parameters on the basis of UV and MS chromatographic profiles, and by NMR spectroscopy, by evaluating the abundance of the reducing-end residues with respect to the total anomeric residues. The results found with the two methods, following a correction of NMR data based on HP-SEC/TDA data, were comparable.

For all the three analysed LMWHs neither the molecular weight of the derived HA1, HA2, HA3 and NA subfractions nor their sulfation degree calculated via NMR exhibited any correlation with the degree of affinity for AT.

The most relevant difference emerging from the comparison of NMR spectra of the three series of LMWH-derived fractions is the relative content of two residues A* and G-(A*): enoxaparin exhibited a significant decrease in their content going from the HA1 to the HA2 fraction; tinzaparin revealed a constant decreasing of these markers from HA1 to HA3; whereas, for dalteparin just a slight decrease of A* and G-(A*) content from HA1 to HA3 was observed, once again confirming this LMWH as the most homogenous one. Although both residues can be considered potentially markers of the heparin binding site for AT, AGA*IA, the trisulfated glucosamine A* was shown to be contained also in NA heparin chains (198). In fact, an evaluation of either A* or G-(A*) potentially undervaluate actual contents of AGA*IA, especially when the first aminosugar residue of the pentasaccharide is a non-6-O-sulfated glucosamine, which dramatically impairs the affinity for AT of the pentasaccharide. Although the presence of the G-(A*) sequence cannot guarantee the complete structural integrity of the active pentasaccharide, its quantitative evaluation can provide a rough estimate of the AGA*IA pentasaccharide content. By combining information obtained by NMR on the G-(A*) content and the chain length derived from molecular weight evaluation, it was thus possible to approximately estimate the AGA*IA content *per* chain.

For HA1 fractions of enoxaparin and dalteparin, the AGA*IA content per chain was estimated about 1.3 and 1.4 respectively, indicating that statistically, some chains may contain more than an active pentasaccharide. For the corresponding HA2 and HA3 fractions, the AGA*IA content was around 1.0. For the graded high affinity fractions of tinzaparin, the AGA*IA content per chain appeared to be slightly lower, starting from one per chain (HA1) to apparently less than one for HA2 and HA3.

Despite the awareness that such an estimation need to be verified, mainly by providing a more precise evaluation of molecular weight of HA fractions and then of

their chain length, the present data confirm the need of structural requirements additional to the presence of AGA*IA to explain at least the different affinity degree of HA2 and HA3 fractions of both enoxaparin and dalteparin, the estimated active pentasaccharide content of which was the same. Structural parameters such as the positioning of AGA*IA within the heparin oligomeric chain, the sulfation pattern of its reducing and non reducing elongating regions, together with their flexibility, mainly depending on epimerization of uronic acid residues, need to be considered and investigated.

Preliminary data on biological activity *in vitro* indicated that the different anti-Xa activities displayed by the analysed fractions are in agreement with the degree of AT affinity and the overall structural considerations. Actually, all HA1 fractions exhibited an anti-Xa potency significantly higher than both the corresponding parent LMWH and HA3 fraction. But, whereas the displayed differences were considerable in the case of enoxaparin and tinzaparin, the differences for dalteparin were less important, confirming once again the structural homogeneity of this LMWH.

The present work represents the first insight into the detailed and comparative structural characterization of three commercial LMWHs differing in manufacturing process. Important and characteristic structural parameters were defined, including the precise oligomeric composition, the relative content of AT interacting species, and their molecular weight, together with the relative content of variously substituted monosaccharide components. Further studies are required to unravel the correlation of structural features with LMWH functional properties.

5.0 Materials and Methods

5.1 Molecular weight evaluation of LMWHs

Materials:

- Viscotek pump VE1121; Degasser on-line dual channel Gastorr 150
- Columns TSK gel G2500 PWXL+TSK gel G3000 PWXL, Tosoh, 7.8mm ID x 30cm, Viscotek; 40°C
- Injection 100 μl
- Detector Viscotek mod.302 TDA equipped with refractive index, viscometer, Light Scattering 90° e 8°, at 40°C.
- Solution $NaNO_3$ 0.1M
- Software Viscotek for data analysis

Method:

- *Sample preparation:*

  Sample was dissolved in 1 ml of $NaNO_3$ 0.1M solution (average concentration was about 5 mg/ml for each sample).

- *Instrumental analysis:*

  HPLC analysis with $NaNO_3$ 0.1M as eluent ; flow-rate: 0.6ml/min;

  temperature: 40° C.

- *Data analysis :*

  Chromatogram analysis was performed with OMNISEC 3.0 software, all molecular weight parameters (Mn,Mw,Mz) and polydispersity of each sample were obtained.

5.2 LMWHs fractionation through size exclusion chromatography

Materials:

- Resin: Bio-gel P10 (polyacrylamide);
- Column: Bio-Rad (5 x 129 cm)
- Eluent: NH_4Cl 0,25 M
- Flow-rate: 7 ml/min
- Fraction-collector Gilson mod. 201 controller
- Pump Gilson Miniplus 2
- Cuvettes macro (4 ml) optical grade quartz
- Spectrophotometer UV/Vis Cary 50 (Varian)
- Millipore 0,22u filters

Method:

- *Eluent preparation:*

  66,75 g NH_4Cl was dissolved in 5l of purified water, the solution was filtered (0,22 u filters) and degassed.

- *Resin preparation:*

  The resin (biogel-P10) was suspended in 2,5 l of purified water and gently stirred until the achievement of a homogenous solution. The solution was incubated for 30 min at room temperature, than the surnatant was eliminated.

  2,5 l of purified water are added again and the procedure was repeated 3 times.

  The solution obtained was finally degassed for 1 h at room temperature.

- *Column preparation:*

  The swollen and degassed resin was packed into the column, than was incubated at room temperature for 24 hours, before washing with 5 l of eluent (flow-rate 0,4 ml/min).

- *Size exclusion Chromatography:*

  150 mg of each sample was dissolved in 5 ml of eluent and applied onto the column. Eluition was performed at a flow-rate of 7 ml/min; flowthrough was collected in 6 ml fractions.

- *Spectrophotometer analysis:*

  Absorbance at 210 nm was evaluated for each fraction, fractions of interest were collected and desalted through size-exclusion chromatography and ultrafiltration.

5.3 LMWH fractions desalting procedure through size-exclusion chromatography

5.3.1 Sephadex G10 column

Materials:

- Resin: Sephadex g10 (Pharmacia);
- column: Pharmacia (2,5 x 180 cm)
- Eluent: EtOH 10% in H_2O
- Flow-rate: 1,2 ml/min
- Fraction-collector Gilson mod. 201 controller
- Pump Gilson Miniplus 2
- Cuvettes macro (4 ml) optical grade quartz
- Spectrophotometer Cary 50 UV/Vis (Varian)
- Millipore 0,22u filters
- Dextran blue (PM 2.000.000 Da)
- K_2CrO_4 (PM=194 Da)

Method:

- *Eluent preparation:*

  500 ml of EtOH was diluted to 5 l of purified water, filtered (0,22 μ) and degassed.

- *Resin preparation:*

  The resin (Sephadex G10) was suspended in 2,5 l of purified water and gently stirred until the achievement of a homogenous solution.

The solution was incubated for 30 min at room temperature, than the surnatant was eliminated. 2,5 l of purified water are added again and the procedure was repeated 3 times.

The solution obtained was finally degassed for 1 h at room temperature.

- *Column preparation:*

The swollen and degassed resin was packed into the column, than was incubated at room temperature for 24 hours, before washing with 2,5 l of eluent (flow-rate 0,4 ml/min).

- *Column calibration:*

The column calibration was obtained by loading a mixture of dextran blue (2,5 mg) and K_2CrO_4 (2,5 mg). Fractions were collected and analysed with spectrophotometer (λ=610 nm and λ=450 nm), V_0 and V_t were calculated.

- *Size exclusion Chromatography:*

From 50 to 150 mg of each sample was dissolved in 5 ml of eluent and applied onto the column. Elution was performed at a flow-rate of 1,2 ml/min; flowthrough was collected in 6 ml fractions

- *Spectrophotometer analysis:*

Absorbance at 210 nm was evaluated for each fraction, fractions of interest were collected and freeze-dried.

5.3.2 TSK columns

Materials:

- Resin: TSK-GEL TOYOPEARL HW40S
- Columns: Pharmacia (2,6x58 cm), Pharmacia (5,5x100 cm)
- Eluent: EtOH 10% in H_2O
- Flow-rate: 1,2 ml/min , 5 ml/min
- Fraction-collector: Gilson mod. 201 controller
- Pump Gilson Miniplus 2
- Cuvettes macro (4 ml) optical grade quartz
- Spectrophotometer Cary 50 UV/Vis (Varian)
- Millipore 0,22u filters
- Dextran blue (PM 2.000.000 Da)
- K_2CrO_4 (PM=194 Da)

Method:

- *Eluent preparation:*

  500 ml of EtOH was diluted to 5 l of purified water, filtered (0,22 μ) and degassed.

- *Resin preparation:*

  The resin (TSK-Gel) was suspended in 2,5 l of purified water and gently stirred until the achievement of a homogenous solution. The solution was incubated for 30 min at room temperature, than the surnatant was eliminated.

  2,5 l of purified water were added again and the procedure was repeated 3 times. The solution obtained was finally degassed for 1 h at room temperature.

- *Column preparation:*

  The swollen and degassed resin was packed into the column, than was incubated at room temperature for 24 hours, before washing with 2,5 l of eluent (flow-rate 0,4 ml/min).

- *Columns calibration:*

  The column calibration was obtained by loading a mixture of dextran blue (2,5 mg and 5mg) and K_2CrO_4 (2,5 mg and 5mg). Fractions were collected and analysed with spectrophotometer (λ=610 nm and λ=450 nm), V_0 and V_t were calculated for each column. Column 2,6x58 cm: V_0=106 ml V_t=206 ml; Column 5,5 x100 cm: V_0=550 ml V_t=1250 ml.

- *Size exclusion Chromatography:*

  From 50 to 150 mg of each sample was dissolved in 5 ml of eluent and applied onto the column. Elution was performed at a flow-rate of 1,2 ml/min; flowthrough was collected in 6 ml fractions

- *Spectrophotometer analysis:*

  Absorbance at 210 nm was evaluated for each fraction; fractions of interest were collected and freeze-dried.

5.4 LMWHs desalting procedure through ultrafiltration

Materials:

- Amicon chamber V=160 ml
- Filter: Millipore (cellulose acetate) NMWL=500 Da
- Purified water

Method:

- *Filter preparation:*

  The filter was washed with purified water and assembled to the chamber. Than was washed with 60 ml of NaCl 5% solution (pressure 3,5 bar) and again with purified water.

- *Ultrafiltration:*

  The sample was loaded into the chamber and desalted under stirring with 3,5 bar of pressure. The retentate was recovered and freeze-dried.

5.5 NMR spectra recording

5.5.1 ^{1}H NMR SPECTRA

Materials:

- D_2O 99%
- NMR tube (Ø = 3 mm)
- Spectrometer Bruker Avance 600 equipped with high sensitivity 5 mm TCI cryoprobe.

Method:

- *Sample preparation:*

  From 5 to 20 mg of each sample were dissolved in 0,3 ml of D_2O 99% water. To eliminate all residues of water the sample was freeze-dried two times and dissolved again in the same amount of D_2O 99%.

- *Average recording conditions:*

  Monodimensional ^{1}H spectra were obtained with presaturation of residual HDO, from 32 to 128 scans and a recycle delay of 10s. The ^{1}H spectra were recorded at 308 °K with 32 K of data points. Spectra were elaborated with the software XWIN-NMR ver. 3.5. Chemical shift values were measured downfield from trimethylsilyl propionate sodium salt (TSP) as standard.

5.5.2 ^{13}C NMR SPECTRA

Materials:

- D_2O 99%
- NMR tube (Ø = 10 mm)
- Spectrometer Bruker Avance 400

Method:

- *Sample preparation:*

  From 50 to 200 mg of each sample were dissolved in 2,5 ml of D_2O 99% water.

- *Average recording conditions:*

  Monodimensional ^{13}C spectra were measured with proton decoupling during acquisition time at 40°C. Recycle delay was 4s and the number of scans 40.000.

5.5.3 HSQC NMR SPECTRA

Materials:

- D_2O 99%
- NMR tube (Ø = 3 mm)
- Spectrometer Bruker Avance 600 equipped with high sensitivity 5 mm TCI cryoprobe.

Method:

- *Sample preparation:*

  From 5 to 20 mg of each sample were dissolved in 0,3 ml of D_2O 99% water. To eliminate all residues of water the sample was freeze-dried two times and dissolved again in the same amount of D_2O 99%.

- *Average recording conditions:*

  Two-dimensional gradient enhanced HSQC spectra were recorded with carbon decoupling during acquisition with 320 increments of 64 scans for each. The matrix size 1Kx512 was zero filled to 4Kx2K by application of a squared cosine function prior to Fourier transformation. Integration of cross-peaks was made using standard Bruker XWINNMR 3.5 software and TOPSPIN 2.0.

Description of the analytical signals used for the HSQC analysis:

The analytical signals were chosen from those with minimal overlap in the HSQC spectra. Signals corresponding to monosaccharides also present in the heparin structure were chosen according to a previously published method (40).

The possibility of detecting and quantifying all minor signals depends on the signal-to-noise ratio obtained in the HSQC spectrum. In the present work, the spectra were recorded using a high-field NMR spectrometer (600 MHz) with a high sensitivity

cryoprobe, permitting accurate quantification of residues present in amounts below 1 to 2%.

Most of the signals present in the anomeric region were directly utilised for the quantification of the corresponding residues, particularly by the integration of A* (Glucosamine trisulfated), Ans-(I) (Glucosamine N-sulfated linked to Iduronic Acid) and Ans-(G) (Glucosamine N-sulfated linked to Glucuronic Acid) signals for the amines and I2s (Iduronic acid 2-O-sulfated) , I(A6s) (Iduronic acid linked to Glucosamine-6-O-sulfated), I(A) (Iduronic acid linked to Glucosamine), G(A*) (glucuronic acid linked to A*), G(Ans) (glucuronic acid linked to Glucosamine-N-sulfated) and G(Anac) (Glucuronic acid linked to Glucosamine-N-acetylated) signals for the glucuronic acids.

The percentage of the linkage region was also calculated by the integration of the anomeric signals evaluating the relative abundance respect to the total amines.

The epoxide signal was added to the total glucuronic acids amount due to the fact that this residue was originated from a sulfated Iduronic acid residue.

For enoxaparin and tinzaparin the evaluation of abundance of the non-reducing end residues ΔU and ΔU2s the H4/C4 signals were chosen for the integration even if the value of $^{1}JC_{4}$–H4 differs from the average value of anomeric signals by ~5 Hz because the overlap of the H1/C1 signal with part of the anomeric signals induces a larger error than that observed by integration of the better separated H4/C4 signals.

All the reducing-end residues were calculated by the integration of the anomeric signals.

For dalteparin the percentage of AM.ol residue was calculated from H2/C2 signals because its $^{1}J_{C2}$–H2 value is much closer to the average of the other glucosamine residues. Given that no other signals compatible with galacturonic acid can be detected in both anomeric and H2/C2 regions of the HSQC spectrum (due to signal overlap), the H5/C5 value was used for in the calculation, even if the value of $_{1}J_{C5–H5}$ differed slightly (by ~25 Hz) from the average value of the anomeric signals of uronic acid residues.

Because of the overlapping of the anomeric signals of A_{nac} residue with A_{ns} residue, was not possible to calculate the percentage of N-Acetylation by using that signal. Then the H2/C2 signals, separated on the HSQC spectrum, were utilised to calculate the percentage of N-Acetylation of each sample.

5.6 NMR evaluation of structural parameters of LMWHs

5.6.1 Evaluation of average sulfation degree

The average disaccharide sulfation degree was calculated using the following formula.

$$\frac{[A_{1NS}\text{-}(G)]+[A_{1NS}\text{-}(I)]+[2\cdot A_1^*]+[Man_{1red}]+[A_{1NS}\text{-}(I_{2S})]+[A_{1NSred\alpha}]+[A_{1NSred\beta}]+[I_{2S}]+[I_{2Sred\alpha}]+[I_{2Sred\beta}]+[G_{2S}]+[A_{6S}]}{100}$$

The percentage of each sulphated residue used to calculate the monosaccharide compositions was used. For Dalteparin also AM_{6S} signal was added; for Enoxaparin also $A_{1MAN1,6}$ and $A_{1GLC1,6}$ and ΔU_{2S} signals were added; for Tinzaparin ΔU_{2S} signal was added. A* signal represent the central glucosamine of the AGA*IA sequence and he is the only glucosamine with 3 sulfates, the coefficient in the formula is 2 because the third sulphate (is position 6) is already contained in the A_{6S} signal.

5.6.2 Evaluation of average molecular weight for a single disaccharide

For LMWHs obtained through β-eliminative cleavage Enoxaparin the following formula was utilised to calculate the average molecular weight for a single disaccharide:

$$\frac{[\Delta U_{2S}]+[\Delta U]}{100}\cdot 337+\frac{1{,}6an}{100}\cdot 337+\frac{100-([\Delta U_{2S}]+[\Delta U])+1{,}6an)}{100}\cdot 355+\text{sulfation degree}\,102+\frac{[A_{2NAc}]}{100}\cdot 43$$

For Tinzaparin the same formula was utilised but the 1,6an factor was not considered.

Whereas for Dalteparin the average molecular weight for a single disaccharide was estimated through a following formula:

$$\frac{anidromannTOT}{100}\cdot 340+\frac{100-(anidromanniTOT)}{100}\cdot 355+\text{sulfation degree}\cdot 102+\frac{[A_{2NAc}]}{100}\cdot 43$$

5.6.3 Evaluation of average chain-length

For Enoxaparin and Tinzaparin the following formula was utilised to evaluate the average chain length:

$$\frac{100}{\textit{r}\text{ed TOT}}$$

Substituting the (red TOT) factor with the percentages of the signals the formula is:

$$\frac{100}{[\text{Unknown}]+[\text{ANSred}\alpha]+[\text{ANSred}\beta]+[\text{ANAc - red}\alpha]+[\text{MNS - red}\alpha]+[1,6\text{ - an.M}]+[1,6\text{ - an.A}]+[\text{I2S - red}\alpha]+[\text{I2Sred}\beta]}$$

For Dalteparin the evaluation is simpler because of the presence of only one residue at reducing end (generated by the depolymerization method with nitrous acid). The following formula was utilised:

$$\frac{100}{[\text{anM}]}$$

5.7 Affinity chromatography

5.7.1 Antithrombin purification

Materials:

- Kybernin P1000 (Behring) Antithrombin from human plasma
- Column: Heparin-Sepharose (Sigma), volume 6ml, 4mg heparin/ml, binding capacity 15 mg of Antithrombin
- Centricon filter YM 10000 (NMWL 10000 Da)
- Equilibrium buffer: Phosphate buffer 10 mM, pH 7.4, NaCl 50 mM
- Elution buffer: Phosphate buffer 10 mM, pH 7.4, NaCl 2,5 M

Method:

- *Sample preparation:*

  80 mg of Kybernin p1000 were dissolved in 4 ml of equilibrium buffer.

- *Affinity chromatography on Heparin-Sepharose:*

  The column was previously washed with 20 ml of equilibrium buffer. The sample was loaded onto the column (flow-rate 1ml/min) and the fraction without affinity for heparin was eluted with 20 ml of equilibrium buffer. Then the antithrombin was eluted with 20 ml of elution buffer. Finally the protein was desalted with Centricon filter and the amount of protein obtained was evaluated through Lowry assay [188].

  The purity degree of the sample previously obtained was estimated through mass spectrometry MALDI/MS (fig 31), in comparison with the starting

commercial sample. About the 30% of the Kybernin P1000 sample resulted to be antithrombin.

Fig 31 MALDI-TOF of purified AT (B) and of Kybernin P1000 (A).

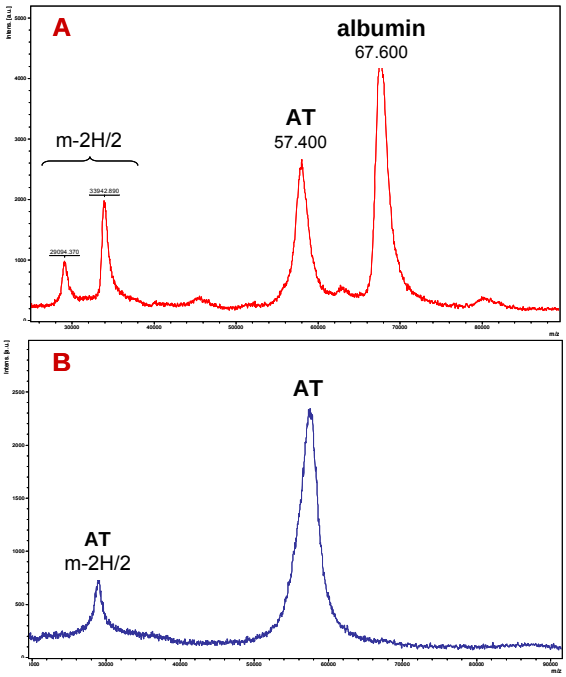

5.7.2 Antithrombin Sepharose preparation

Materials:

- Resin: Sepharose4CnBr activated
- Eluent: : Phosphate buffer 10 mM, pH 7.4, NaCl 0,1 M

Method:

- *Coupling procedure:*

  The antithrombin was coupled to UFH (unfractionated heparin) to preserve the heparin binding site during the coupling procedure to the resin. 15 mg of UFH were added to AT solution and dissolved in 5 ml of eluent solution. The solution was incubated under stirring for 1h at 4°C.

- *AT-Sepharose coupling procedure:*

  The AT-UFH solution was added to 1 g of Sepharose4CnBr activated resin (previously incubated in 5 ml of HCl 1mM o/n at 4°C and washed with 250 mM HCl). The resin was dissolved in $NaHCO_3$ 0,1 M final solution and the AT-UFH was finally added and incubated under stirring for 2 h at 24°C. In these conditions the coupling between the resin and the AT is favourable and the heparin binding site in protected by the presence if heparin (Fig. 32).

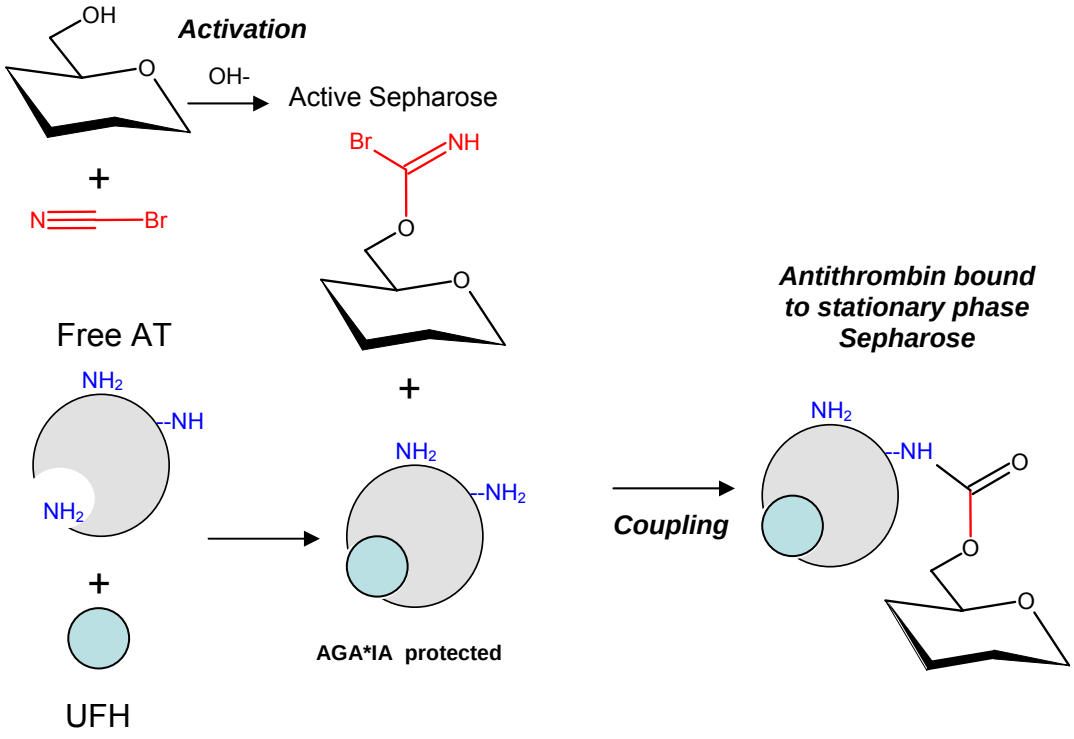

Fig 32 Coupling of the Antithrombin to the stationary phase

5.7.3 Affinity column preparation

Materials:

- Columns: Pharmacia (0,6x 12cm), Pharmacia (1,6x30 cm), Pharmacia (1,6x60 cm)
- Equilibrium buffer: Tris HCl buffer 50 mM, pH 7.4, NaCl 50 mM
- Elution buffer: Tris HCl buffer 50 mM, pH 7.4, NaCl 3 M
- Acetate buffer: Sodium acetate 0,1 M, NaCl 1,5 M

Method:

- *Analytical column preparation:*

  The AT-Sepharose complex was transferred onto the column Pharmacia (0,6x 12cm) at 4°C. Then the column was washed with $NaHCO_3$ (flow-rate 0,5 ml/min) and the absorbance at 280 nm of the collected fractions was measured. The washing procedure was repeated until the absorbance at 280 nm was 0 (with this parameter we can obtain an estimation of the Antithrombin not linked to the resin). The amount of AT not linked was evaluated (molar extinction coefficient ε_{280}=6,28) and the efficiency of the coupling procedure was about 98%. The total amount of AT linked to the resin was about 20 mg. Finally the column was washed with 20 ml of elution buffer , 20 ml of purified water, 20 ml of acetate buffer, 20 ml of purified water and 20 ml of equilibrium buffer.

- *Semi-preparative column preparation:*

  The column (1,6x 30 cm) was prepared as described above. In this case the total amount of AT linked to the resin was 100 mg.

- *Preparative column preparation:*

  The column (1,6x 60 cm) was prepared as described above. In this case the total amount of AT linked to the resin was 1 g.

5.7.4 Affinity chromatography toward Antithrombin

Materials:

- Equilibrium buffer: Tris HCl buffer 50 mM, pH 7.4, NaCl 50 mM
- Elution buffer: Tris HCl buffer 50 mM, pH 7.4, NaCl 3 M
- Fraction-collector Gilson mod. 201 controller
- Pump Gilson Miniplus 2
- Cuvettes micro (0,8 ml)
- Spectrophotometer Cary 50 UV/Vis (Varian)
- Millipore 0,22u filters

Method:

- *Buffers preparation:*

  Both buffers, Equilibrium and Elution, was prepared with purified water, filtered with Millipore filter (0,22 µ) and incubated at 4°C for at least 1 h before using.

- *Binding capacity evaluation:*

  The binding capacity of each column was estimated using UFH like standard. A single chromatography was performed and the NA fraction was reloaded again onto the column, when was no possible to isolate a high affinity fraction from the NA fraction reloaded the amount of UFH loaded was considered the maximum binding capacity of the column.

- *Analytical chromatography:*

  The sample (1,5 mg, equal to the binding capacity of the column) was dissolved in 1,5 ml of equilibrium buffer and loaded onto the column (flow rate 0,5 ml/min). The fraction with no affinity toward the antithrombin was eluted with 12 ml of equilibrium buffer and collected in a single fraction called NA fraction. The fraction with high affinity toward the antithrombin was eluted with 10 ml of elution buffer and collected in a single fraction named HA fraction. The column was finally washed with about 70 ml of equilibrium buffer before a new experiment. The amount of LMWHs for each fraction was estimated through an uronic acid assay (187).

- *Semi preparative chromatography:*

  The sample (15 mg, equal to the binding capacity of the column) was dissolved in 1,5 ml of equilibrium buffer and loaded onto the column (flow rate 1 ml/min). The fractions with no affinity toward the antithrombin were eluted with 65 ml of equilibrium buffer and collected in 13 fractions (vol. = 5 ml) and called NA fractions. The fractions with high affinity toward the antithrombin were eluted with 65 ml of elution buffer and collected in 12 fractions named HA fractions. The column was finally washed with about 350 ml of equilibrium buffer before a new experiment. The amount of LMWHs for each fraction was estimated through an uronic acid assay (187).

- *Preparative chromatography:*

The sample (50 mg, equal to the binding capacity of the column) was dissolved in 5 ml of equilibrium buffer and loaded onto the column (flow rate 5 ml/min). The fractions with no affinity toward the antithrombin were eluted with 600 ml of equilibrium buffer and collected in 24 fractions (vol. = 25 ml) and called NA fractions. The fractions with high affinity toward the antithrombin were eluted with 600 ml of elution buffer and collected in 24 fractions (vol. = 25 ml) named HA fractions. The column was finally washed with about 1 L of equilibrium buffer before a new experiment. The amount of LMWHs for each fraction was estimated through a uronic acid assay (187).

5.7.5 Isolation of fractions with different affinity toward AT

Materials:

- Equilibrium buffer: Tris HCl buffer 50 mM, pH 7.4, NaCl 50 mM
- Elution buffer: Tris HCl buffer 50 mM, pH 7.4, NaCl 3 M
- Fraction-collector Gilson mod. 201 controller
- Pump Gilson Miniplus 2
- Cuvettes micro (0,8 ml)
- Spectrophotometer Cary 50 UV/Vis (Varian)
- Millipore 0,22u filters

Method:

- *Buffers preparation:*

  Both buffers, Equilibrium and Elution, were prepared with purified water, filtered with Millipore filter (0,22 µ) and left at 4°C for at least 1 h before using.

- *Semi-preparative column:*

  50 mg of sample (equal to 3 times the binding capacity of the column) was dissolved in 1,5 ml of equilibrium buffer and loaded onto the column (flow rate 1 ml/min). The fractions with no affinity toward the antithrombin were eluted with 65 ml of equilibrium buffer and collected in 13 fractions (vol. = 5 ml) and called NA fractions. The fractions with high affinity toward the antithrombin were eluted with 65 ml of elution buffer and collected in 12 fractions named HA fractions. The column was finally washed with about 350 ml of equilibrium buffer before a new experiment. The amount of LMWHs for each fraction was estimated through an uronic acid assay (187). The HA fractions were

collected, named HA1, freeze-dried and desalted through size exclusion chromatography. The NA fractions were collected and loaded again onto the column. A second chromatography was performed. HA fractions were collected and named HA2 fraction, freeze-dried and desalted through size exclusion chromatography. NA fractions were collected and loaded for a second time onto the column. A third chromatography was performed and HA fraction was now named HA3. NA fractions were collected and loaded for a fourth time. After the last chromatography was no possible to isolate any HA fractions, the NA fractions obtained were collected and named NArel, freeze dried and desalted through size exclusion chromatography.

- *Preparative column:*

  150 mg of sample (equal to 3 times the binding capacity of the column) was dissolved in 5 ml of equilibrium buffer and loaded onto the column (flow rate 5 ml/min). The same experiment described above was performed and HA1, HA2, HA3, and NAr fractions were obtained and desalted through size exclusion chromatography.

5.8 Lowry assay [188]

Materials:

- Solution A: $CuSO_4$ 0,5% + sodium tartrate 1%
- Solution B: Na_2CO_3 2% dissolved in NaOH 0,1 M
- Solution D: Folin reagent dissolved in purified water (1 :1)
- Standard: BSA 200 µg/ml dissolved in purified water
- Equilibrium buffer: Tris HCl buffer 50 mM, pH 7.4, NaCl 50 mM
- Cuvettes micro (0,8 ml)
- Spectrophotometer Cary 50 UV/Vis (Varian)

Method:

- *Buffers preparation:*

  50 ml of B solution was added to 1 ml of A solution, obtaining C solution.

- *Procedure:*

  The calibration curve was obtained with 0,1 , 0,2 , 0,3 and 0,5 ml of standard solution diluted to 0,6 ml with equilibrium buffer. The sample was diluted 1 : 3 with purified water and 0,05 ml of the new solution was assayed. 3 ml of C solution were added to each sample and calibration curve point. The solutions were incubated for 10 min at room temperature. 0,4 ml of D solution were added and the samples were incubated for 30 min at room temperature. The absorbance at 550 nm was estimated for each sample.

5.9 Carbazole assay [187]

Materials:

- Carbazole solution: carbazole 0,125% dissolved in EtOH
- Equilibrium buffer: Tris HCl buffer 50 mM, pH 7.4, NaCl 50 mM
- Hydrolysis Solution: NaB_4O_7 0,25 M dissolved in H_2SO_4 98%
- Standard solution: LMWH 1 mg/ml dissolved in equilibrium buffer
- Pyrex tubes
- Cuvettes micro (0,8 ml)
- Spectrophotometer Cary 50 UV/Vis (Varian)

Method:

- *procedure:*

  The calibration curve was obtained with 0,01 , 0,02 , 0,03 and 0,05 ml of standard solution diluted to 0,5 ml with equilibrium buffer. 0,5 ml of sample solution was transferred onto the pyrex tubes. 2,5 ml of hydrolysis solution were added to a single tube. All samples were incubated at 100°C for 10 min then were cooled in water for 3 min. 0,1 ml of carbazole solution were added. Tubes were stirred and incubated at 100° for 15 min then cooled in water for 3 min. The samples were finally transferred in micro cuvettes and the absorbance at 530 nm was estimated.

- *Method validation:*

  The samples were contained in fractions differing for the concentration of LMWHs but also for the NaCl concentration. To demonstrate that the measures obtained through the carbazole assay were totally independent from the NaCl concentration the same sample of LMWH was dissolved in 3 different buffers with crescent NaCl concentration (from 0,5 M to 2,5 M) and assayed. The result confirms the independence from the NaCl concentration. The limits of detections

and the limits of quantifications were finally estimated with Enoxaparin like a standard.

5.10 Ion exchange chromatography

The ion exchange chromatography with Amberlite was used to eliminate some Tris-HCl traces from the samples before the NMR analysis.

Materials:

- Column: Amberlite IR-120 (H+) (2x12.5 cm)

Method:

- *Resin preparation:*

  The resin was rigenerated with 200 ml of HCl 4% and washed with 600 ml of purified water.

- *Procedure:*

  The sample was loaded onto the column and eluted with water. Flowthrough was collected in a single fraction until the pH was near to the neutrality. NaOH was added to the sample solution until the pH was about 6.5.

5.11 Chelex chromatography

The chelex resin was used in batch to eliminate ion Ca^{++} traces from the samples before the NMR analysis.

Materials:

- Resin: chelex (exchange capacity 0,4 meq/ml of resin)

Method:

- *Procedure:*

  The resin, extensively washed with purified water, was added to the sample solution (amount calculated on the basis of the quantity of the sample). The solution was incubated under stirring for 30 min at room temperature. The resin was removed from the sample solution with 0,22 µm Millipore filter.

5.12 HPLC/ESI-MS

Materials

- HPLC: dionex ultimate 3000
- Column: Superdex 75 1,5x30 cm
- Resin: dextran based
- Eluent: H_2O/MeOH 80:20 NH_4HCO_3 30 mM
- Flow-rate: 50 µl/min
- Injection: 250 µg dissolved in 50 µl of purified water
- Instrument: ESI qTOF MicrotofQ
- Temperature: 180 °C
- program: Bruker DataAnalysis

Method

Subfractions HA1, HA2, HA3 and NAr were analysed by high performance size-exclusion chromatography (HP-SEC) coupled to an electrospray ionization source, equipped with a hybrid quadrupole/time-of-flight (ESI-Q-TOF) mass spectrometer.

HP-SEC was performed on a prepacked Superdex 75 column (7 x 300 mm, GE Healthcare) equilibrated with mobile phase containing NH_4HCO_3 30 mM in H_2O/CH_3OH 80:20 (v/v). Samples were loaded by autosampler injection of 50 µl of sample solution at the concentration of 5 mg/ml in water and eluted in isocratic condition at 50 µl/min via a high performance liquid chromatographic (HPLC) system coupled to an electrospray ionization source.

All ESI mass spectra were carried out using the optimized ionization and desolvation conditions of the source working in the negative ion mode on a micrOTOF$_Q$ (Bruker Daltonics, Bremen, Germany) at a resolution of 15 000, in the mass range from m/z 300 to m/z 2500.

Ion dissociation was avoided by using the following source parameters: capillary voltage at 3500 V; nitrogen used as nebulizer and drying gas, nebulizer gas was set

at 0.7 bar , drying gas at a temperature of 200°C and a flow rate of 5l/min. The ESI-Q-TOF mass spectrometer was externally calibrated using negative Na formate clusters of a sodium formate solution produced from an appropriate mixture of sodium hydroxide and formic acid solutions. Quadratic calibration was performed to increase the mass accuracy. Mass distribution was obtained from the ESI MS data processed by the DataAnalysis software (Version 3.4 , Bruker Daltonik).

To verify the IP-RP-HPLC/ESI-MS profiles, samples were analyzed at the same concentration (50 µl of a solution 5 mg/ml) by chromatographic separation on a 3µm Knauer reversed-phase C4 (4.6 x 150 mm) by eluting with a linear gradient from 90% eluent A (H2O) to 70% eluent B (CH3OH), both in 10mM dibutylammonium acetate (DBA), at a flow rate of 0.4 mL/min.

5.13 Activity anti-factor Xa

Materials

- Coagulometer: ACL mod 7000
- Buffer: Tris buffer pH 8.0
- Chromogenic solution: S-2765

Method

The samples were dissolved in 0,2 ml of Tris buffer (pH 8,4) in different concentrations and 0,05 ml of human plasma and 0,05 ml of antithrombin III were added. The coagulometer collect 0,06 ml from the sample solution, 0,06 ml from the chromogenic solution (S-2765), 0,03 ml of factor Xa and after 5 min add 0,03 ml of acetic acid and finally measure the absorbance at 405 nm. The standard solutions were obtained with LMWHs BRP (standard LMWH for assay).

6.0 References

1 Fransson LA. Glycosaminoglycans. In: Aspinall GO, ed. The Polysaccharides. Orlando, FL: Academic Press, 1985; vol. 3:337–413.

2 Roden L, Ananth S, Campbell P, Curenton T, Ekborg G, Manzella S, Pillion D, Meezan E. Heparin – an introduction. In: Lane DA, Bjork, Lindahl U, eds. Heparin and Related Polysaccharides. New York: Plenum Press, 1992; 1–20.

3 Lindahl U, Lidholt K, Spillmann D, Kjelle´n L. More to ‘‘heparin’’ than anticoagulation. Thromb Res 1994; 75:1–32.

4 Lever R, Page CP. Novel drug development opportunities for heparin. Nat Rev Drug Discov 2002; 1:140–148.

5 Casu B, Lindhal U. Structure and biological interactions of heparin and heparan sulfate. Adv Carbohydr Chem Biochem 2001; 57:159–206.

6 Lindahl U. Heparin – from anticoagulant drug into the new biology. Glycocon J 2000; 17:597–605.

7 Van Boeckel C, Petitou M. The unique antithrombin binding domain of heparin: a lead to new synthetic antithrombotics. Angew Chem Int Ed 1993; 32:1671–818.

8 Turnbull JE. Integral glycan sequencing of heparan sulfate and heparin saccharides. Methods Mol Biol 2001; 171:129–39.

9 Casu B. Structure and biological activity of heparin. Adv Carbohydr Chem Biochem 1985; 43:51–132.

10 Conrad HE. Heparin binding proteins. San Diego, CA: Academic Press, 1998.

11 Sasisekharan R, Venkataraman G. Heparin and heparan sulfate: biosynthesis, structure and function. Curr Opin Chem Biol 2000; 6:626–31

12 Capila I, Linhardt RJ. Heparin–protein interactions. Angew Chem Int Ed 2002; 41:390–412.

13 Linhardt RJ. Heparin: structure and activity. J Med Chem 2003; 46:2551–64.

14 Bianchini P, Liverani L, Mascellani G, Parma B. Heterogeneity of unfractionated heparins studied in connection with species, source, and production processes. Semin Thromb Hemost 1997; 23:3–10.

15 Guerrini M, Bisio A, Torri G. Combined quantitative 1H and 13C nuclear magnetic resonance spectroscopy for characterization of heparins. Semin Thromb Hemost 2001; 27:473–482.

16 Sudo M, Sato K, Chaidedgumjorm A, Toyoda H, Toida T, Imanari T. 1H Nuclear magnetic resonance spectroscopic analysis for determination of glucuronic acid and iduronic acid in dermatan sulfate, heparin and heparin sulfate. Anal Biochem 2001; 297:42–51.

17 Yamada S, Murakami T, Tsuda H, Yoshida K, Sugahara K. Isolation of porcine heparin tetrasaccharides with glucuronate 2-O-sulfate. J Biol Chem 1995; 270:8695–8705.

18 Fransson L-A° , Malmstrom A, Sjoberg I, Huckerby TN. Periodate oxidation and alkaline degradation of heparin-related glycans. Carbohydr Res 1980; 80:131–145.

19 Islam T, Butler M, Sikkander SA, Toida T, Linhardt RJ. Further evidence that periodate cleavage of heparin occurs primarily through the antithrombin binding site. Carbohydr Res 2002; 337:2239–2243.

20 Casu B, Guerrini M, Naggi A, Torri G, De-Ambrosi L, Boveri G, Gonella S, Cedro A, Ferro L, Lanzarotti E, Paterno` M, AttoliniM, Valle MG. Characterization of sulfation patterns of beef and pig mucosal heparins by nuclear magnetic resonance spectroscopy. Arzneim-Forsh (Drug Res) 1996; 46:472–477.

21 Stringer SE, Kandola BS, Pye DA, Gallagher JT. Heparin sequencing. Glycobiology 2003; 13:97–107.

22 Krueger J, Salvimirta M, Sturiale L, Gimenez-Gallego G, Lindahl U. Sequence analysis of heparan sulfate epitopes with graded affinities for fibroblast growth factors 1 and 2. J Biol Chem 2001; 276:30744–30752.

23 Thanawiroon C, Rice KG, Toida T, Linhardt RJ. Liquid chromatography/ mass spectrometry sequencing approach for highly sulfated heparin-derived oligosaccharides. J Biol Chem 2004; 279:2608–2615.

24 Mourier AJ, Viskov C. Chromatographic analysis and sequencing approach of heparin oligosaccharides using cetyltrimethylammonium dynamically coated stationary phases. Anal Biochem 2004.

25 Yamada S, Yamane Y, Tsuda H, Yoshida K, Sugahara K. A major commontrisulfated hexasaccharide core sequence, hexuronic acid (2 sulfate)-glucosamine(N-sulfate)–iduronic acid–N-acetylglucosamine–glucuronic acid–glucosamine (N-sulfate), isolated from the low sulfated irregular region of porcine intestinal heparin. J Biol Chem 1998; 273:1863–1871.

26 Lam LH, Silbert JE, Rosenberg RD. The separation of active and inactive forms of heparin. Biochem Biophys Res Comm 1976; 69:570–577.

27 Hook M, Bjork I, Hopwood J, Lindahl U. Anticoagulant activity of heparin: separation of high-activity and low-activity heparin species by affinity chromatography on immobilized antithrombin. FEBS Lett 1976; 66:90–93.

28 Andersson LO, Barrowcliffe TW, Holmer E, Johnson EA, Sims GEC. Anticoagulant properties of heparin fractionated by affinity chromatography on matrix-bound antithrombin III and by gel filtration. Thromb Res 1976; 9:575–583.

29 Lindahl U, Ba¨ ckstro¨m G, Thunberg L, Leder IG. Evidence for a 3-O-sulfated d-glucosamine residue in the antithrombin-binding sequence of heparin. Proc Natl Acad Sci USA 1980; 77:6551–6555.

30 Thunberg L, Backstrom G, Lindahl U. Further characterization of the antithrombin-binding sequence in heparin. Carbohydr Res 1982; 100:393–410.

31 Petitou M, Casu B, Lindahl U. 1976–1983, a critical period in the history of heparin: the discovery of the antithrombin binding site. Biochimie 2003; 85:83–89.

32 Rosenfeld L, Danishefsky I. Location of specific oligosaccharides in heparin in terms of their distance from the protein linkage region in native proteoglycan. J Biol Chem 1988; 263:262–266.

33 Pejler G, Danielsson A, Bjork, Lindahl U, Nader HB, Dietrich, CP. Structure and antithrombin binding properties of heparin isolated from the clams Anomalocardia brasiliana and Tivela macroides. J Biol Chem 1987; 262:11413–11421.

34 Bisio A, Guerrini M, Yates EA, Torri G, Casu B. NMR identification of structural environment for 2,3- and 2,3,6-tri-sulfated glucosamine residues in heparin with high and no affinity for antithrombin. Glycoconj 1997; J14:89.

35 Toida T, Hileman RE, Smith AE, Petinka IV, Linhardt RJ. Enzymatic preparation of heparin oligosaccharides containing antithrombin III binding sites. J Biol Chem 1996; 271:32040–32047.

36 Shriver Z, Raman R, Venkataraman G, Drummond K, Turnbull J, Toida T, Linhardt R, Biemann K, Sasisekharan R. Sequencing of 3-O-sulfate containing heparin decasaccharides with a partial antithrombin III binding site. Proc Natl Acad Sci USA 2000; 97:10359–10364.

37 Guerrini M, Raman R, Venkataraman G, Torri G, Sasisekharan R, Casu B. A novel computational approach to integrate NMR spectroscopy and capillary electrophoresis for

structure assignment of heparin and heparan sulphate oligosaccharides. Glycobiology 2002; 12:713–719.

38 Yamada S, Yoshida K, Sugiura M, Sugahara K, Khoo K-K, Morris HR, Dell A. Structural studies on the bacterial lyase-resistant tetrasaccharides derived from the antithrombin III-binding site of porcine intestinal heparin. J Biol Chem 1993; 268:4780–4787.

39 Lindahl U. Further characterization of the heparin–protein linkage region. Biochim Biophys Acta 1996; 130:368–382.

40 Iacomini M, Casu B, Guerrini M, Naggi A, Pirola A, Torri G. ‘‘Linkage region’’ sequences of heparins and heparan sulfates: detection and quantification by nuclear magnetic resonance spectroscopy. Anal Biochem 1999; 274: 50–58.

41 Hanhenberger R, Jakobson A. M., Ansari A, Wehler T, Svahn CM, Lindahl U.
Low-sulfated oligosaccharides derived from heparan sulate inhibit normalangiogenesis. Glycobiology 1993; 3:567–573.

42 Casu B, Choay J, Ferro DR, Gatti G, Torri G, Petitou M, Sinay P. Controversial glycosaminoglycan conformations. Nature 1986; 322:215–216.

43 Casu B. Conformation of individual residues and chains segments of glycosaminoglycans in solution by spectroscopic methods. In: Arnott F, Reeves DA, Morris, eds. Molecular Biophysics of the Extracellular Matrix. Clifton, NJ: Humana Press, 1983:69–93.

44 Ferro D.R., Provasoli A, Ragazzi M, Torri G, Casu B, Petitou M, Sinay P, Choay J. Evidence for conformational equilibrium of the sulfated l-iduronate residue in heparin and in synthetic mono- and oligosaccharides. J Am Chem Soc 1986; 108:6773–6778.

45 Ferro D, Ragazzi M, Provasoli A, Perly B, Torri G, Casu B, Petitou M, Sinay P, Choay J. Conformers population of l-iduronic acid residues in glycosaminoglycan sequences. Carbohydr Research 1990; 195:157–167.

46 Ragazzi M, Ferro D, Perly B, Sinay¨ P, Petitou M, Choay J. Conformation of the pentasaccharide corresponding to the binding site of heparin for antithrombin III. Carbohydr Res 1990; 195:169–185.

47 Van Boeckel CAA, van Aelst SF, Wagenaars GN, Mellema J-R. Synthesis and conformational analysis of iduronic acid-containing heparin trisaccharides. Rec Trav Chim Pays Bas 1987; 106:19–29.

48 Mickailov D, Linhardt RJ, Mayo KH. NMR conformation of heparin-derived hexasaccharide. Biochem J 1997; 328:51–61.

49 Angulo J, de Paz J-L, Nieto PM, Martin-Lomas M. Synthesis and conformational analysis of a heparin hexasaccharide. Israel J Chem 2001; 40:289–299.

50 Casu B, Petitou M, Provasoli M, Sinay P. Conformational flexibility: a new concept for explaining binding and biological properties of iduronic acid containing glycosaminoglycans. Trends Biochem Sci 1988; 13:221–225.

51 Mulloy B, Forster M, Jones C, Davies DB. NMR and molecular modelling studies in the solution conformation of heparin. Biochem J 1993; 293:849–858.

52 Casu B, Guerrini M, Torri G. Structural and conformational aspects of the anticoagulant and antithrombotic activity of heparin and dermatan sulfate. Current Pharmac Design 2004; 10:939–949.

53 Mulloy B, Forster MJ, Jones C, Drake AF, Johnson EA, Davies DB. The effect of variation of substitution on the solution conformation of heparin: a spectroscopic and molecular modelling study. Carbohydr Res 1994; 255:1–26.

54 Esko JD, Sellek SB. Order out of chaus: assembly of ligand binding sites in heparin sulphate. Annu Rev Biochem 2002; 71:435-471.

55 Prydz K, Dalen KT. Synthesis and sorting of proteoglycans. J Cell Sci 2000; 113:193-205.

56 Esko JD, Zhang L. Influence of core protein sequence on glycosaminoglycan assembly. Curr Opin Struct Biol 1996; 6:663-670.

57 Gotting C, Kuhn J, Zhan R, Brinkmann T, Kleesiek K. Molecular cloning and expression of human UDP-d-xylose: proteoglycan core protein β-D-xylosyltranferaseand its first isoform XT-II. J Mol Biol 2000; 304:517-528.

58 Bai X, ZhouD, Brown JR, Crawford BE, Hennet T, Esko JD. Biosynthesis of the linkage region of glycosaminoglycans: cloning and activity of galactosyltranferase II, the sixth member of the β1,3-galactosyltranferase family (β3GalT6). J Biol Chem 2001; 276:48189-48195.

59 Kitagawa H, Tone Ym Tamura J, Neumann KW, Ogawa T, Oka S, Kawasaki T, Sugahara K. Molecular cloning and expression of glucuronyltranferase I involved in the biosynthesis of glycosaminoglycan-protein linkage region of proteoglycans. J Biol Chem 1998; 273:6615-6618.

60 Tone Y, Kitagawa H, Imiya K, Oka S, Kawasaki T, Sugahara K. Characterization of recombinant human glucuronyltransferase I involved in the biosynthesis of glycosaminoglycan-protein linkage region of proteoglycans. FEBS Lett 1999; 459:415-420.

61 Monograph 01/2008:0828 Heparins, Low-Molecular_mass, European Pharmacopoeia 2008; Edition 6.0:2041–2042.

62 Johnson EA, Kirkwood TB, Stirling Y, et al. Four heparin preparations: anti-Xa potentiating effect of heparin after subcutaneous injection. Thromb Haemost 1976; 35: 586–591.

63 Andersson LO, Barrowcliffe TW, Holmer E, et al. Anticoagulant properties of heparin fractionated by affinity chromatography on matrix-bound antithrombin III and by gel filtration. Thromb Res 1976; 9: 575–583.

64 Lane DA, Macgregor IR, Michalski R, et al. Anticoagulant activities of four unfractionated and fractionated heparins. Thromb Res 1978; 12: 257–271.

65 Barrowcliffe TW, Johnson EA, Eggleton CA, et al. Anticoagulant activities of high and low molecular weight heparin fractions. Br J Haematol 1979; 41:573–583.

66 Holmer E, Lindahl U, Backstrom G, et al. Anticoagulant activities and effects on platelets of a heparin fragment with high affinity for antithrombin. Thromb Res 1980; 18: 861–869.

67 Thomas DP, Merton RE, Barrowcliffe TW, et al. Effects of heparin oligosaccharides with high affinity for antithrombin III in experimental venous thrombosis. Thromb Haemost 1982; 47: 244–248.

68 Barrowcliffe TW, Merton RE, Havercroft SJ, et al. Low-affinity heparin potentiates the action of high-affinity heparin oligosaccharides. Thromb Res 1984; 34: 125–133.

69 Hirsh J, Warkentin T, Raschke R, Granger C, Ohman E, Dalen J. Heparin and low molecular weight heparin. Mechanism of action, pharmacokinetics, dosing consideration, monitoring safety and efficacy. Chest 1998; 114:489S-501S.

70 Fareed J,. Basic and applied pharmacology of low molecular weight heparins. Pharm Ter 1995;16S-24S.

71 Hoppenstead DA, JeskeW, Fareed J, Bermes Jr EW. The role of tissue factor pathway inhibitor in the mediation of the antithrombotic actions of heparin and low molecular weight heparin. Blood Coagul Fibrinolyisis 1995; (Suppl1):S57-S64.

72 Fareed J, Walenga JM, Hoppenstead D, Huam X, Racanelli R. Comparative study on the in vitro and in vivo activities of seven low-molecular weight heparins. Haemostasis 1988;18 (suppl3):3-15.

73 Planes A, Vochelle N, Ferru J, Przyrowski D, Clerc J, Fagola M, Planes M. Enoxaparin, low molecular weight heparin: its use in the prevention of deep vein thrombosis following total hip replacement. Haemostasis 1986; 16:152-158.

74 Koopman MMW, Prandoni p, Piovena F. Treatment of venous thrombosis with intravenous unfractionated heparin administered in the hospital as compared with subcutaneous low molecular weight heparin administered at home. NEJM 1996;337(17):1251.

75 Levme M, Gent M, Hirsch J. A comparison of low-molecular-weight administered primarily at home with unfractionated heparin administered in the Hospital for proximal deep-vein thrombosis. N Engi J Med 1996- 334-677-681.

76 Samama MM, Cohen AT, Darmon JY, Desjardms L, Elder A, Janbon C, Leizorovicz A, Nguyen H, Olsson CG, Turpie AG, Weisslinger N. A comparison with placebo for the prevention of venous thromboembolism in acutely ill medical patients. N Engl J Med 1999; 341:793-800.

77 Zacharski LR, Ornsteing DL. Heparin and cancer. Thromb Haemost 1998-80:10-23.

78 Kay R, Wong KS, Lu UL. Low-molecular-weight heparin for the treatment of acute ischemic stroke. N Engi J Med 1995; 333:1588-1593.

79 Gillis S, Dann EJ, Eldor A. A low molecular weight heparin in the prophylaxis and treatment of disseminated intravascular coagulation in acute promyeloctic leukemia. Eur J Haematol 1995; 54:59-60.

80 Aguilar D, Goldhaber SZ. Clinical uses of low molecular weight heparins. Chest 1999; 115:1418-1423.

81 Hirsh J, Raschke R. Heparin and low-molecular-weight heparin. Chest 2004126:179S-203S.

82 Hirsh J, Warkentin TE, Shaughnessy SG. Heparin and low-molecular-weight heparin. mechanisms of action, pharmacokinetic, dosing, monitoring, efficacy and safety. Chest 2001; 119:64S-94S.

83 Ragazzi, M., Ferro, D.R, Provasoli, A. et al., Confirmation of the unsaturated ironic acid residues of glucosnminoglycan disaccharides J. Carbohydr Chem; 1993 12, 523.

84 J Bendix, M.G., Capila, Linhardt, II.J., Conformational study of synthetic A4-uronate monosaccharides and glycosaminoglycan-derived disaccharides Carbohydr. Res. 1998; 309, 135.

85 J Kiss. J.. Eliminative degradation of carbohydrate containing ironic acid residues. Adv. Carbohydr. Chem Biochem. 1974; 29, 230.

86 Shively . E., Conrad, H. E., Formation of anhydrosugar in the chemical depolyrnerization of heparin. Biochemistry 1976; 15, 3932.

87 Fussi, E, Process for obtaining low molecular weight heparins. Etzropean Patent GB2. 1982; 002, 4068.

88 Santini, F, Bisio, A., Guerrini, M. et al., Modification under basic conditions of the minor sequences of heparin containing 2,3 or 2.3,6 sulfated D-gluccmqmine residues Car- bohydr. Res. 302, 103 (1997)

89 Holme. K.R., Liang, W, Yang, Z. et al. Non anticoagulant action of glycosaminoglycans, 139-162 Plenum Press 1996; New York.

90 Fareed J., Hoppensteadt, D., Jeske, W et al., Low molecular weight aspirin a developmental perspective. EXP. Opin Invest. brags 1997; 6, 705.

91 Casu, B., Oreste, Torri, G. et aL, The structure of heparin oligosaccharide fragments with high anti-(factorXa) activity containing the minimal antithrombin Ill binding sequence. Biochem. 1981; 197, 599.

92 Shriver, Z., Sundays, M., Venkatnmman G. et as., Cleavage of the antithrombin III binding site in heparin by renominates and its implication in the generation of low molecular weight heparin. Procl. Natl. Acad. 2000 SCSI 57, 10365.

93 Yu, G., Le Bran, L., Gunky, N. S. ei al., Heparinase I arts on a synthetic aspirin tetrasaccharide corresponding to the antithrombin III binding site. Thromb. Res. 2000, 100, 549.

94 De Ambrosi, L., Recchia, W, Fermri G., Process of the controlled preparation of 1-molecular weight glycosaminoglycans. US Patent 4987222 1991.

95 Gray E., Mulloy B., Trevor W. Barrowcliffe, Heparin and low-molecular-weight heparin. Thromb. Haemost. 2008; 99: 807–818.

96 Torri G., Casu B., Gatti G., Petitou M.,Choay J., Mono and bi-dimensional 500 MHz 1H-NMR spectra of a pentasaccharide corresponding to the binding sequenze of heparin to antithrombin III: evidence for conformational peculiarity of the sulfated iduronate residue. Biochem Biophys Res Comm 1985;128:134-140.

97 Atha DH.,Lormeau JC, Petitou M, Rosenberg RD. Contribution of monosaccharideresidues in heparin binding to Antithrombin III. Biochemistry 1985; 24:6723-6729.

98 Choay J,Petitou M., Structure activity relationship in heparin: a synthetic pentasaccharide with high affinity to Antothrombn III and eliciting high anti-factor Xa activity**.** Biochem Biophys Res Comm 1983;116:492-499.

99 Walenga JM, Fareed J. Preliminary biochemical and farmacologic studies on a chemically synthesized pentasaccharide. Semin Thromb Hemost 1985;11:89-99.

100 Choay J. Biologic studies on chemically synthesized petasaccharide and tetrasaccharide fragments. Thromb Hemost 1985;11:81-85.

101 Riensenfeld J.,Thunberg L., Lindhal U. The antithrombin binding sequence of heparin. Location of essential N-sulfate groups. J. Biol. chem. 1981;256:2389-2394.

102 Petitou M. syntetic heparin fragments: new and efficient tools for the study of heparin and its interactions. Nouv. Rev. Fr. Hematol. 1984;26:221-226.

103 Herbert JM., Hérault JP., Bernat A., Petitou M., Meuleman DG. Biochemical and pharmacological properties of SANORG 34006, a potent and long-acting synthetic pentasaccharide. Blood 1998; 91:4197-4205.

104 Faaij RA, Burggraaf J. A Phase I single rising dose to study to investigate the safety, tolerance and pharmacokinetics of subcutaneous SanOrg 34006 in healthy male and female elderly volunteers. Thromb. Hemost. 1999; (Suppl):abstract 15547.

105 Emmanuele RM, Fareed J. The effect of molecular weight on the bioavailability of heparin. Thromb Res 1987; 48:591-596.

106 Brieger D, Dawes J. Production method affects the pharmacokinetic and ex vivo biological properties of low molecular weight heparins. Thromb Heamost 1997; 77:317-322.

107 Mousa SA, Mohamed S. Inhibition of endothelial cell tube formation by the low molecular weight heparin, tinzaparin, is mediated by tissue factors pathway inhibitor. Thromb Heamost 2004; 92:627-633.

108 Mousa SA, Kaiser B. Tissue factor pathway inhibitor in thrombosis and beyond: role of heparin. Drugs Future 2004; 29:751-766.

109 Boneu B, Caranobe C, Cadroy Y, Dol F, Gabaig AM, Dupouy D, Sie P. Pharmacokinetic studies of standard unfractionated heparin, and low molecular weight heparins in the rabbit. Semin Thromb Hemost 1988; 14:18-27.

110 Sutr AH, Massicotte P, Leaker M, Andrew M, Heparin therapy in pediatric patients. Semin Thromb Hemost 1997; 23:303-319.

111 Silverman GA, Bird PI, Carrel RW, Chuch FC, Coughlin PB, Gettings PGW, Irving JA, Lomas DA, Luke CJ, Moyer RW, Pemberton PA, Remold-O'donnel E, Salvesen GS, Travis J, Whisstock JC. Te serpins are an expanding superfamily of structurally similar but functionally diverse proteins. J Biol chem. 2001; 276:33293-33296.

112 Gettins PG. Serpin structure, mechanism, and function. Chem Rev 2002-102:4751-4804.

113 Rawhngs ND, Tolle DP, Barrett AJ. MEROPS: the peptidase database Nucleic Acids Res 2004; 32:D160-D164.

114 Barrett AJ, Salvesen G., eds. Protease Inhibitors. Amsterdam: Elsevier 1986.

115 Huntmgton JA, Carrell RW. The serpins: nature's molecular mousetraps Sci Prog 2001; 84:125-136.

116 Gettins PGW, Patston PA, Olson ST. Serpins: Structure, Function and Biol-ogy. Austin, TX: R.G. Landes Co., 1996.

117 Hunt LT, Dayhoff MO. A surprising new protein superfamily containing ovalbumm, antithrombin-III, and alpha 1-proteinase inhibitor. Biochem Bio-phys Res Commun 1980; 95:864-871.

118 Irving JA, Steenbakkers PJ, Lesk AM, Op dCH, Pike RN, Whisstock JC Serpins in prokaryotes. Mol Biol Evol 2002; 19:1881-1890.

119 Bird PI. Serpins and regulation of cell death. Results Probi Cell Differ 1998; 24:63-89

120 Carrell RW, Evans DL, Stein PE. Mobile reactive centre of serpins and the control of thrombosis [published erratum appears in Nature 1993- 364 (6439):737]. Nature 1991; 353:576-578.

121 Mottonen J, Strand A, Symersky J, Sweet RM, Danley DE, Geoghegan KF Gerard RD, Goldsmith EJ. Structural basis of latency in plasminogen activator inhibitor-1. Nature 1992; 355:270-273.

122 Zhou A, Huntington JA, Carrell RW. Formation of the antithrombin hetero-dimer In vivo and the onset of thrombosis. Blood 1999; 94:3388-3396.

123 Schechter I, Berger A. On the size of the active site in proteases I Papain. Biochem Biophys Res Commun 1967; 27:157-162.

124 Esnouf RM. An extensively modified version of MolScript that includes greatly enhanced coloring capabilities. J Mol Graph Modell 1997- 15-132.

125 Merritt EA, Murphy MEP. Raster 3d version 2.0 - a program for photorealistic molecular graphics. Acta Crystalogr 1994; D50:869-873.

126 Olson ST, Swanson R, Day D, Verhamme I, Kvassman J, Shore JD. Reso-lution of Michaelis complex, acylation, and conformational change steps in the reactions of the serpin, plasminogen activator inhibitor-1, with tissue plasmi-nogen activator and trypsin. Biochemistry 2001; 40:11742-11756.

127 Ye S, Chech AL, Belmares R, Bergstrom RC, Tong Y, Corey DR, Kanost MR,Goldsmith EJ. The structure of a Michaelis serpin-protease complex Nat Struct Biol 2001; 8:979-983.

128 Huntington JA, Read RJ, Carrell RW. Structure of a serpin-protease complex shows inhibition by deformation. Nature 2000; 407:923-926.

129 Kaslik G, Patthy A, Balint M, Graf L. Trypsin compiexed with alpha1-proteinase inhibitor has an increased structural flexibility. FEBS Lett 1995-370:179-183.

130 Stavridi ES, O'Malley K, Lukacs CM, Moore WT, Lambris JD, Christianson DW, Rubm H, Cooperman BS. Structural change in alpha-chymotrypsin induced by complexation with alpha 1-antichymotrypsin as seen by enhanced sensitivity to proteolysis. Biochemistry 1996; 35:10608-10615.

131 Peterson FC, Getting PG. Insight into the mechanism of serpin-proteinase inhibition from 2D [1H-15N] NMR studies of the 69 kDa alpha 1-proteinase inhibitor Pittsburgh-trypsin covalent complex. Biochemistry 2001; 40:6284-6292.

132 Bedsted T, Swanson R, Chuang YJ, Bock PE, Bjork I, Olson ST. Heparin and calcium ions dramatically enhance antithrombin reactivity with factor IXa by generating new interaction exosites. Biochemistry 2003; 42:8143-8152.

133 Rezaie AR, Olson ST. Calcium enhances heparin catalysis of the antithrombin-factor Xa reaction by promoting the assembly of an intermediate heparin-antithrombin-factor Xa bridging complex. Demonstration by rapid kinetics studies. Biochemistry 2000; 39:12083-12090.

134 Danielsson A, Bjork I. Mechanism of inactivation of trypsin by antithrombin. Biochem J 1982; 207:21-28.

135 Chuang YJ, Swanson R, Raja SM, Bock SC, Olson ST. The antithrombin PI residue is important for target proteinase specificity but not for heparin activation of the serpin.

Characterization of PI antithrombin variants with altered proteinase specificity but normal heparin activation. Biochemistry2001; 40:6670-6679.

136 Derechin VM, Blinder MA, Tollefsen DM. Substitution of arginine for Leu444 in the reactive site of heparin cofactor II enhances the rate of thrombin inhibition. J Biol Chem 1990; 265:5623-5628.

137 Verhamme IM, Bock PE, Jackson CM. The preferred pathway of glycosaminoglycan accelerated inactivation of thrombin by heparin cofactor II. J Biol Chem 2004; 279:9785-9795.

138 Rezaie AR. Role of exosites 1 and 2 in thrombin reaction with plasminogen activator inhibitor-1 in the absence and presence of cofactors. Biochemistry 1999; 38:14592-14599.

139 Wallace A, Rovelli G, Hofsteenge J, Stone SR. Effect of heparin on the glia derived nexin thrombin interaction. Biochem J 1989; 257:191-196.

140 Evans DL, McGrogan M, Scott RW, Carrell RW. Protease specificity and heparin binding and activation of recombinant protease nexin I. J Biol Chem 1991; 266:22307-22312.

141 Knauer DJ, Majumdar D, Fong PC, Knauer MF. SERPIN regulation of factor XIa. The novel observation that protease nexin 1 in the presence of heparin is a more potent inhibitor of factor XIa than Cl inhibitor. J Biol Chem 2000; 275:37340-37346.

142 Pratt CW, Church FC. Heparin binding to protein C inhibitor. J Biol Chem 1992; 267:8789-8794.

143 Hermans JM, Jones R, Stone SR. Rapid inhibition of the sperm protease acrosin by protein C inhibitor. Biochemistry 1994; 33:5440-5444.

144 Ecke S, Geiger M, Resch I, Jerabek I, Sting L, Maier M, Binder BR. Inhibition of tissue kallikrein by protein C inhibitor. Evidence for identity of protein C inhibitor with the kallikrein binding protein. J Biol Chem 1992; 267:7048-7052.

145 Loebermann H, Tokuoka R, Deisenhofer J, Huber R. Human alpha 1-proteinase inhibitor. Crystal structure analysis of two crystal modifications, molecular model and preliminary analysis of the implications for function. J Mol Biol 1984; 177:531-557.

146 Huber R, Carrell RW. Implications of the three-dimensional structure of alpha 1-antitrypsin for structure and function of serpins. Biochemistry 1989-28:8951-8966.

147 Bjork I, Olson ST. Antithrombin. A bloody important serpin. Adv Exp Med Biol 1997; 425:17-33.

148 Hirsh J. Blood tests for the diagnosis of venous and arterial thrombosis. Blood 1981; 57:1-8.

149 Kojima T. Targeted gene disruption of natural anticoagulant proteins in mice. Int J Hematol 2002; 76 (Suppi 2):36-39.

150 Desai UR. New antithrombin-based anticoagulants. Med Res Rev 2004-24:151-181.

151 Sie P, Ofosu F, Fernandez F, Buchanan MR, Petitou M, Boneu B. Respective role of antithrombin III and heparin cofactor II in the in vitro anticoagulant effect of heparin and of various sulphated polysaccharides. Br J Haematol 1986; 64:707-714.

152 Casu B, Lindahl U. Structure and biological interactions of heparin and heparan sulfate. Adv Carbohydr Chem Biochem 2001; 57:159-206.

153 Esko JD, Selleck SB. Order out of chaos: assembly of ligand binding sites in heparan sulfate. Annu Rev Biochem 1905; 71:435-471.

154 Lindahl U, Thunberg L, Backstrom G, Riesenfeld J. The antithrombin-binding sequence of heparin. Biochem Soc Trans 1981; 9:499-51.

155 Casu B, Oreste P, Torri G, Zoppetti G, Choay J, Lormeau JC, Petitou M,Sinay P. The structure of heparin oligosaccharide fragments with high anti-(factor Xa) activity containing the minimal antithrombin Ill-binding sequence. Chemical and 13C nuclear-magnetic-resonance studies. Biochem J 1981; 197:599-609.

156 Petitou M, Casu B, Lindahl U. 1976-1983, a critical period in the history of heparin: the discovery of the antithrombin binding site. Biochimie 2003-85:83-89.

157 Borg JY, Owen MC, Soria C, Soria J, Caen J, Carrell RW. Proposed heparin binding site in antithrombin based on arginine 47. A new variant Rouen-II, 47 Arg to Ser. J Clin Invest 1988; 81:1292-1296.

158 Olson ST, Bjork I, Bock SC. Identification of critical molecular interactions mediating heparin activation of antithrombin: implications for the design of improved heparin anticoagulants. Trends Cardiovasc Med 2002-12:198-205.

159 Jin L, Abrahams JP, Skinner R, Petitou M, Pike RN, Carrell RW. The anticoagulant activation of antithrombin by heparin. Proc Nati Acad Sci USA 1997; 94:14683-14688.

160 Li W, Johnson DJ, Esmon CT, Huntington JA. Structure of the antithrombm-thrombin-heparin ternary complex reveals the antithrombotic mechanism of heparin. Nat Struct Mol Biol 2004; 11:857-862.

161 Johnson DJ, Huntington JA. Crystal structure of antithrombin in a heparin-bound intermediate state. Biochemistry 2003; 42:8712-8719.

162 Arocas V, Bock SC, Raja S, Olson ST, Bjork I. Lysine 114 of antithrombin is of crucial importance for the affinity and kinetics of heparin pentasaccharide binding. J Biol Chem 2001; 276:43809-43817.

163 Mushunje A, Zhou A, Huntington JA, Conard J, Carrell RW. Antithrombin 'DREUX' (Lys 114Glu): a variant with complete loss of heparin affinity. Thromb Haemost 2002; 88:436-443.

164 Desai U, Swanson R, Bock SC, Bjork I, Olson ST. Role of arginine 129 in heparin binding and activation of antithrombin. J Biol Chem 2000; 275:18976-18984.

165 Schedin Weiss S, Desai UR, Bock SC, Gettins PG, Olson ST, Bjork I. Importance of lysine 125 for heparin binding and activation of antithrombin. Biochemistry 2002; 41:4779-4788.

166 Schedin-Weiss S, Desai UR, Bock SC, Olson ST, Bjork I. Roles of N-terminal region residues Lysll, Argl3, and Arg24 of antithrombin in heparin recognition and in promotion and stabilization of the heparin-induced conformational change. Biochemistry 2004; 43:675-683.

167 Nordenman B, Bjork I. Influence of ionic strength and pH on the interaction between high-affinity heparin and antithrombin. Biochim Biophys Acta 1981; 672:227-238.

168 Nordenman B, Bjork I. Binding of low-affinity and high-affinity heparin to antithrombin. Ultraviolet difference spectroscopy and circular dichroism studies. Biochemistry 1978; 17:3339-3344.

169 Olson ST, Shore JD. Binding of high affinity heparin to antithrombin III. Characterization of the protein fluorescence enhancement. J Biol Chem 1981; 256:11065-11072.

170 Olson ST, Srinivasan KR, Bjork I, Shore JD. Binding of high affinity heparin to antithrombin III. Stopped flow kinetic studies of the binding interaction.J Biol Chem 1981; 256:11073-11079.

171 Carrell RW, Stein PE, Fermi G, Wardell MR. Biological implications of a 3A structure of dimeric antithrombin. Structure 1994; 2:257-270.

172 Schreuder HA, de Boer B, Dijkema R, Mulders J, Theunissen HJ, Grootenhuis PD, Hoi WG. The intact and cleaved human antithrombin III complex as a model for serpin-proteinase interactions. Nat Struct Biol 1994;1:48-54.

173 Whisstock JC, Pike RN, Jin L, Skinner R, Pei XY, Carrell RW, Lesk AM. Conformational changes in serpins. II. The mechanism of activation of antithrombin by heparindagger. J Mol Biol 2000; 301:1287-1305.

174 van Boeckel CA, Grootenhuis PD, Visser A. A mechanism for heparin-induced potentiation of antithrombin III. Nat Struct Biol 1994; 1:423-425.

175 Meagher JL, Olson ST, Gettins PG. Critical role of the linker region between helix D and strand 2A in heparin activation of antithrombin. J Biol Chem 2000; 275:2698-2704.

176 Belzar KJ, Zhou A, Carrell RW, Gettins PG, Huntington JA. Helix D elongation and allosteric activation of antithrombin. J Biol Chem 2002; 277:8551-8558.

177 Bjork I, Fish WW. Production in vitro and properties of a modified form of bovine antithrombin, cleaved at the active site by thrombin. J Biol Chem 1982; 257:9487-9493.

178 Skinner R, Chang WS, Jin L, Pei X, Huntington JA, Abrahams JP, Carrell RW,Lomas DA. Implications for function and therapy of a 2.9A structure of binary-complexed antithrombin. J Mol Biol 1998; 283:9-14.

179 Olson ST, Bjork I. Role of protein conformational changes, surface approxi-mation and protein cofactors in heparin-accelerated antithrombin-proteinase reactions. Adv Exp Med Biol 1992; 313:155-165.

180 Bray B, Lane DA, Freyssinet JM, Pejier G, Lindahl U. Anti-thrombin activities of heparin. Effect of saccharide chain length on thrombin inhibition by heparin cofactor II and by antithrombin. Biochem J 1989; 262:225-232.

181 Langdown J, Johnson DJ, Baglin TP, Huntington JA. Allosteric activation of antithrombin critically depends upon hinge region extension. J Biol Chem 2004; 279:47288^7297.

182 Izaguirre G, Zhang W, Swanson R, Bedsted T, Olson ST. Localization of an antithrombin exosite that promotes rapid inhibition of factors Xa and IXa dependent on heparin activation of the serpin. J Biol Chem 2003; 278:51433-51440.

183 Olson ST, Chuang YJ. Heparin activates antithrombin anticoagulant function by generating new interaction sites (exosites) for blood clotting proteinases. Trends Cardiovasc Med 2002; 12:331-338.

184 Dementiev A, Petitou M, Herbert JM, Gettins PG. The ternary complex of antithrombin-anhydrothrombin-heparin reveals the basis of inhibitor specificity. Nat Struct Mol Biol 2004; 11:863-867.

185 Huntington JA. Mechanisms of glycosaminoglycan activation of the serpins in hemostasis. J Thromb Haemost 2003; 1:1535-1549.

186 Guerrini et al. Complex glycosaminoglycans: profiling substitution patterns by two dimensional NMR spectroscopy. Anal Biochem. 2005 337; 35-47.

187 T Bitter, HM Muir. A Modified Uronic Acid Carbazole Reaction. Anal. Biochem. 4 (4); 330-334 1962.

188 O. H. Lowry, N. J. Rosebrough, A.L. Farr, R. J. Randall. Protein measurement with the folin phenol reagent. *J. Biol. Chem.* 193, 265-275 1951.

189 Guerrini M, Guglieri S Naggi A, Sasisekharan R, Torri G,. Low Molecular Weight Heparins: Structural Differentiation by Bidimensional Nuclear Magnetic Resonance Spectroscopy. Semin Thromb Hemost 2007;33:478–487.

190 Bertini, S., Bisio, A.,Torri, G., Bensi, D., Terbojevich, M. Molecular Weight Determination of Heparin and Dermatan Sulfate by Size Exclusion Chromatography with a Triple Detector Array. *Biomacromol.*, 2005, 6, 168-173.

191 Guerrini et al. Antithrombin-binding Octasaccharides and Role of Extensions of the Active Pentasaccharide Sequence in the Specificity and Strength of Interaction. Journal of Biological chemistry. In press 2008.

192 U.R. Desai, R.J. Linhardt, Molecular weight of heparin using 13C nuclear magnetic resonance spectroscopy, J. Pharm. Sci. 84 (2) 212–215 1995.

193 Yates, E.A., Santini, F., De Cristofano, B., Payre, N., Cosentino, C., Guerrini, M., Naggi, A., Torri, G., Hricovini, M. Effect of substitution pattern on 1H, 13C NMR chemical shifts and 1JC-H coupling constants in heparin derivatives. Carbohydr. Res. 329, 239-247, 2000.

194 Hochuli, M., Wuthrich, K., and Steinmann, B. Two-dimensional NMR spectroscopy of urinary glycosaminoglycans from patients with different mucopolysaccharidoses. NMR Biomed. 16, 224-236, 2003.

195 Bisio, A., Guglieri, S., Frigerio, M., Torri, G., Vismara, E., Cornelli, U., Bensi, D., Gonella, S., and De Ambrosi, L. Controlled γ-ray irradiation of heparin generates oligosaccharides enriched in highly sulfated sequences. Carbohydr. Polym. 55, 101-112, 2004 .

196 Heikkinen, S., Toikka, M.M., Karhunen, P.T., and Kilpeläinen, I.A. Quantitative 2D HSQC (Q-HSQC) via suppression of J-dependence of polarization transfer in NMR spectroscopy: application to wood lignin. J. Am. Chem. Soc. 125, 4362-4367, 2003.

197 Seyrek E., Dubin Paul L., Henriksen J. Nonspecific electrostatic binding characteristics of the heparin-antithrombin interaction. Biopolymers 2007; 86 (3);249-59.

198 Casu B, Torri G. Structural characterization of low molecular weight heparins. Semin Thromb Hemost, 25(3) 17-25, 1999.

1.0 INTRODUCTION 1

1.1 HEPARIN 2
1.1.1 *Monosaccharide residues* 3
1.1.2 *Major disaccharide units* 5
1.1.3 *Undersulfated sequences* 7
1.1.4 *Specific sequences* 9
1.1.5 *Molecular conformation of heparin and sequences* 12
1.1.6 *Biosynthesis of heparin and HS* 15
1.1.7 *Nuclear Magnetic Resonance for structural analysis of heparin and HS* 18

1.2 LOW MOLECULAR WEIGHT HEPARINS 22
1.2.1 *Therapeutic applications of LMWHs* 23
1.2.2 *Different depolymerization methods* 28
1.2.3 *Synthetic heparin polysaccharides* 31

1.3 HEPARIN vs LOW MOLECULAR WEIGHT HEPARINS 34

1.4 ANTITHROMBIN 36
1.4.1 *Serpin structure* 36
1.4.2 *The suicide substrate mechanism* 37
1.4.3 *Physiological functions* 39
1.4.4 *Mechanism of heparin binding* 41
1.4.5 *Acceleration of protease inhibition* 43

2.0 AIM OF THE WORK 46

3.0 RESULTS 47

3.1 GEL PERMEATION CHROMATOGRAPHY 47

3.2 AFFINITY CHROMATOGRAPHY 49

3.3 MOLECULAR WEIGHT EVALUATION 50

3.4 NMR CHARACTERIZATION 57

3.5 ACTIVITY 64

4.0 DISCUSSION 66

5.0 MATERIALS AND METHODS 70

5.1 MOLECULAR WEIGHT EVALUATION OF LMWHs 70

5.2 LMWHs FRACTIONATION THROUGH SIZE EXCLUSION CHROMATOGRAPHY 71

5.3 LMWHs FRACTIONS DESALTING PROCEDURE THROUGH SIZE EXCLUSION CHROMATOGRAPHY 73

5.3.1 *Sephadex G10 column* 73

5.3.2 *TSK columns* 75

5.4 LMWHs FRACTIONS DESALTING PROCEDURE THROUGH ULTRAFILTRATION 77

5.5 NMR SPECTRA RECORDING 78

5.5.1 *^{1}H NMR spectra* 78

5.5.2 *^{13}C NMR spectra* 79

5.5.3 *HSQC NMR spectra* 80

5.6 NMR EVALUATION OF STRUCTURAL PARAMETERS OF LMWHs 82

5.6.1 *Evaluation of average sulfation degree* 82

5.6.2 *Evaluation of average molecular weight for a single disaccharide* 83

5.6.3 *Evaluation of average chain-length* 84

5.7 AFFINITY CHROMATOGRAPHY 85
5.7.1 *Antithrombin purification* 85
5.7.2 *Antithrombin sepharose preparation* 87
5.7.3 *Affinity column preparation* 89
5.7.4 *Affinity chromatography toward Antithrombin* 90
5.7.5 *Isolation of fractions with different affinity toward AT* 93

5.8 LOWRY ASSAY [188] 95

5.9 CARBAZOLE ASSAY [189] 96

5.10 ION EXCANGHE CHROMATOGRAPHY 97

5.11 CHELEX CHROMATOGRAPHY 98

5.12 HPLC/ESI-MS 99

5.13 ACTIVITY ANTI-FACTOR Xa 101

6.0 REFERENCES 102

1D	Monodimensional.
1JC-H	one-bond proton-carbon coupling constant.
2D	two-dimensional.
3D	three-dimensional.
3JH-H	three-bonds proton-proton coupling constant.
AGA*IA	pentasaccharidic sequence (binding AT).
AM_{6S}	Anhydromannitol.
APTT	activated partial thromboplastin time.
Arg	Arginine.
Asn	Asparagine.
AT	antithrombin III.
AT-bd	antithrombin binding domain.
AT-BR	antithrombin bindign region.
BSA	bovin serum albumin.
CS	condroitin sulphate.
D	Polydispersity.
D2O	deuterium hydroxide.
Da	Daltons.
DS	dermatan sulphate.
DVT	deep venous thrombosis.
ECS	endothelial cells.
ESI	electron spry ionization.
etOH	ethanol.
FDA	food and drug administration.

FGF(s)	fibroblast growth factor(s),
GAG(s)	glycosaminoglycan(s).
Gal	D-galactose.
GalNacT-I	β1-4N-acetylgalactosaminyltranferase-I.
GalT-I	galactosyltransferase I.
GalT-II	galactosyltransferase II.
GlcA	D-glucuronic acid.
GlcAT-I	glucuronyltransferase I.
GlcN	D-glucosamine.
GlcN,3,6S (or A*)	N,3-O,6-O-trisulfated D-glucosamine.
GlcN,6S	N,6-O-disulfated-D-glucosamine.
GlcNAc	N-acetyl-D-glucosamine.
GlcNS	N-sulfated-D-glucosamine.
Gly	glycine.
HA	high affinity.
HP	heparin.
HPLC	high pressure liquid chromatography.
HS	heparan sulfate.
HSQC	heteronuclear single quantum coherence.
HST	hexasulfated trisaccharide.
IdoA	L-iduronic acid.
IdoA2S	L-iduronic acid 2-O-sulfate.
IIa	factor IIa (thrombin).
IV	Intravenous.

LALLS	low angle laser light scattering.
LMWH	low molecular weight heparin.
LR	linkage region.
Lys	Lysine.
MALDI	matrix assisted laser desorbtion ionization.
Mn	molecular weight (number average).
MSD	monosulfated disaccharide.
Mw	molecular weight (weight average).
Mz	molecular weight (Z-average).
NA	N-acetylated.
NA	no affinity.
NDSTs	N-deacetylase/N-sulfotranseferase.
NMR	nuclear magnetic resonance.
NOE	nuclear Overhauser effect.
NOESY	nuclear Overhauser effect spectroscopy.
NR	non-reducing end.
NS	N-sulfated.
NSD	nonsulfated disaccharide.
R	reducing end.
RALLS	right angle laser light scattering.
RCL	reactive centre loop.
SC	subcutaneous.
Ser	serine.
TDA	triple detector assay.

TFPI	tissue factor pathway inhibitor.
TIC	total ion chromatogram.
Tris	tromethamine.
tr-NOE	transferred nuclear Overhauser effect.
TSD	trisulfated disaccharide.
TSP	trimethylsilyl propionate sodium.
U	units.
UFH	unfractionated heparin.
VTE	venous thromboembolic disorders.
WHO	world health organization.
Xa	factor Xa.
Xyl	D-xylose.
XylT	xylosyltransferase.
ΔU	4,5-unsaturated uronic acid.
ΔU2s	4,5-unsaturated-2-sulfated uronic acid.
ε	extinction molar coefficient.